General Projective Approach to Transport Coefficients of Condensed Matter Systems and Application to an Atomic Wire

Dissertation (kumulativ)

zur Erlangung des Grades eines
Doktors der Naturwissenschaften (Dr. rer. nat.)

dem Fachbereich Physik der Universität Osnabrück
vorgelegt von

Dipl.-Phys. Christian Bartsch

Osnabrück, im Januar 2010

Betreuer, Hauptberichterstatter: Prof. Dr. Jochen Gemmer

Mitberichterstatter: Prof. Dr. Michael Rohlfing

Constituent Parts

General Projective Approach to Transport Coefficients of Condensed Matter Systems and Application to an Atomic Wire

Dissertation (Cumulative)

Christian Bartsch[1, *]

[1] *Fachbereich Physik, Universität Osnabrück, Barbarastrasse 7, D-49069 Osnabrück, Germany*

(Dated: January 29, 2010)

We present a novel approach to the investigation of transport coefficients in condensed matter systems, which is based on a pertinent time-convolutionless (TCL) projection operator technique. In this context we analyze in advance the convergence of the corresponding perturbation expansion and the influence of the occurring inhomogeneity. The TCL method is used to establish a formalism for a consistent derivation of a Boltzmann equation from the underlying quantum dynamics, which is meant to apply to non-ideal quantum gases. We obtain a linear(ized) collision term that results as a finite non-singular rate matrix and is thus adequate for further considerations, e.g., the calculation of transport coefficients. In the work at hand we apply the provided scheme to numerically compute the diffusion coefficient of an atomic wire and especially analyze its dependence on certain model properties, in particular on the width of the wire.

PACS numbers: 05.30.-d, 05.70.Ln, 72.10.-d, 05.60.Gg

Contents

I. INTRODUCTION

The investigation of transport phenomena is a long-established research field in physics, especially because many transport effects are present in everyday life, e.g., electrical conduction and heat conduction [6]. Both these phenomena are usually described (phenomenologically) by Fourier's law [7] in most ordinary macroscopic situations. Whenever this law is valid, one speaks of normal, regular or diffusive transport. However, when it comes to smaller systems the characterization of the transport becomes more difficult, i.e., when the size of the regarded systems reaches the nanoscale. This especially concerns the foregoing downsizing of technical devices, e.g., computer processors. In this case quantum effects may become important and non-regular transport may occur, i.e., the validity of Fourier's law is not self-evident. One important representative of such (low-dimensional) systems is a so-called atomic wire, which is, e.g., assumed to consist of an array of a certain sort of atoms linearly and regularly arranged on some crystal surface. There are experimental approaches to construct such atomic wires, e.g., by self-assembly [8]. Moreover, atomic wires may become relevant for technical applications as conductor on the nanoscale in the future.

The main intention of the work at hand is to provide a novel approach which allows for the investigation of transport behavior of closed quantum systems in general, bottom-up from first principles, i.e., from the Schrödinger equation. In detail, we concretely aim at determining transport properties like diffusion coefficients and conductivities for concrete systems. In the work at hand we especially address the determination of a diffusion coefficient of a 1-d atomic wire. This system is of particular interest, since it has surely quantum mechanical character and because a stringent derivation of a diffusion coefficient or a conductivity of an atomic wire is not existent so far.

There are several approaches to transport in quantum systems, one of them is provided by the Kubo formula which arises in the context of linear response theory [9, 10]. However, one generally needs to know the corresponding current-current-correlation function in detail to obtain a conductivity from the Kubo formula. To find the

*Electronic address: cbartsch@uos.de

current-current-correlation function one normally has to diagonalize the system, since the time dependence occurring therein refers to the Heisenberg picture. The systems we consider in the work at hand are many-particle systems and therefore very high dimensional, so that a complete diagonalization is normally not accessible. Hence, the Kubo formula may not be directly evaluated without further efforts.

Instead of that we suggest here an access to the transport properties via a Boltzmann equation. However, there is a priori no Boltzmann equation available in quantum systems, there is only a description of the microscopic dynamics given by the Schrödinger equation. So to nevertheless follow this approach we have to somehow generate us a pertinent Boltzmann equation from the underlying quantum dynamics. There are some ideas pointing out how such a mapping of the quantum dynamics onto a Boltzmann equation may be performed, e.g., [11–13]. However, they often feature some conceptual difficulties, e.g., infinitely many dynamical variables, singular scattering rates in the collision term, non-linear collision terms. Thus, it seems to be challenging to apply them to concrete models in order to obtain quantitative results, e.g., calculate transport coefficients. Moreover, they partly involve rather ill-controlled assumptions such as, e.g., full factorizability of occupation number operators at all times.

So, instead of following one of these ideas, we introduce in the work at hand an alternative, novel approach to the mapping of quantum dynamics onto a Boltzmann equation. This approach is based on a time-convolutionless (TCL) projection operator method [14–16]. It allows for a consistent systematic derivation of a collision term of a Boltzmann equation on the basis of the Schrödinger equation without uncontrolled assumptions. So far, the application of projection operators methods within the framework of transport theoretical investigations is quite an unusual approach. (Projection operator methods have barely been used in transport theory.) Therefore, our approach represents a truly novel access to transport. Simultaneously, transport theory, especially in the context of closed systems, is a new field of application for projection operator techniques, which are commonly used in the context of open systems. In particular, this means that problems, which may possibly arise when using such methods, have to be reviewed again. Concretely this aims at the convergence of the corresponding perturbation expansion, which the TCL method is based on, i.e., the influence of higher orders beyond the leading, to which the expansion is typically truncated, and the influence of the inhomogeneity, which depends on the initial state. Both features are explicitly analyzed in the work at hand.

Eventually, we obtain a formalism which yields a collision term of a Boltzmann equation, that essentially avoids the previously mentioned shortcomings. I.e., the number of dynamical occupation numbers is finite and in principle directly controllable, the collision term is a priori linear and contains only finite rates. Or in other words, the resulting equations of motion are (numerically) manageable and therefore a good starting point for further investigations, e.g., for calculating transport coefficients.

Thus, in the final step of our main approach we utilize the obtained linear Boltzmann equation to compute diffusion coefficients via a pertinent method.

We especially present an important application of the provided scheme, namely we quantitatively determine the diffusion coefficient for an atomic wire. In particular, we analyze the dependence of the diffusion coefficient on certain model properties, especially on the width of the atomic wire.

Apart from this application, the established formalism for determining transport coefficients may in principle be applied to any system which can be expressed as a non-ideal quantum gas with pertinent scattering mechanisms (impurity-scattering, electron-phonon-scattering, electron-electron-scattering). This may potentially address a large amount of various condensed matter systems.

The work at hand is organized as follows. In the remainder of Sec. I we shortly introduce two common approaches in transport theory, namely the Kubo formula (Sec. I A) and the Boltzmann equation (Sec. I B). Sec. II serves as a guideline to the appended article components [1–5], i.e., it summarizes their main contents and shows their relation to the main approach. In Sec. II A we give a short overview to the TCL projection operator technique and investigate two problems which may become relevant in the context of this method, i.e., in Sec. II A 1 we discuss the convergence of the corresponding perturbation expansion and in Sec. II A 2 we analyze the influence of occurring inhomogeneity. In Sec. II B we present our main approach, i.e., we establish a formalism based on the TCL method that allows for a consistent mapping of quantum dynamics onto Boltzmann equations for non-ideal quantum gases. By means of that scheme we exemplary compute the diffusion coefficient for a 3-d Anderson model in Sec. II C. In Sec. II D we then present the main application, where we numerically determine the diffusion coefficient of an atomic wire and analyze its dependence on certain model properties, especially on the wire width. Finally, Sec. III closes with a short summary and conclusion.

A. Linear Response Theory: Kubo Formula

One important approach to transport in quantum systems is provided by the Kubo formula (KF) which arises in the context of linear response theory [9, 10]. In general, linear response theory analyzes the response of a system to an external perturbation. The response is supposed to scale linearly with the perturbation, i.e., the corresponding perturbation series is truncated to the linear order, that is, the perturbation has to be weak. Furthermore, the perturbation must appear as an additional term in

the Hamiltonian. An application of linear response theory to electrical conductance leads to the Kubo formula. Here a current is caused as response to an external electric field which manifests itself in a potential term additional to the unperturbed Hamiltonian. The respective response coefficient corresponds to the (frequency dependent) electrical conductivity and is given by the Kubo formula [9, 10]

$$L(\omega) = \frac{1}{V} \int_0^\infty \mathrm{d}t \; \mathrm{e}^{-\imath\omega t} \int_0^\beta \mathrm{d}\beta' \; \mathrm{Tr}\Big\{ \rho_0 \, \hat{j}(0) \, \hat{j}(t + \imath\beta') \Big\} \,, \quad (1)$$

where ω is the frequency of the external field; V refers to the volume of the system; β is the inverse temperature; and ρ_0 denotes the Gibbsian equilibrium state. The KF provides a relation between the conductivity and the current-current correlation function. However, the evaluation of the latter is generally difficult, since it requires the diagonalization of the system, which is often impossible. This also applies for the atomic wire which is investigated in the work at hand.

Moreover, for transport which exclusively arises from an internal density gradient of some quantity, e.g., heat conduction, the cause of the current cannot be incorporated as an additional energy term in the Hamiltonian. Hence, the above derivation of a Kubo formula from linear response theory may not be accomplished analogously. Therefore, the validity of a Kubo-type formula for density gradient driven transport is in principle questionable.

B. Boltzmann Equation

Originally the Boltzmann equation (BE) has been introduced in the context of classical mechanics (kinetic gas theory) [17, 18]. It describes the time evolution of some particle distribution function $\rho(\mathbf{r}, \mathbf{v}, t)$ in the classical phase space of configurations $\mathbf{r}$ and velocities $\mathbf{v}$. The classical BE is typically applied for dilute gases. Without external forces the BE reads

$$\frac{\partial \rho(\mathbf{r}, \mathbf{v}, t)}{\partial t} + \mathbf{v} \cdot \nabla_{\mathbf{r}} \, \rho(\mathbf{r}, \mathbf{v}, t) = \left. \frac{\partial \rho(\mathbf{r}, \mathbf{v}, t)}{\partial t} \right|_{\mathrm{coll}} , \quad (2)$$

with some drift term $\mathbf{v} \cdot \nabla_{\mathbf{r}} \, \rho(\mathbf{r}, \mathbf{v}, t)$ and some collision term on the r.h.s.. The latter describes the change of the probability distribution due to two-particle collisions. For the collision term one usually implements the so-called "Stosszahlansatz", which essentially means that colliding particles are not correlated before the collision. The collision generates correlation between the colliding particles, but it is assumed that there are many intermediate collisions with other particles until the same particles collide again, so that the correlations are effectively wiped out. The Stosszahlansatz is also known as the assumption of molecular chaos.

In general the collision term is non-linear. However, it may potentially be linearized for distributions $\rho(\mathbf{r}, \mathbf{v}, t)$ close to the equilibrium distribution.

Within the frame of quantum mechanics there are many suggestions which address the mapping of the dynamics of non-ideal quantum gases onto Boltzmann equations. Routinely these BE are of the form $\dot{n}_k + T_k^{\mathrm{drift}} = T_k^{\mathrm{col}}$ where $T^{\mathrm{drift}}, T^{\mathrm{col}}$ are the drift and the collision term respectively, the n's correspond to mean occupation numbers and k denotes the (quasi-) momenta. One important approach by Peierls [11] includes classical transition rates between two occupation number eigenstates, which are obtained by means of Fermi's Golden Rule, in the derivation of the collision term. The rates are weighted by the squared interaction matrix elements connecting those two eigenstates. This already implies some kind of random phase approximation which in some sense corresponds to the Stosszahlansatz for the classical BE. (For similar approaches see [19, 20].) There are also other approaches based on Green's function methods [12, 21, 22] and again others relying on full factorizability of occupation number operators [13, 23, 24]. For a more detailed overview see [4].

Generally, these approaches often feature some conceptual difficulties, i.e., they often yield rather formal expressions for the collision term involving, e.g., singular scattering rates and infinitely many dynamical variables. Moreover, the resulting collision terms are non-linear and thus have to be linearized for many practical purposes in the context of linear non-equilibrium physics, e.g., the calculation of transport coefficients.

II. PROJECTIVE APPROACH TO DIFFUSION COEFFICIENTS

This main part of this cumulative dissertation essentially serves as a guideline and overview to the appended article components [1–5]. It describes the interconnections between them, and shows in how far they are related to the main global approach. We also briefly summarize their main contents and results.

The main approach of the work at hand basically consists of two steps. We firstly establish a formalism, based on the so-called TCL projection operator technique, which allows for a consistent mapping of quantum dynamics onto a collision term of a Boltzmann equation. The latter is done by projecting onto certain occupation numbers. This derivation constitutes the primary part of the scheme presented in the work at hand and takes considerably more space than the afterwards following determination of a diffusion coefficient from the obtained collision term. Eventually, we use the established scheme mainly to calculate a diffusion coefficient for a (quasi-) 1-d atomic wire.

In the first step, and only there, we need to apply the TCL projection operator method. To this end a short introduction to this approach including its characteristic

resulting equations of motion is presented in the following Sec. II A.

A. TCL Projection Operator Method

The method which is used here to construct a linear(ized) collision term from the quantum dynamics is the time-convolutionless (TCL) projection operator method [14–16], which is shortly introduced in this paragraph. In the work at hand the TCL method is followed as detailed in [15]. This perturbative technique , as the well-known Nakajima-Zwanzig (NZ) projection operator method [25, 26], is generally applied in order to describe reduced dynamics of quantum systems with a Hamiltonian of the type $H = H_0 + \lambda V$ where λV has to be small in some sense. It produces autonomous equations of motion for the variables of interest ("relevant information"). Projection operator techniques are commonly used approaches in the context of open systems. However, their following application to transport investigations in closed quantum systems is a novel concept. Generally, the full dynamics of the quantum system are given by the Liouville-von Neumann equation,

$$\frac{\partial}{\partial t}\,\rho(t) = -\frac{\imath}{\hbar}\,[\,\lambda V(t), \rho(t)\,] = \mathcal{L}(t)\,\rho(t)\,. \tag{3}$$

Now and in the following all equations are denoted in the interaction picture. In order to apply this method one firstly has to construct a suitable projection (super) operator $\mathcal{P}$ which projects any density matrix $\rho(t)$ onto its relevant part. "Relevant part" here implies that $\mathcal{P}\rho(t)$, in spite of being significantly less complex than $\rho(t)$, should still contain all variables of interest. Note that these relevant variables for all following applications presented in the work at hand refer to time-dependent expectation values of pertinently defined operators, describing, e.g., occupation numbers. Furthermore, $\mathcal{P}$ has to satisfy the characteristic trait of a projection operator $\mathcal{P}^2\,\rho(t) = \mathcal{P}\,\rho(t)$. The TCL scheme yields a closed time-local differential equation for the dynamics of $\mathcal{P}\rho$,

$$\frac{\partial}{\partial t}\,\mathcal{P}\,\rho(t) = \mathcal{K}(t)\,\mathcal{P}\,\rho(t) + \mathcal{I}(t)\,(1-\mathcal{P})\,\rho(0)\;, \tag{4}$$

and consequently avoids the often troublesome time-convolution which appears, e.g., in the context of the Nakajima-Zwanzig technique. The TCL generator $\mathcal{K}(t)$ is given by a systematic perturbative expansion in orders of the interaction strength λ

$$\mathcal{K}(t) = \sum_{i=1}^{\infty} \lambda^i \mathcal{K}_i(t)\,, \tag{5}$$

which is in principle formally exact.

From Eq. (4) one may identify two major problems that can arise for the practical applicability of the TCL method. Especially, since the investigations in the work at hand are of novel nature, these difficulties deserve further consideration. The first problem is common to many perturbative methods and concerns the convergence of the expansion (5). One typically aims at a truncation to leading order of the perturbative expansion (5) for concrete applications, which is typically, and certainly for all models considered in the work at hand, the second order, since the odd cumulants of the expansion (5) vanish. Therefore, one has to determine $\mathcal{K}_2(t)$. In the literature [15] one finds

$$\mathcal{K}_2(t) = \int_0^t \mathrm{d}t_1\,\mathcal{P}\,\mathcal{L}(t)\,\mathcal{L}(t_1)\,\mathcal{P}\;. \tag{6}$$

However, a leading order approximation can only be expected to yield reliable results if the higher orders are negligible, compared to the leading, on the relevant dynamical time scales. This question of the convergence of the TCL expansion is especially addressed in [2].

The second main difficulty is the influence of the inhomogeneity $\mathcal{I}(t)\,(1-\mathcal{P})\,\rho(0)$ occurring in Eq. (4), which is typically neglected in order to obtain manageable equations of motion. This inhomogeneity depends on the initial state $\rho(0)$. Formally the inhomogeneity only vanishes for certain initial states, namely those featuring $\mathcal{P}\,\rho(0) = \rho(0)$. Nevertheless, there are indications that the influence of the inhomogeneity may also become negligible for other initial states. The validity of Eq. (4) without inhomogeneity for other initial states not obeying the above mentioned relation is particularly discussed in [3].

1. *Convergence of the TCL Expansion*

The legitimacy of a leading order approximation of the TCL method of course crucially depends on the influence of the neglected higher orders. Since the TCL expansion is exact, deviations from a leading order result must be incorporated in the higher orders. Detailed considerations on this point are presented in Ref. [2].

The problem of the convergence always arises whenever a perturbative method is applied in terms of some truncation, not only in the context of the TCL method (see also [1]). Both Refs. [1, 2] investigate the occurrence of statistical dynamics of certain time dependent expectation values in some abstract quantum systems with similar results. Ref. [1] applies a perturbative method based on the so-called Hilbert space average method (HAM), which relies on a pertinent truncation of the Dyson series [27]. In that context the validity of the truncation is analyzed by (numerically) evaluating the next higher order of the Dyson series, which is unfortunately numerically very extensive.

Now, Ref. [2] analyzes the influence of higher orders of the TCL expansion in the context of a leading order TCL approach to the dynamics of certain expectation values $a(t) = \mathrm{Tr}\{\rho(t)A\}$ of some observables A. Numerical calculations obtained from an exact diagonalization of the

Schrödinger equation show that the second order TCL prediction becomes wrong for certain "structured" interactions, even if a clear separation of time scales, i.e., a Markov approximation, exists. The failure of the second order TCL prediction may occur at very small times of the order of the correlation time, but also at later times of the order of the relaxation time. The latter may refer to localization effects which appear, e.g., in the context of the 3-d Anderson in the chaotic regime. These results clearly indicate that an analysis of higher orders is necessary.

To repeat, since the TCL expansion as a whole is exact, the deviations from the correct result have to be incorporated in the higher orders. The strategy to check the convergence of the TCL expansion, which is particularly pursued here in [2], is to find an estimation of the next higher, i.e., the fourth order in comparison to the second. The fourth order turns out to be already a quite complicated object. In the literature [15] $\mathcal{K}_4(t)$ is given as

$$\begin{aligned}\mathcal{K}_4(t) \;=\; & \int_0^t \mathrm{d}t_1 \int_0^{t_1} \mathrm{d}t_2 \int_0^{t_2} \mathrm{d}t_3 \\ & \mathcal{P}\,\mathcal{L}(t)\,\mathcal{L}(t_1)\,\mathcal{L}(t_2)\,\mathcal{L}(t_3)\,\mathcal{P} \\ & - \;\mathcal{P}\,\mathcal{L}(t)\,\mathcal{L}(t_1)\,\mathcal{P}\,\mathcal{L}(t_2)\,\mathcal{L}(t_3)\,\mathcal{P} \\ & - \;\mathcal{P}\,\mathcal{L}(t)\,\mathcal{L}(t_2)\,\mathcal{P}\,\mathcal{L}(t_1)\,\mathcal{L}(t_3)\,\mathcal{P} \\ & - \;\mathcal{P}\,\mathcal{L}(t)\,\mathcal{L}(t_3)\,\mathcal{P}\,\mathcal{L}(t_1)\,\mathcal{L}(t_2)\,\mathcal{P}\;. \end{aligned} \tag{7}$$

An exact evaluation of the fourth order, which of course would be desirable, turns out to be almost impossible, analytically and numerically, already for the relatively abstract and simple models considered in Refs. [1, 2]. Instead there are two feasible estimations of $\mathcal{K}_4(t)$ established on the basis of pertinent approximations.

One of them, which refers to the so-called Van Hove-structure, estimates the fourth order compared to the second for very small times of the order of the correlation time. However, numerics indicate that for certain interactions the fourth order may become non-negligible at larger times, even if it is negligible at small times.

For the detection of such a behavior there is another estimation of $\mathcal{K}_4(t)$ suggested in Ref. [2], which again incorporates the time dependence of the fourth order. These two estimations are able to successfully explain the deviations from the second order prediction indicated by the numerics concerning the simple models analyzed in [2].

However, both of them rely on more or less rough approximations, so that neither of them can be viewed as a sufficient criterion for a valid leading order prediction. E.g., the Van Hove-structure rather represents a criterion for exclusion in the sense that a leading order result cannot be reliable if the interaction does not have Van Hove-structure.

Moreover, although these estimations may be much easier obtained than the exact fourth order, it becomes difficult to evaluate them for more realistic systems, like those we address with our main approach (Sec. II B). This, in particular, also refers to the atomic wire, which represents the main application in the work at hand. Typically the corresponding Hilbert spaces are very high dimensional and the occurring interactions are very complicated in these cases. Therefore, we do not aim at a direct application of these criteria in our main approach.

However, despite all insufficiencies the investigations in [2] provide a systematic analysis of higher orders of the TCL expansion and are able to demonstrate that there are systems where a leading order truncation is not good enough. It is simultaneously shown that the corresponding deviations are caused by the next higher, i.e., the fourth order.

At the end of this section we give some further general comments concerning the validity of a leading order truncation of the TCL method.

The criteria established in [2] can also be only of necessary nature, since they only take the fourth, i.e., the next higher order into account and do not provide any information about the influence of higher orders. In principle, higher orders beyond the fourth may dominate the leading order as well, when the fourth order does not, though that will probably occur only in a few cases.

The influence of higher orders of the TCL expansion may decrease if there are additional dynamical variables incorporated in the projection. By this means one would obtain a more detailed picture of dynamics, but at the same time the second order result becomes more complex. In our main approach (Sec. II B) this would correspond to a finer graining in momentum space, the latter being introduced below.

Although the analyses in [2] show examples where the second order truncation of TCL gives wrong results even if a clear separation of time scales is fulfilled, this Markov approximation is nevertheless commonly a good indicator for the validity of a second order approximation, if no analyzations of higher orders are available. That is, a "reasonable" leading order result may indicate the legitimacy of leading order truncation.

In our main approach we do not explicitly evaluate the estimations of the fourth order explained in this Sec., we rather perform a leading order TCL truncation without further analyzations of higher orders. We briefly comment on the justification of this proceeding at the beginning of Sec. II B.

2. *Influence of the Inhomogeneity*

The inhomogeneity appearing in the equation of motion for the relevant part of the density matrix (Eq. (4)) depends on the initial state $\rho(0)$. It only vanishes exactly for certain specific initial states, namely those featuring $\mathcal{P}\rho(0) = \rho(0)$. However, in Ref. [3] there are investigations concerning the dynamical typicality of quantum mechanical expectation values, which show that applying Eq. (4) without inhomogeneity also yields reasonable results for the vast majority of possible initial states if

the Hilbert space of the regarded system is high dimensional, i.e., that the inhomogeneity becomes negligible for the vast majority of possible initial states.

The approach followed in [3] is based on the Hilbert space average method (HAM) [28, 29]. We obtain the following very general main result which applies when the dimension of the Hilbert space n is large.

It is shown that, for large enough systems the vast majority of all pure states featuring a common expectation value of the observable A at a given time will yield very similar expectation values of the same observable at any later time. As a consequence dynamics of expectation values of individual initial states are then typically well described by the dynamics of the ensemble average. That is, there is a typical time evolution for the expectation values. Particularly, this typicality is independent of the concrete form of the dynamics, which may be a standard exponential decay into equilibrium or something completely different.

This result has important consequences on the applicability of projection operator theories in general and particularly for the TCL method, too. Note that the above mentioned ensemble average may be expressed as a mixed state. Now, if the projection operator is constructed to project onto an expectation value $a(t)$ as dynamical variable, the density matrix of the ensemble average is at least approximately of the form of the initial state, which leads to a vanishing inhomogeneity in Eq. (4), i.e., $\mathcal{P}\rho(0) = \rho(0)$. Thus, a TCL calculation based on Eq. (4) without inhomogeneity describes the dynamics of $a(t)$ for the ensemble average as initial state. The dynamical curves of the vast majority of possible initial states are very close to the dynamical curve of the ensemble average at any time t. Hence Eq. (4) yields also a reasonable description for the most initial states and consequently, the inhomogeneity has to be negligible not only for specific initial states, but for the most initial states at least for large enough Hilbert spaces. There of course are states for which the inhomogeneity is not negligible, but their statistical weight is low, i.e., they are few compared to the number of states for which the inhomogeneity is negligible. This result of course provides an immense extension for the validity of corresponding TCL calculations without inhomogeneity.

Note that the typicality arguments presented here are valid for almost any quantum system as long as the corresponding Hilbert space is large enough, which is surely the case for more realistic systems, and particularly for those addressed in our main approach in Sec. II B. The quality of the arguments even improves with growing dimension.

B. Derivation of Master Equations for Coarse Grained Occupation Numbers in Non-Ideal Quantum Gases

After having now extensively discussed the two main problems concerning the applicability of the TCL projection operator method, that is, the convergence of the TCL expansion, i.e., the influence of higher orders beyond the leading, and the relevance of the inhomogeneity, the TCL method is exclusively used in leading order approximation and with neglected inhomogeneity in the following. Proceeding this way seems reasonable, because there is a similar approach concerning the determination of lifetimes of electrons in metals [30], which yields results that are in good accordance with pertinent experiments. That is, $\mathcal{K}_2(t)$ has to be evaluated.

In this Sec. and Ref. [4] we introduce our main approach based on the TCL projection operator technique which addresses the mapping of quantum dynamics onto master equations for some coarse grained occupation numbers. The corresponding rate matrix may be interpreted as a linear(ized) collision term of a Boltzmann equation. This collision term may afterwards (Secs. (II C,II D)) be used to determine a diffusion coefficient. We especially apply this scheme to find a diffusion coefficient for an atomic wire. But there are also many other thinkable applications to various kinds of condensed matter systems.

The systems we discuss here may in general be all sorts of quantum gases, which are routinely used to describe condensed matter systems,

$$H = \underbrace{\sum_{\mathbf{k}} \varepsilon_{\mathbf{k}} a_{\mathbf{k}}^{\dagger} a_{\mathbf{k}}}_{H_0} + V \tag{8}$$

$a_{\mathbf{k}}^{\dagger}, a_{\mathbf{k}}$ are electronic creation/annihilation operators in some momentum eigenmodes and $\varepsilon_{\mathbf{k}}$ denotes the corresponding dispersion relation. The latter depends on the underlying model which is assumed to describe the non-interacting electrons. V refers to different pertinent interaction types, i.e., electron-impurity-scattering, electron-phonon-interaction and electron-electron-interaction. All of them are treated as small perturbations (in the sense of the TCL method).

A crucial feature of the approach is an adequate coarse graining in momentum space defined by partitioning the complete momentum space into grains labelled by a Greek index κ. The remaining variables $d^{\kappa}(t)$ are essentially the joined occupation numbers of the grains, which can be written as expectation values of suitable operators, so that all considerations from the previous paragraphs apply here. The coarse graining is incorporated in the projection and is eventually responsible for the finite rates in the collision term.

The concrete form of the graining has a decisive influence on the form of the resulting rate matrix. A finer graining, i.e., a higher number of retained dynamical vari-

ables, will produce a more detailed picture of the dynamics, but will also give rise to a higher dimensional rate matrix. Moreover, the concrete choice of the graining may have a crucial influence on the complexity of the resulting rate matrix, which we demonstrate by a simple example in the following Sec. II C.

Performing the TCL formalism in leading order approximation finally yields a master equation for the dynamics of the joined occupation numbers $d^\kappa(t)$

$$\dot{d^\eta}(t) = \sum_{\kappa\neq\eta} R_{\eta\kappa}(t) d^\kappa(t) - \sum_{\kappa\neq\eta} R_{\kappa\eta}(t) d^\eta(t) \ . \qquad (9)$$

This equation yields a linear(ized) collision term, i.e., a rate matrix of finite dimension with finite, non-singular rates $R_{\eta\kappa}$. That is, we obtain numerically manageable equations of motion which are adequate for, e.g., the computation of a diffusion coefficient. The master equation property, i.e.,

$$R_{\eta\eta}(t) = -\sum_{\kappa\neq\eta} R_{\kappa\eta}(t) \qquad (10)$$

stems from the conservation of the total particle number.

The concrete form of the rates $R_{\eta\kappa}(t)$ of course depends on the interaction mechanism V and may be found in Ref. [4] respectively. The interpretability of the resulting rate matrix as a collision term of a Boltzmann equation is supported by the fact that individual terms appearing in the expressions for the rates $R_{\eta\kappa}(t)$ may be understood as certain collision processes. Here we demonstrate this point for the case of the electron-electron-interaction. There are four terms occurring in the corresponding rates which may be viewed as contributing to a, say, "scattering rate" from a state $\mathbf{i}$ in domain κ into a state $\mathbf{k}$ in domain η. This rate has to be understood in the sense that it describes how an occupation of state $\mathbf{i}$ over equilibrium changes the occupation of state $\mathbf{k}$. Since the electron-electron-interaction describes two-particle collisions under conservation of the complete electronic momentum, there are four thinkable collision processes in which the states $\mathbf{i}$ and $\mathbf{k}$ participate. Each of them is represented by one of the four terms occurring in the rates. These are

$$\begin{aligned}
&\text{I:} && f_{\mathbf{l}}(1-f_{\mathbf{i-k+l}})(1-f_{\mathbf{k}}) \\
&\text{II:} && f_{\mathbf{k}} f_{\mathbf{i-k+l}}(1-f_{\mathbf{l}}) \\
&\text{III:} && -f_{\mathbf{k}}(1-f_{\mathbf{i+k-l}})(1-f_{\mathbf{l}}) \\
&\text{IV:} && -f_{\mathbf{l}} f_{\mathbf{i+k-l}}(1-f_{\mathbf{j}}) \ . \qquad (11)
\end{aligned}$$

The corresponding collision processes are illustrated in Figs. 1-4.

E.g., process I leads to an increase of the occupation of state $\mathbf{k}$, when $\mathbf{i}$ is occupied over equilibrium, i.e., the corresponding rate term is positive. This process may occur, when state $\mathbf{l}$ is occupied and the states $\mathbf{i}-\mathbf{k}+\mathbf{l}$ and $\mathbf{k}$ are unoccupied. Process II is the reverse process to I and therefore in principle leads to a decrease of the occupation of state $\mathbf{k}$. The corresponding rate term is nevertheless positive, because an occupation of state $\mathbf{i}$ over equilibrium in some sense blocks this process and thus "lessens the decrease" of the occupation of state $\mathbf{k}$. The term belonging to process III is negative, since this process reduces the occupation of state $\mathbf{k}$, and IV is the reverse process to III, analogously.

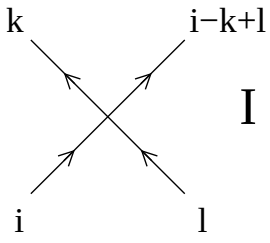

FIG. 1: Sketch of scattering process I

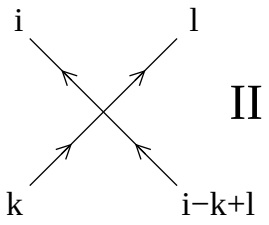

FIG. 2: Sketch of scattering process II

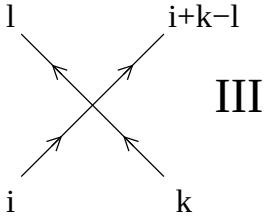

FIG. 3: Sketch of scattering process III

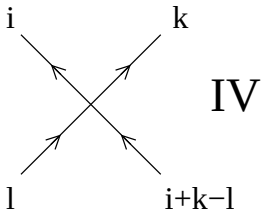

FIG. 4: Sketch of scattering process IV

C. Diffusion Coefficient of a 3-d Anderson Model

We particularly demonstrate the influence of the choice of the graining by a simple application of the previously introduced method. This application addresses the calculation of the diffusion coefficient of a 3-d Anderson model with weak uncorrelated on-site disorder, see Ref. [4]. We assume that this model is suitably described by a Hamiltonian of quantum gas-type with electron-impurity scattering. The Hamiltonian reads

$$H = \underbrace{\sum_{\mathbf{n}} \varepsilon_{\mathbf{n}} a^\dagger_{\mathbf{n}} a_{\mathbf{n}}}_{H_{0,\mathrm{el}}} + \underbrace{\sum_{\mathbf{k},\mathbf{q}} \frac{W(\mathbf{q})}{\sqrt{\Omega}} a^\dagger_{\mathbf{k+q}} a_{\mathbf{k}}}_{V} \ . \qquad (12)$$

Here $W(\mathbf{q})$ simply denotes the corresponding spatial Fourier component of the random impurity potential and Ω corresponds to the total number of discrete (quasi-)momenta, i.e., Ω scales with the volume of the crystal.

In this case the resulting expression for the rates reads

$$R_{\eta\kappa}(t) = \int_0^t \mathrm{d}\tau \frac{2}{\hbar^2 N_\kappa} \sum_{\substack{\mathbf{i}\in\kappa,\\ \mathbf{k}\in\eta}} \frac{|W(\mathbf{k}-\mathbf{i})|^2}{\Omega} \cos[\frac{1}{\hbar}(\varepsilon_{\mathbf{i}} - \varepsilon_{\mathbf{k}})\tau] \ , \qquad (13)$$

where N_κ denotes the number of individual states within the grain κ.

In order to concretely evaluate the rates (15) we implement a specific coarse graining, which is in detail explained in [4]. Now for this graining and due to the disorder being uncorrelated one obtains a very simple rate matrix, that is, all non-diagonal elements of the rate matrix are equal, the rate matrix is symmetric and therefore yields symmetric detailed balance. As a consequence, for this graining the so-called relaxation time approximation [31] is exactly fulfilled. This simple structure of course strongly facilitates the computation of a diffusion coefficient, as shown in [4].

D. Main Application: Derivation of Diffusion Coefficients of an Atomic Wire

In this Sec. we present the main application of the projective approach introduced in Sec. II B and Ref. [4]. This application is in more detail investigated in Ref. [5]. We intend to find a description of electronic diffusion in (quasi-) 1-d atomic wires formed on some crystal surface or embedded within some crystal bulk. The diffusion is induced by coupling to "external" surface or bulk phonons. We accordingly compute a linear(ized) collision term by exploiting the scheme provided in Sec. II B and determine the corresponding diffusion coefficient by using a pertinent formula (see [5]). We especially analyze the dependence of the diffusion coefficient on the width of the atomic wire and on some below defined cross hopping perpendicular to the wire.

Generally, low dimensional systems are often candidates for non-regular transport behavior and it is not a priori clear how diffusive transport is induced in those systems. Diffusive transport implies that a total electronic current has to decay with time due to some scattering processes. This may arise, e.g., by electron-electron-scattering, but only due to Umklapp processes (, e.g., [31]), since normal scattering processes leave the total electronic momentum unchanged. It is commonly believed that electronic diffusion mainly arises due to electron-phonon-scattering, at least for high enough temperatures, so we concentrate here on this scattering mechanism in our application.

We describe the atomic wire on the basis of a (quasi-) 1-d tight-binding-model of length L, which consists of B parallel rows. Besides the hopping along the wire, given by the hopping strength $T_\parallel$, we allow hopping between neighboring rows perpendicular to the wire with the lateral hopping strength $T_\perp$.

The Hamiltonian of this model corresponds to a quantum gas model with electron-phonon-scattering. That is, the method introduced in Sec. II B and Ref. [4] especially applies to this case. It reads

$$H = \underbrace{\sum_{\mathbf{j}}\sum_{r=1}^{B}\varepsilon_{\mathbf{j},r}a^\dagger_{\mathbf{j},r}a_{\mathbf{j},r}}_{H_{0,\mathrm{el}}} + \underbrace{\sum_{\mathbf{i}}\omega_{\mathbf{i}}b^\dagger_{\mathbf{i}}b_{\mathbf{i}}}_{H_{0,\mathrm{ph}}} + \underbrace{(\sum_{\mathbf{k},\mathbf{q}}\sum_{r,s=1}^{B}\frac{W_{rs}(\mathbf{q})}{\sqrt{\Omega}}a^\dagger_{\mathbf{k}+\mathbf{q},r}a_{\mathbf{k},s}b_{\mathbf{q}}+h.c.)}_{V}, \quad (14)$$

with $\Omega = BL$. The $a^\dagger_{\mathbf{j},r}/a_{\mathbf{j},r}$ are electronic creation/annihilation operators in some pertinent momentum modes and $\varepsilon_{\mathbf{j},r}$ is the corresponding electronic dispersion relation. $b^\dagger_{\mathbf{i}}/b_{\mathbf{i}}$ are (bosonic) phononic creation/annihilation operators in some phonon eigenmodes and $\omega_{\mathbf{i}}$ is the phononic dispersion relation. V denotes the electron-phonon-coupling with some coupling elements $W_{rs}(\mathbf{q})$.

In this case the resulting rates are given by

$$R_{\eta\kappa}(t) = \int_0^t \mathrm{d}\tau \frac{2}{\hbar^2 N_\kappa}\sum_{\substack{\mathbf{i},s\in\kappa,\\ \mathbf{k},r\in\eta}}\frac{|W_{rs}(\mathbf{k}-\mathbf{i})|^2}{\Omega}(1+g_{\mathbf{k}-\mathbf{i}}+g_{\mathbf{i}-\mathbf{k}}) \cdot\cos[\frac{1}{\hbar}(\varepsilon_{\mathbf{i},s}-\varepsilon_{\mathbf{k},r})\tau], \quad (15)$$

where $g_{\mathbf{q}}$ is the thermal equilibrium distribution on the phonon mode $\mathbf{q}$, that is, the Bose distribution.

To determine the diffusion coefficient, we use a formula, which is essentially similar to a formula suggested in [32] and references therein. By that means we are able to numerically obtain quantitative values for diffusion coefficients, which are essentially converged over the grain size, i.e., the corresponding values do not change much, when the graining is made finer and finer. The results are displayed in Figs. 5,6.

We observe a significant dependency of the diffusion coefficient on the width of the wire. For a sufficiently large lateral coupling the resulting "curve" of diffusion coefficients over the wire width shows large jumps on top of that. This also implies that the diffusion becomes nearly 0 for certain wire widths. These features may clearly be classified as effects of the finite wire width, which lies on the nanoscale. They evidently demonstrate the quantum character of the model considered here, because a diffusion coefficient of a macroscopic system, e.g., a macroscopic wire cannot be dependent on the wire width.

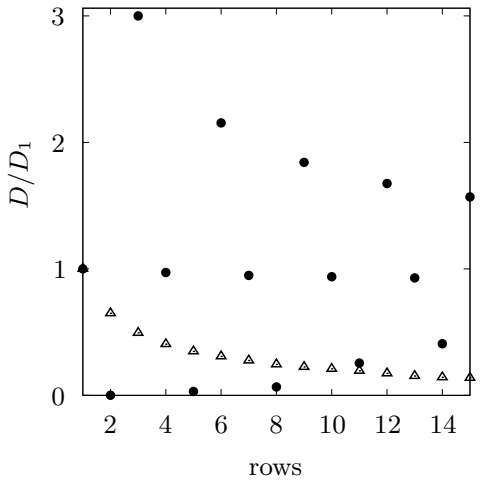

FIG. 5: Plot of the diffusion coefficient D against the number of rows, i.e., the width for $T_\perp = 2T_\parallel$ (black dots) and $T_\perp = T_\parallel$ (white triangles). The plot is normalized to the D obtained for 1 row, denoted by D_1. Other parameters: $E_B = 3$eV, $T_\parallel = 0.75$eV, $T = 300$K, half filling.

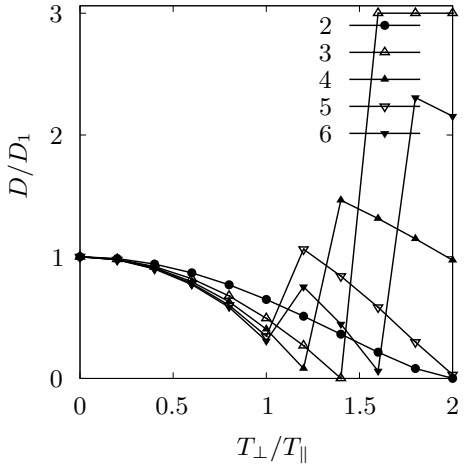

FIG. 6: Plot of the diffusion coefficient D against the lateral coupling $T_\perp$ for different widths, i.e., different numbers of rows, according to the legend. The plot is normalized to the D obtained for 1 row, denoted by D_1. Other parameters: $E_B = 3$eV, $T_\parallel = 0.75$eV, $T = 300$K, half filling.

III. SUMMARY AND OUTLOOK

The work at hand provides a novel access to the investigation of transport coefficients in condensed matter systems, which is based on the TCL projection operator method. As preliminary analysis we explicitly discussed the convergence of the perturbative TCL expansion and demonstrated that deviations from a leading order truncation may occur due to the influence of the next higher order for certain abstract quantum systems. Furthermore, it is shown that the inhomogeneity occurring in connection with the TCL method typically becomes irrelevant for the vast majority of possible initial states in the case of high dimensional Hilbert spaces.

As main approach, we used a leading order TCL truncation to obtain a formalism, which allows for a consistent mapping of quantum dynamics onto a Boltzmann equation. A projection onto certain sets of coarse grained occupation numbers in momentum space leads to a linear(ized) collision term which results as a rate matrix of finite dimension that contains only non-singular finite rates. These features render the obtained Boltzmann equation numerically manageable and adequate for further applications. In the work at hand we especially exploited that Boltzmann equation to compute diffusion coefficients.

An exemplary application to a 3-d Anderson model demonstrated the crucial influence of the coarse graining on the form of the resulting collision term. In this case a specific graining led to a very simple rate matrix which strictly obeys the relaxation time approximation. Eventually, we applied the provided scheme to determine the diffusion coefficient of an atomic wire numerically. In particular, we showed that there is a significant dependency of the diffusion coefficient on the width of the atomic wire, if the lateral coupling is large enough. This may be clearly classified as a finite size effect.

To obtain more realistic values for the diffusion coefficient of the atomic wire, which could possibly be compared with experiments, one would probably concretize some model properties, e.g., one could choose more realistic electron-phonon coupling elements. Furthermore, we considered the electrons themselves to be non-interacting with each other. It is not definitely clear if this assumption is completely legitimate, since the electron-electron-interaction may have a substantial influence, especially for 1-d systems. The calculated diffusion coefficients may be converted into conductivities via a pertinent generalized Einstein relation [33]. The atomic wire analyzed in the work at hand is of course an important application, but the established formalism is by no means restricted to it. There are many systems in the context of condensed matter physics which may be expressed as a non-ideal quantum gas and therefore be addressed by this approach. One may think of, e.g., electronic diffusion in bulk metals, primarily due to phonon-coupling. Or one may think of regular heat conduction in bulk metals arising from Umklapp processes occurring in phonon-phonon scattering processes.

Acknowledgments

At this point I would like to thank several persons who supported me in the last years during the time of my PhD thesis.

First of all, I sincerely thank my supervisor Prof. Dr. J. Gemmer for his immense support, his helpful advice and his constant interest in the proceeding of this work during the last years. He was also the supervisor of my diploma thesis and interested me in the research

field of transport and relaxation in quantum mechanics. I thank him for giving me the possibility to write my PhD thesis in his group and for the pleasant working atmosphere.

Furthermore, I would like thank present and former colleagues from the Physics Department at the University of Osnabrück, Dr. R. Steinigeweg for his helpful advice and fruitful discussions and especially my room colleague Dr. M. Kadiroğlu for the pleasant atmosphere and for many professional and private conversations; further I thank T. Pobandt, J. Ummethum, K. Wedderhoff, M. Ogiewa and H. Wichterich; H. Niemeyer; Dr. R. Schnalle and Dr. M. Brüger; P. Hage; C. Abè, L. Urban, V. Zielke. I also thank Dr. P. Vidal (University of Stuttgart) for fruitful collaboration; Dr. M. Michel (University of Surrey). Moreover, I thank Prof. Dr. M. Rohlfing for writing the second report on this dissertation and Prof. Dr. K. Betzler and Dr. J. Klare for being members of the examination committee.

Financial support by the DFG through the Graduate Colleague 695 is gratefully acknowledged, too.

Finally, I am also grateful to my family who supported me very much during the time of my PhD thesis.

---

[1] C. Bartsch and P. Vidal, Eur. Phys. J. Special Topics **151**, 29 (2007).
[2] C. Bartsch, R. Steinigeweg, and J. Gemmer, Phys. Rev. E **77**, 011119 (2008).
[3] C. Bartsch and J. Gemmer, Phys. Rev. Lett. **102**, 110403 (2009).
[4] C. Bartsch, R. Steinigeweg, and J. Gemmer (2010), invited for resubmission to Phys. Rev. E.
[5] C. Bartsch and J. Gemmer (2010), to be submitted to Europhys. Lett..
[6] R. Steinigeweg, Ph.D. Thesis (University of Osnabrück) (2008).
[7] D. Meschede, *Gerthsen Physik* (Springer, 2006), Springer Lehrbuch, 23rd ed.
[8] A. Kühnle, T.R. Linderoth, and F. Besenbacher, J. A. C. S. **125**, 14680 (2003).
[9] R. Kubo, M. Toda, and N. Hashitsume, *Statistical Physics II. Nonequilibrium Statistical Mechanics* (Springer, Berlin, 1991).
[10] G. D. Mahan, *Many Particle Physics, Physics of Solids and Liquids* (Springer, 2000), 3rd ed.
[11] R. E. Peierls, *Quantum Theory of Solids* (Clarendon, Oxford, 2001).
[12] L. P. Kadanoff and G. Baym, *Quantum Statistical Mechanics* (Benjamin, New York, 1962).
[13] L. Erdös, M. Salmhofer, and H.-T. Yau, arXiv:math-ph/0302034 (2003).
[14] H. P. Breuer, J. Gemmer, and M. Michel, Phys. Rev. E **73**, 016139 (2006).
[15] H. P. Breuer and F. Petruccione, *Theory of Open Quantum Systems* (Oxford University Press, Oxford, 2007).
[16] S. Chaturvedi and F. Shibata, Z. Phys. B **35**, 297 (1979).
[17] L. Boltzmann, *Vorlesungen über Gastheorie* (Akademische Druck- und Verlagsanstalt, 1981).
[18] C. Cercignani, *The Boltzmann Equation and its Applications* (Springer, New York, 1988).
[19] S. Lepri, R. Livi, and A. Politi, Phys. Rep. **377**, 1 (2003).
[20] J. Jäckle, *Einführung in die Transporttheorie* (Vieweg, Braunschweig, 1978).
[21] J. Rammer and H. Smith, Rev. Mod. Phys. **58**, 323 (1968).
[22] D. N. Zubarev, V. Morozov, and G. Ropke, *Statistical Mechanics of Nonequilibrium Processes: Basic Concepts, Kinetic Theory* (John Wiley and Sons, 1996).
[23] H. Haug, *Statistische Physik: Gleichgewichtstheorie und Kinetik* (Springer, Berlin Heidelberg, 2006).
[24] L. A. Banyai, *Lectures on Non-Equilibrium Theory of Condensed Matter* (World Scientific, 2006).
[25] S. Nakajima, Progr. Theor. Phys. **20**, 948 (1958).
[26] R. Zwanzig, J. Chem. Phys. **33**, 1338 (1960).
[27] W. Nolting, *Grundkurs Theoretische Physik 5/2: Quantenmechanik-Methoden und Anwendungen* (Springer, Berlin Heidelberg, 2006).
[28] J. Gemmer, M. Michel, and G. Mahler, *Quantum Thermodynamics* (Springer, Berlin, 2004).
[29] J. Gemmer and G. Mahler, Eur. Phys. J. B **31**, 249 (2003).
[30] M. Kadiroğlu and J. Gemmer, Phys. Rev. B **79**, 134301 (2009).
[31] C. Kittel, *Introduction to Solid State Physics* (John Wiley and Sons, 2004).
[32] M. Kadiroğlu and J. Gemmer, Phys. Rev. B **76**, 024306 (2007).
[33] R. Steinigeweg, H. Wichterich, and J. Gemmer, Europhys. Lett. **88**, 10004 (2009).

EPJ manuscript No.
(will be inserted by the editor)

Statistical Relaxation in Closed Quantum Systems and the Van Hove-Limit

Christian Bartsch[1,a] and Pedro Vidal[2,b]

[1] Universtität Osnabrück, Fachbereich Physik, Barbarastraße 7, D-49069 Osnabrück
[2] Universität Stuttgart, I Institut für Theoretische Physik, Pfaffenwaldring 57 // IV 70550 Stuttgart

Abstract. We analyze the dynamics of occupation probabilities for a certain type of design models by the use of two different methods. On the one hand we present some numerical calculations for two concrete interactions which point out that the occurrence of statistical dynamics depends on the interaction structure. Furthermore we show an analytical derivation for an infinite system that yields statistical behaviour for the average over the whole ensemble of interactions in the Van Hove-limit.

Original publication Eur. Phys. J. Special Topics **151**, 29 (2007)
available at http://www.epjst-journal.org/

1 Introduction

The emergence of statistical behaviour from microscopic dynamics is of special interest for two reasons. Its existence is evident from countless experiments, nevertheless its explanation seems subtle. And if statistical dynamics are established, their description is much simpler than the description of microscopic dynamics. From first principles the dynamics of quantum systems are controlled by the Schrödinger equation. Nevertheless, it has been observed that statistical relaxation may appear in such systems for certain quantities under certain conditions. The dynamics of the quantities P_n are called statistical if they are given by a master equation of the form

$$\frac{\partial}{\partial t}P_n = \sum_m R(m \to n)P_m - \sum_m R(n \to m)P_n \ . \tag{1}$$

This is a set of coupled rate equations whose solutions decay exponentially in time.

In this contribution the dynamics for a certain type of modular design model are approached from two different sides. On the one hand, we show numerical calculations of the time evolution of occupation probabilities for a finite size version of the model with two concrete types of interactions. Furthermore we will present an analytical derivation that analyzes the dynamics of these variables for an average over all possible interactions in the Van Hove-limit and in the limit of an infinitely large system size, in the sense that the number of energy levels in the bands of the modules N goes to ∞, whereas the number of modules M is always 2, i.e., M is still finite.

The numerics are consistent with the analytical results for an interaction which is kept very general and represents the majority of all interactions. Nevertheless, there can be completely exceptional interactions that yield substantially different dynamics.

[a] e-mail: cbartsch@uos.de
[b] e-mail: pedro@itp1.uni-stuttgart.de

2 Numerical calculations

2.1 Design model

The model we investigate for the occurrence of statistical dynamics is a simple design model depicted in Fig. 1 (see also [1–4]).

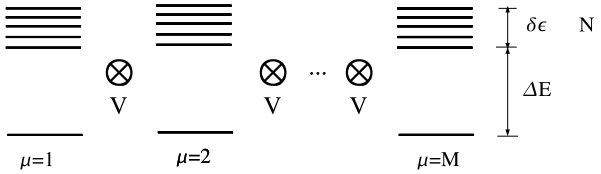

Fig. 1. Sketch of the design model

It consists of M one-dimensionally arranged identical modules that are coupled to the two neighbouring modules via the interaction V. Each subunit consists of a single ground state and an energy band. These are separated by the band gap ΔE. The model can be characterized by some rough system parameters; N is the number of levels in each band, $\delta\epsilon$ denotes the band width ($\delta\epsilon \ll \Delta E$) and λ gives the average interaction strength. The Hamiltonian can be split into a local part H_0 and an interaction V

$$H = H_0 + \lambda V \ . \tag{2}$$

The interaction is chosen to be weak such that one can assume local energy conservation and restrict to the subspace of the states where one system is in the excited state and all other systems are in the ground state. In this contribution only chains with two modules ($M = 2$) are regarded. V shall have an off-diagonal block form in the eigenbasis representation of H_0 in the relevant subspace, thus the Hamiltonian is given by

$$H = \left(\begin{array}{cc|cc} \ddots & & 0 & \\ & \Delta E + \frac{i}{N-1}\delta\epsilon & & V \\ 0 & & \ddots & \\ \hline & & \ddots & 0 \\ & V^\dagger & & \Delta E + \frac{j}{N-1}\delta\epsilon \\ & & 0 & \ddots \end{array}\right) \ . \tag{3}$$

The relevant space is divided into two subspaces each containing the states where the μ-th subsystem is in the excited state ($\mu = 1, 2$). V is normalized by

$$\frac{\mathrm{Tr}\{V^2\}}{2N^2} = 1 \ . \tag{4}$$

One can now define the occupation probability in the μ-th subsystem P_μ. According to the predictions of the Hilbert Space Average Method (HAM) in second order (see contribution

Breuer/Gemmer) the time evolution of the P_μ is controlled by coupled rate equations which means that the dynamics are statistical

$$\frac{dP_1}{dt} = RP_2 - RP_1 \ , \qquad \frac{dP_2}{dt} = RP_1 - RP_2 \ , \tag{5}$$

$$\text{with} \qquad R = 2\pi\lambda g \qquad \text{and} \qquad g = \frac{N}{\delta\epsilon} \ . \tag{6}$$

The rate is completely determined by the system parameters and is the same rate that appears in the context of Fermi's Golden Rule. In fact, HAM uses some kind of stepwise iteration of Fermi's Golden Rule. One also obtains some necessary conditions for the system parameters,

$$K_1 = \lambda^2 \frac{N}{\delta\epsilon^2} \ll 1 \ , \tag{7}$$

$$K_2 = 2\lambda \frac{N}{\delta\epsilon} \geq 1 \ . \tag{8}$$

A more detailed derivation can be found in [1–4].

In particular, these results do not depend on the concrete realization of V. So, in principle, they should be valid for any possible interaction structure.

2.2 Numerical calculations for two concrete interactions

In this paragraph we are going to compare the dynamics of the P_μ obtained from the rate equations (5) with the numerical solution of the Schrödinger equation for two specific interactions. The system parameters are adjusted in a way that the criteria (7) and (8) are well fulfilled.

For the first interaction the matrix elements of V in the eigenbasis representation of H_0 are chosen as random Gaussian distributed complex numbers. For the second interaction all matrix elements of V are set to be equal, say, $V_{ij} = 1$. The random interaction possesses no structure at all, whereas the opposite holds true for the constant interaction.

Figure 2 and Fig. 3 show the time evolution of $P_1(t)$ for both interactions. The initial state is selected to have $P_1(0) = 1$.

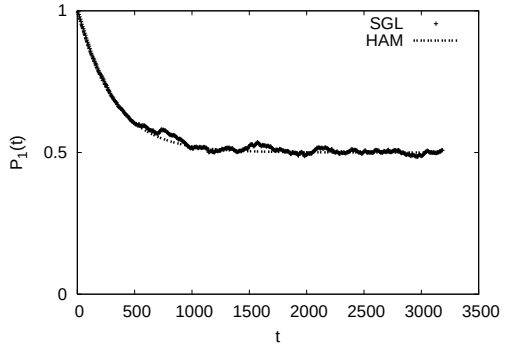

Fig. 2. Dynamics of $P_1(t)$ for a completely random interaction, parameters: $N = 500$, $\delta\epsilon = 0.5$, $\lambda = 0.0005$.

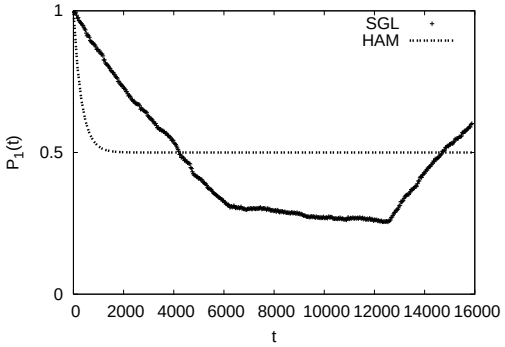

Fig. 3. Dynamics of $P_1(t)$ for a constant interaction with $V_{ij} = 1$, parameters: $N = 500$, $\delta\epsilon = 0.5$, $\lambda = 0.0005$.

One finds a very good agreement between both curves for the random interaction. Therefore the rate equations predicted by HAM are valid and the dynamics are statistical. For the constant

interaction there is no correspondence at all, so one finds no statistical relaxation in this case, although the system parameters, which are the same for both interactions, fulfill the criteria (7) and (8). Referring to Sec. 3 the random interaction represents the average over all possible interactions very well, whereas the constant interaction demonstrates that there can be complete exceptions from the average. It becomes obvious that the concrete structure of the interaction can be indeed significant for the occurrence of statistical relaxation.

The HAM calculation, as well as Fermi's Golden Rule, relies on second order perturbation theory, i.e., the time evolution operator is expressed by the Dyson series in second order truncation

$$|\psi(\tau)\rangle = (\hat{1} - \frac{i}{\hbar}U_1(\tau) - \frac{1}{\hbar^2}U_2(\tau) + ...)|\psi(0)\rangle \tag{9}$$

with the first and second order terms

$$U_1(\tau) = \int_0^\tau d\tau' V(\tau') \ , \tag{10}$$

$$U_2(\tau) = \int_0^\tau d\tau' \int_0^{\tau'} d\tau'' V(\tau')V(\tau'') \ . \tag{11}$$

If this expansion is justified, all higher orders, including $U_2(\tau)$, must be small compared to $U_1(\tau)$ in the relevant time regime. We use $\mathrm{Tr}\{\mathrm{UU}^\dagger\}$ to measure the size of the respective contributions. HAM produces a "best guess" for the time evolution of the P_μ for a short time step ($P_\mu(t+\tau)$) on the basis of $P_\mu(t)$ by using the appropriate truncation of the Dyson series,

$$P_\mu(t+\tau) - P_\mu(t) \approx f(\tau)(P_{\mu-1}(t) + P_{\mu+1}(t) - 2P_\mu(t)) \ , \tag{12}$$

where $f(\tau)$ corresponds to a double time integral over the autocorrelation function of V (see also [2]). One usually expects that this autocorrelation function has decayed completely after some decay time τ_c. After τ_c $f(\tau)$ grows linearly with τ and equation (12) can be iterated which eventually results in the corresponding rate equations (5). Figure 4 and Fig. 5 show a comparative calculation of $U_1(\tau)$ and $U_2(\tau)$ for both analyzed interactions. Whereas $U_1(\tau)$ is equal for both interactions, $U_2(\tau)$ will depend on the structure.

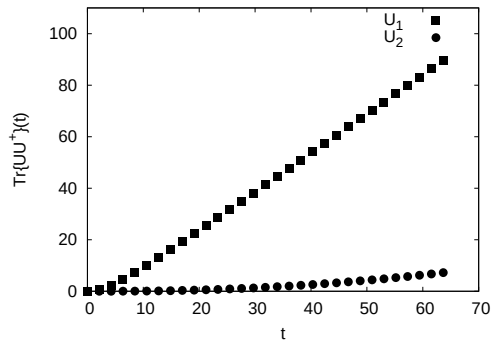

Fig. 4. Dyson terms for a completely random interaction, parameters: $N = 500$, $\delta\epsilon = 0.5$, $\lambda = 0.0005$.

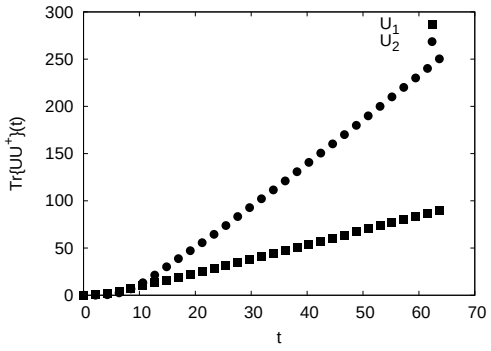

Fig. 5. Dyson terms for a constant interaction with $V_{ij} = 1$, parameters: $N = 500$, $\delta\epsilon = 0.5$, $\lambda = 0.0005$.

$U_1(\tau)$ and $U_2(\tau)$ must be compared in the time regime where equation (12) is iterated, i.e., in the region after τ_c (here $\tau_c \approx 25$). This turns out to be equivalent to the beginning of the linear regime of $U_1(\tau)$. For the completely random interaction one finds that $U_1(\tau) \gg U_2(\tau)$ at time τ_c, so the second order truncation seems to be suggestive in this case. There is no reason why higher orders beyond the second should have a decisive influence, since the second order already leads to a very good approximation. This corresponds to the numerical calculations that

showed statistical relaxation. For the constant interaction $U_2(\tau)$ is already larger than $U_1(\tau)$ at time τ_c. So the truncation is not justified which conforms to the numerically calculated non-statistical dynamics. It should be remarked that this breakdown of the exponential behaviour is actually a problem of the structure of the interaction. It cannot be solved by simply decreasing the average interaction strength λ. This is demonstrated in Fig. 6. λ is chosen too small to

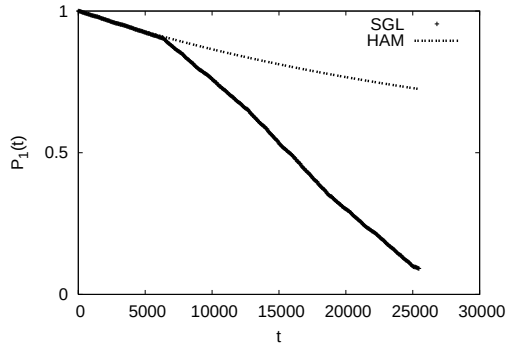

Fig. 6. Dynamics of $P_1(t)$ for a constant interaction with $V_{ij} = 1$, parameters: $N = 500$, $\delta\epsilon = 0.5$, $\lambda = 0.00005$.

fulfill criteria (8). One again finds no complete decay into equilibrium here. However, one can see that Fermi's Golden Rule is fulfilled because of the good agreement at the very beginning. The deviation at some certain time nearly coincides with the Heisenberg time that is equivalent to the recurrence time of the autocorrelation function of V in our model with equidistant local energies ($\tau_H \approx 6200$). At this time the assumption of a completely decayed autocorrelation function necessarily becomes wrong and therefore the rate can no longer be considered as constant. Since the relaxation time of $P_1(t)$ is increased by a smaller λ, while the Heisenberg time is not, this finite size effect becomes important.

Generally, the full evaluation of the second order Dyson term or even higher orders is numerically and analytically very extensive. Instead of that one can introduce a specific structural requirement for the interaction to estimate those contributions. In [5] Van Hove used a similar interaction structure to derive the possible occurrence of statistical relaxation. Basically, this would mean that V features this so called Van Hove-structure, if V^2 is dominated by its diagonal elements in some sense. If the interaction does not have Van Hove-structure, then statistical relaxation cannot emerge. If the interaction possesses Van Hove-structure, the dynamics are possibly but not inevitably statistical. So it can be regarded as a necessary criteria. One finds that the random interaction fulfills the Van Hove-structure, whereas the constant interaction does not. In this sense the resulting dynamics for both examples are explained correctly. In principle, the Van Hove-structure gives an estimation for the proper convergence of the respectively used perturbation expansion. It indicates that the higher orders should be small compared to the leading one, at least for times in the order of the relaxation time.

3 Analytic derivation of the solution of the rate equation

This Section is devoted to the derivation of the solution of the probability for the excitation to be on the left $P_1(t)$ or right hand side $P_2(t)$ for the case where the interaction is modeled by complex Gaussian entries in V. We will not show the total derivation as some intermediary results are too long but rather try to explain the main steps. This is why some results are just stated. What we mean by solution is the following. If we keep the interaction V as a random matrix with its probability distribution instead of fixing it, then the time evolution operator, $e^{-i(H_0+\lambda V)t}$, becomes a random evolution operator. Thus $P_1(t)$ also contains this

random character. We can then calculate its average, $\mathbf{E}[P_1(t)] = \int p(V)dV P_1(t)$, where $p(V)$ is the probability distribution over the random interaction. $p(V)$ is the product of the probability distribution of the complex Gaussian elements which can be written in a more compact form as $p(V) = \frac{1}{Z}e^{-\frac{N}{\sigma}\mathrm{Tr}\{V^2\}}$, where Z is the partition function. We will calculate this average in the limit where the number of energy levels per subunit (there are 2 subunits in the present case) N tends to ∞ and in the Van Hove limit. The Van Hove limit is given by $\lim_{\lambda\to 0}\lim_{t\to\infty}\lambda^2 t = T$. We call T the macroscopic time. This limit represents some long time-weak coupling limit. We will actually not calculate $\mathbf{E}[P_1(t)]$ directly. We will calculate $\mathbf{E}[P_1(t) - P_2(t)]$. Since we know that $P_1(t) + P_2(t) = 1$ always holds (may it be averaged or not), we can obtain $\mathbf{E}[P_1(t)]$ from it.

The main idea of the proof and the below presented expansion is that, in the limits considered, the interference effects vanish. For this graphs are introduced which represent pairs of histories of the state of the system. The vanishing of interference effects means that for two different pairs of histories the contribution is much smaller than for equal or similar pairs. In some sense the quantum feature of interference becomes negligible when the limits are taken, thus making it more classical. It is basically this fact that allows for an autonomous equation to exist. For a pair of histories, or a graph, it is the random interaction, after averaging, that will decide on the weight given to it. It will also decide which class of pairs of histories, or graphs, are preponderant, thus contributing the most. These will be called simple graphs. We start by writing down the observable we wish to consider and inserting the expansion of the time evolution operator.

$$P_1(t) = \langle\psi_0|e^{iHt}\sum_{l=1}^{N}|1,l\rangle\langle 1,l|e^{-iHt}|\psi_0\rangle \tag{13}$$

$$P_1^l(t) = \langle\psi_0|e^{iHt}|1,l\rangle\langle 1,l|e^{-iHt}|\psi_0\rangle \tag{14}$$

Every index l represents the dependency on E_l and $|\mu,l\rangle$ is a basis ket for the state being in unit μ on energy level E_l.
Loosely speaking the idea is to expand the time evolution operator in powers of the interaction. We have then powers of the random matrix over which we can average. Some parts won't contribute in the limit $N\to\infty$ and others won't contribute in the Van Hove limit. In the limit $N\to\infty$ we will keep our local spectrum bounded and so the energy level variables, E_l, will turn into continuous variables, E. $P_1^l(t)$ will become then $P_1(E,t)$. We expand the evolution operator as

$$e^{-iHt} = \sum_n(-i\lambda)^n\Gamma_n(t)\ , \tag{15}$$

$$\Gamma_n(t) = \int_0^t\dots\int_0^t ds_0\dots ds_n e^{-iH_0 s_0}V\dots Ve^{-iH_0 s_n}\delta\left(t-\sum_{j=0}^{n}s_j\right)\ . \tag{16}$$

We thus have

$$P_1^l(t) = \sum_{n,m}(i\lambda)^m(-i\lambda)^n\langle\psi_0|\Gamma_m^\dagger(t)|1,l\rangle\langle 1,l|\Gamma_n(t)|\psi_0\rangle\ , \tag{17}$$

$$P_1^l(t) = \sum_{n,m}\sum_{l_n,l'_m=1}^{N}\sum_{p_n,p'_m=1}^{2}\psi_0^*(p'_m,l'_m)\psi_0(p_n,l_n)i^m(-i)^n\lambda^{n+m}\langle p'_m,l'_m|\Gamma_m^\dagger|1,l\rangle\langle 1,l|\Gamma_n|p_n,l_n\rangle\ . \tag{18}$$

We notice that if $n+m$ is odd, $\langle p'_m,l'_m|\Gamma_m^\dagger|1,l\rangle\langle 1,l|\Gamma_n|p_n,l_n\rangle$ is proportional to an odd number of random variables with average zero. The average of an odd number of random variables centered around zero is zero and so all terms with odd $n+m$ don't contribute to the average. For $n+m$ to be even we need both to be even or both to be odd. The variables p'_m and p_n

here stand for the unit 1 or 2. Since the interaction matrix makes an excitation hop from unit 1 to unit 2 and vice versa, we notice that if n is even, then the product $\langle 1,l|\Gamma_n|p_n,l_n\rangle$ is zero if p_n is equal to 2. Thus p_n has to be equal to 1. For n odd we will only have a contribution for $p_n=2$. We make this explicit in formula (19).

$$\begin{aligned}
P_1^l(t) &= \sum_{n,m}\lambda^{2(n+m)}\sum_{l_{2n},l'_{2m}=1}^{N}\psi_0^*(1,l'_{2m})\psi_0(1,l_{2n})i^{2m}(-i)^{2n}\langle 1,l'_{2m}|\Gamma^\dagger_{2m}|1,l\rangle\langle 1,l|\Gamma_{2n}|1,l_{2n}\rangle \\
&+ \sum_{n,m}\lambda^{2(n+m)+2}\sum_{l_{2n+1},l'_{2m+1}=1}^{N}\psi_0^*(2,l'_{2m+1})\psi_0(2,l_{2n+1})i^{2m+1}(-i)^{2n+1}\times \\
&\langle 2,l'_{2m+1}|\Gamma^\dagger_{2m+1}|1,l\rangle\langle 1,l|\Gamma_{2n+1}|2,l_{2n+1}\rangle \qquad (19)\\
&= F_1^l(t)+F_2^l(t) \qquad (20)
\end{aligned}$$

Notice that the first contribution is related to the initial state of unit 1 and the second to the unit 2. Of course, we have a similar expression for $P_2^l(t)$,

$$P_2^l(t) = G_2^l(t)+G_1^l(t)\ . \qquad (21)$$

When subtracting P_2^l from P_1^l we can group terms with the same initial data dependence that is F_1^l with G_1^l , and F_2^l with G_2^l. We then have

$$\mathbf{E}[P_1^l(t)-P_2^l(t)] = \mathbf{E}[F_1^l(t)-G_1^l(t)]+\mathbf{E}[F_2^l(t)-G_2^l(t)]\ . \qquad (22)$$

We will thus compute one of these, the other being analogue. Inserting (16) in $\langle 1,l|\Gamma_n|p_n,l_n\rangle$ and identities after each interaction term we have

$$\begin{aligned}
(-i)^n\langle 1,l|\Gamma_n|p_n,l_n\rangle &= \int_0^t\dots\int_0^t ds_0\dots ds_n e^{-iE_l s_0}e^{-iE_{l_1}s_1}\dots e^{-iE_{l_n}s_n}\delta\left(t-\sum_{j=0}^n s_j\right) \qquad (23)\\
&\times (-i)^n\langle 1,l|V|p_1,l_1\rangle\langle p_1,l_1|V|p_2,l_2\rangle\dots\langle p_{n-1},l_{n-1}|V|p_n,l_n\rangle\ .
\end{aligned}$$

For a shorter notation we define

$$\begin{aligned}
K^n(t,\{E_{l_j}\}) &= (-i)^n\int_0^t\dots\int_0^t ds_0\dots ds_n e^{-iE_l s_0}e^{-iE_{l_1}s_1}\dots e^{-iE_{l_n}s_n}\delta\left(t-\sum_{j=0}^n s_j\right), \qquad (24)\\
L^n(\{l_j\},\{p_i\}) &= \langle 1,l|V|p_1,l_1\rangle\langle p_1,l_1|V|p_2,l_2\rangle\dots\langle p_{n-1},l_{n-1}|V|p_n,l_n\rangle\ . \qquad (25)
\end{aligned}$$

All of the randomness is encoded in $L^n(\{l_j\},\{p_i\})$ and we know the $\{p_i\}$ variables are determined if n is odd or even. With this notation we have for the first term in Eq. (19)

$$\begin{aligned}
&\sum_{l_{2n},l'_{2m}=1}^{N}\psi_0^*(1,l'_{2m})\psi_0(1,l_{2n})i^{2m}(-i)^{2n}\langle 1,l'_{2m}|\Gamma^\dagger_{2m}|1,l\rangle\langle 1,l|\Gamma_{2n}|1,l_{2n}\rangle \\
&= \sum_{\{l_i,l'_j\}}\psi_0^*(1,l'_{2m})\psi_0(1,l_{2n})K^{2n}(t,\{E_{l_i}\})\bar{K}^{2m}(t,\{E_{l'_i}\})L^{2n}(\{l_j\},\{p_j\})\bar{L}^{2m}(\{l'_j\},\{p'_j\}). \qquad (26)
\end{aligned}$$

To average we must average over $L^n\bar{L}^m$. This term is a product of Gaussian complex variables. It only contributes if these variables correlate. This will introduce relations between the different indices $\{l_i,l'_j,l\}$. According to Wigner's theorem we have the following formula to calculate the average over a product of Gaussian random variables.

$$\mathbf{E}[X_1\dots X_{2n}] = \sum_{C_\pi}\prod_{(i,j)\in C_\pi}\mathbf{E}[X_iX_j] \qquad (27)$$

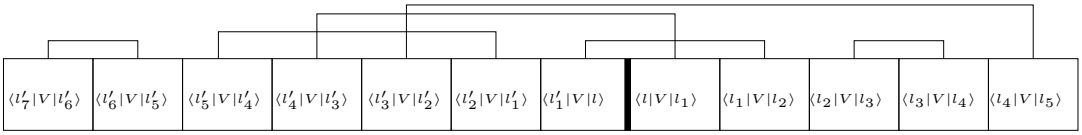

Fig. 7. Example of graph representation for a pairing with $n = 5$ and $m = 7$. This graph represents the following contribution:
$\mathbf{E}[\langle l_7'|V|l_6'\rangle\langle l_6'|V|l_5'\rangle] \times \mathbf{E}[\langle l_5'|V|l_4'\rangle\langle l_2'|V|l_1'\rangle] \times \ldots \mathbf{E}[\langle l_1'|V|l\rangle\langle l_1|V|l_2\rangle] \times \mathbf{E}[\langle l_2|V|l_3\rangle\langle l_3|V|l_4\rangle]$.
All p_j indices are omitted for lighter notation.

Here C_π is a permutation of the set of indices $\{1, \ldots 2n\}$. In the present case each X_j corresponds to matrix elements of the type $\langle p_1, l_1|V|p_2, l_2\rangle$. The pairings induce a graph structure on $L^n\bar{L}^m$. Pictorially an example is given in Fig. 1. The average of one pairing is given in Eq. (28).

$$\mathbf{E}[\langle 1, l_i|V|2, l_{i+1}\rangle\langle 2, l_j|V|1, l_{j+1}\rangle] = \frac{\sigma}{N}\delta_{l_i,l_{j+1}}\delta_{l_{i+1},l_j} \tag{28}$$

Notice that the averaging enforces identities amongst $\{l_i, l_{i+1}, l_j, l_{j+1}\}$ and hence amongst the energies $\{E_{l_i}, E_{l_{i+1}}, E_{l_j}, E_{l_{j+1}}\}$ in Eq. (26). The question is then how much graphs weight and what kinds of graphs are important. We focus on the weight they have.

Over many pairings the delta functions are responsible for the graph structure. However, we notice the weight of every pair will always be the same. Thus we conclude the weight of a graph on $L^{2n}\bar{L}^{2m}$ in (26) is given by $\left(\frac{\sigma}{N}\right)^{n+m}$. $\mathbf{E}[L^{2n}(\{l_j\}, \{p_j\})\bar{L}^{2m}(\{l_j'\}, \{p_j'\})]$ is represented by a graph and enforces identities amongst the energies $\{E_{l_i}, E_{l_i'}\}$. We can then rewrite (26) as

$$\sum_{\text{graphs } C_\pi(2n,2m)} \left(\sum_{\text{indep.}\{l_i,l_j'\}} \left(\frac{\sigma}{N}\right)^{n+m} \psi_0^*(1, l_{2m}')\psi_0(1, l_{2n})K_\pi^{2n}(t, \{E_{l_i}, E_{l_i}'\})\bar{K}_\pi^{2m}(t, \{E_{l_i}, E_{l_i'}\}) \right). \tag{29}$$

Here $K_\pi^{2n}(t, \{E_{l_i}, E_{l_i}'\})\bar{K}_\pi^{2m}(t, \{E_{l_i}, E_{l_i'}\})$ stands for the function $K^{2n}\bar{K}^{2m}$ from Eq.(26) but with the identities amongst the energy variables imposed. It can be shown that for $C_\pi(2n, 2m)$ graphs the maximum of independent $\{l_i, l_j'\}$ is $n + m$ and that we only have this for a certain class of graphs, which we will call simple graphs (S. graphs). For this class of graphs holds that the identity $l_{2n} = l_{2m}'$ is fulfilled. The fact that this identity is fulfilled implies that $\psi_0^*(1, l_{2m}')\psi_0(1, l_{2n}) = P_1^{l_{2n}}(t = 0)$.

We would then have

$$\sum_{w_1} \cdots \sum_{w_{n+m}} \left(\frac{\sigma}{N}\right)^{n+m} \to \sigma^{n+m} \prod_{j=1}^{n+m} \int dE_j = \sigma^{n+m} \int dE \ . \tag{30}$$

The w_j here represent the independent l_j and $\int dE$ is a short notation for the multiple integrals. The sums over independent variables turn into integrals over, what has become, continuous energy variables E_j. The limit as $N \to \infty$ of the average of Eq.(26) then becomes

$$\begin{aligned} &\mathbf{E}[F_1(E_0, t)] = \lim_{N\to\infty} \mathbf{E}[F_1^l(t)] \qquad (31)\\ &= \sum_{n,m} (\lambda^2)^{n+m} \sum_{\text{S graphs } C_\pi(2n,2m)} \sigma^{n+m} \left(\int dE P_1(E_{2n}, t = 0)K_\pi^{2n}(t, \{E_i\})\bar{K}_\pi^{2m}(t, \{E_j\}) \right). \end{aligned}$$

E_0 is the now continuous variable E_l. We now explain what type of graphs contribute in the way previously described. Among all graphs the ones of the type shown in Fig. 8 are simple graphs. Figure 8 represents graphs where $\bar{n}$ random variables from the left hand side are paired with one on the right hand side, and in between each pair of this left-right type of pairs we have a certain amount of pairings with their nearest neighboring random variables. That is,

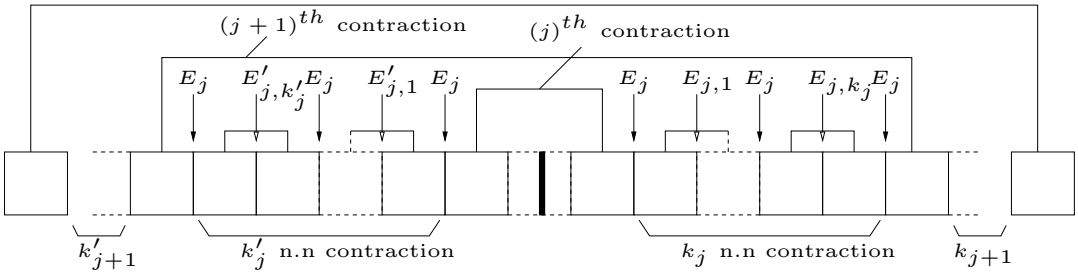

Fig. 8. Sketch of simple graphs

.

in between the j^{th} pairing from left to right and the $(j+1)^{th}$ pairing from left to right we have k'_j pairings on the left and k_j pairings on the right. It is very important to notice that the information of the graph is now coded in the set of number $\{\bar{n}, k'_j, k_j\}$ which determine uniquely the graph. For such graphs the exponentials of the $K^n\bar{K}^m$ factors in Eq. (26) and Eq. (31) in between the j^{th} and $(j+1)^{th}$ contraction have the form

$$C_j = (-i)^{k_j+1} e^{-iE_j \sum_{l=1}^{k_j+1} s_l^j} \left(\prod_{q=1}^{k_j} -ie^{-iE_{j,q} s_{jq}} \right) (i)^{k'_j+1} e^{iE_j \sum_{l=1}^{k_j+1} \tau_l^j} \left(\prod_{q'=1}^{k'_j} ie^{iE'_{j,q'} \tau_{jq'}} \right). \quad (32)$$

C_j depends on many variables ($C_j = C_j(E_j, E_{j,q}, E'_{j,q'}, s_{jq}, \tau_{jq'}, s_l^j, \tau_l^j)$) which we didn't write explicitly. In order to calculate the contribution of a graph we need to integrate the product of all C_j functions over all of these variables respecting the delta functions of Eq. (24). It can be shown that in the Van Hove limit each integral over the functions depending on $E_{j,q}$, s_{jq}, $E'_{j,q'}$ and $\tau_{jq'}$ can be replaced by a given constant. We have then

$$C_j(E_j, s_l^j, \tau_l^j) = (-i)^{k_j+1} e^{-iE_j \sum_{l=1}^{k_j+1} s_l^j} \Theta^{k_j} (i)^{k'_j+1} e^{iE_j \sum_{l=1}^{k_j+1} \tau_l^j} \bar{\Theta}^{k'_j} \quad (33)$$

and

$$Q(C_\pi(\bar{n}, \{k_i, k'_j\}), E_0, t) = \left(\int dE P_1(E_{2n}, t=0) K_\pi^{2n}(t, \{E_i\}) \bar{K}_\pi^{2m}(t, \{E_j\}) \right) \quad (34)$$

$$= \prod_{j=1}^{\bar{n}} \int dE_j P_1(E_{\bar{n}}, 0) \prod_{l=1}^{k_j+1} \int_0^\infty ds_l^j \prod_{l=1}^{k'_j+1} \int_0^\infty d\tau_l^j \delta\left(t - \sum_{j,l} s_l^j \right) \delta\left(t - \sum_{j,l} \tau_l^j \right) C_j(E_j, s_l^j, \tau_l^j).$$

For the integration over the time variables we have the identity (35).

$$\prod_{j=1}^{\bar{n}} \prod_{l=1}^{k_j+1} \int_0^\infty ds_l^j \delta\left(t - \sum_{j,l} s_l^j \right) = \prod_{j=1}^{\bar{n}} \int_0^\infty ds_j \delta\left(t - \sum_j s_j \right) \prod_{l=1}^{k_j+1} \int_0^\infty ds_l^j \delta\left(s_j - \sum_l s_l^j \right) \quad (35)$$

We have the same identity for the τ variables. We see that with this identity we can make the integrations over the s_l^j variables and τ_l^j variables easily because the exponential in C_j depends on $\sum_{l=1}^{k_j+1} s_l^j$ and $\sum_{l=1}^{k'_j+1} \tau_l^j$.

$$\tilde{C}_j(E_j, s_j, \tau_j, k_j, k'_j) = \prod_{l=1}^{k_j+1} \int_0^\infty ds_l^j \delta\left(s_j - \sum_l s_l^j \right) \prod_{l=1}^{k'_j+1} \int_0^\infty d\tau_1^j \delta\left(\tau_j - \sum_l \tau_l^j \right) C_j(E_j, s_l^j, \tau_l^j)$$

$$= (-i)^{k_j+1} (i)^{k'_j+1} e^{-iE_j s_j} \frac{(s_j)^{k_j}}{k_j!} \Theta^{k_j} e^{iE_j \tau_j} \frac{(\tau_j)^{k'_j}}{k'_j!} \bar{\Theta}^{k'_j} \quad (36)$$

We then have by Eq. (34), (35) and (36)

$$\begin{aligned} &Q(C_\pi(\bar{n},\{k_i,k_j'\}),E_0,t) \\ &=\prod_{i=1}^{\bar{n}}\int dE_i \prod_{j=0}^{\bar{n}}\int ds_j \int d\tau_j \tilde{C}_j(E_j,s_j,\tau_j,k_j,k_j')\delta\left(t-\sum_j s_j\right)\delta\left(t-\sum_j \tau_j\right). \end{aligned} \tag{37}$$

$F_1^l(t)$ has become $F_1(E_0,t)$ due to $E_l \to E_0$. Since our graphs are determined by the variables $\{\bar{n},k_j,k_j'\}$ and we have to sum over all possible graphs, this sum over all graphs becomes a sum over all possible values of $\{\bar{n},k_j,k_j'\}$.

$$\mathbf{E}[F_1(E_0,t)] = \sum_{\text{all even } \bar{n}} (\sigma\lambda^2)^{\bar{n}} \sum_{\{k_i,k_j'\}} (\sigma\lambda^2)^{k_i+k_j'} Q(C_\pi(\bar{n},\{k_i,k_j'\}),E_0,t) \tag{38}$$

The fact that $\bar{n}$ is restricted to even numbers comes from Eq. (20). That means, $F_1(E_0,t)$ is the contribution when we have an even number of interaction matrices on the left and on the right. This is guaranteed when $\bar{n}$ is even. $G_1(E_0,t)$ turns out to be the sum over all odd $\bar{n}$. By grouping together all terms which are to the power of k_j and k_j' we can now sum over these.

$$\begin{aligned} &\sum_{k_j,k_j'} (\sigma\lambda^2)^{k_j+k_j'} Q(C_\pi(\bar{n},\{k_i,k_j'\}),E_0,t) = \\ &e^{-it\sigma\lambda^2(\Theta-\bar{\Theta})}\prod_{i=1}^{\bar{n}}\int dE_i P_1(E_{\bar{n}},0)\prod_{j=0}^{\bar{n}}\int_0^\infty ds_j d\tau_j \delta\left(t-\sum s_j\right)\delta\left(t-\sum \tau_j\right) e^{-iE_j(s_j-\tau_j)} \end{aligned} \tag{39}$$

In the first exponent $\Theta-\bar{\Theta}$ is thus the imaginary part of Θ. We have not derived this constant but it turns out to have the following imaginary part.

$$\Theta-\bar{\Theta} = -i2\pi \tag{40}$$

Thus

$$\lim_{\text{Van Hove}} e^{-it\sigma\lambda^2(\Theta-\bar{\Theta})} = e^{-2\pi\sigma T}\ . \tag{41}$$

We now turn to the first part of Eq. (22). By Eq. (38) and Eq. (39) we have an expression for $\mathbf{E}[F_1(E,t)]$. A similar one can be obtained for $\mathbf{E}[G_1(E,t)]$. We group these together in the following equations.

$$\begin{aligned} \mathbf{E}[F_1(E,t)-G_1(E,t)] &= \sum_{\text{all even } \bar{n}} (\sigma\lambda^2)^{\bar{n}} \sum_{\{k_i,k_j'\}} (\sigma\lambda^2)^{k_i+k_j'} Q(C_\pi(\bar{n},\{k_i,k_j'\}),E,t) \qquad (42)\\ &\quad - \sum_{\text{all odd } \bar{n}} (\sigma\lambda^2)^{\bar{n}} \sum_{\{k_i,k_j'\}} (\sigma\lambda^2)^{k_i+k_j'} Q(C_\pi(\bar{n},\{k_i,k_j'\}),E,t) \\ &= \sum_{\text{all } \bar{n}} e^{-it\sigma\lambda^2(\Theta-\bar{\Theta})}\prod_{i=1}^{\bar{n}}\int dE_i P_1(E_{\bar{n}},0)\prod_{j=0}^{\bar{n}} \qquad (43)\\ &\quad (-\sigma\lambda^2)^{\bar{n}}\int_0^\infty ds_j d\tau_j \delta\left(t-\sum s_j\right)\delta\left(t-\sum \tau_j\right) e^{-iE_j(s_j-\tau_j)} \end{aligned}$$

To calculate the integral part we introduce a change of variables, Eq. (44), in the last line of Eq. (43).

$$\alpha_j = \lambda^2\frac{s_j+\tau_j}{2}, b_j = \frac{s_j-\tau_j}{2} \tag{44}$$

$$(-\sigma)^{\bar{n}}\prod_{j=0}^{\bar{n}}\int_0^T d\alpha_j \delta\left(T-\sum_0^{\bar{n}}\alpha_j\right)\int_{\frac{-\alpha_j}{\lambda^2}}^{\frac{+\alpha_j}{\lambda^2}} db_j \delta\left(\sum_{j=0}^{\bar{n}} b_j\right) e^{-i\sum_{j=0}^{\bar{n}} b_j E_j} \tag{45}$$

In the Van Hove limit Eq. (45) turns into

$$(-\sigma)^{\bar{n}} \frac{T^{\bar{n}}}{\bar{n}!} \prod_{j=0}^{\bar{n}-1} 2\pi\delta\left(E_j - E_{\bar{n}}\right) \ . \tag{46}$$

Inserting Eq. (46) in Eq. (43) we obtain

$$\begin{aligned}
&\lim_{\text{Van Hove}} \int dE \left(\mathbf{E}[F_1(E,t) - G_1(E,t)]\right) \\
&= \sum_{\text{all } \bar{n}} e^{-2\pi\sigma T} \prod_{j=1}^{\bar{n}} \int dE_j P_1(E_{\bar{n}},0)(-\sigma)^{\bar{n}} \frac{T^{\bar{n}}}{\bar{n}!} \prod_{j=0}^{\bar{n}-1} 2\pi\delta\left(E_j - E_{\bar{n}}\right) \\
&= \sum_{\text{all } \bar{n}} e^{-2\pi\sigma T} \int dE P_1(E,0) \frac{(-2\sigma\pi T)^{\bar{n}}}{\bar{n}!} \\
&= e^{-4\pi\sigma T} \int dE P_1(E,0) \ .
\end{aligned} \tag{47}$$

In the same manner we can calculate $\int dE \left(\mathbf{E}[F_2(E,t) - G_2(E,t)]\right)$ in the Van Hove limit which will have the same form as Eq.(47) but will depend on $P_2(E,0)$ instead of $P_1(E,0)$. Using these last results in Eq. (22) we finally have

$$\lim_{\text{Van Hove}} \lim_{N\to\infty} \left(\mathbf{E}[P_1(t) - P_2(t)]\right) = e^{-4\pi\sigma T} \left(P_1(0) - P_2(0)\right) \ . \tag{48}$$

These give us the solutions to the rate equations with a rate of $4\pi\sigma$.

4 Conclusion

The analytical derivation has shown that the dynamics of the occupation probabilities of single subunits are statistical for the average over the whole ensemble of possible interactions for $N \to \infty$ and in the Van Hove-limit. This means that if "most" members of the ensemble (a dense subset of the ensemble) give the same type of relaxation, then there is statistical relaxation which is then a typical feature for members of the ensemble. The numerical calculations for a finite size version of the system demonstrate that the occurrence of statistical relaxation actually depends on the structure of a concrete realization of the interaction. A random interaction reproduces the results for the average. Nevertheless, the example of the constant interaction indicates that there are exceptions as the dynamics are not statistical at all in this case. The fact that a fixed randomly chosen interaction reproduces the same type of relaxation as the average strongly supports that the statistical relaxation is a typical feature because it represents the majority of all possible interactions very well.

References

1. J. Gemmer, M. Michel, G. Mahler, *Quantum Thermodynamics*, (Springer, 2004)
2. M. Michel, G. Mahler, J. Gemmer, Phys. Rev. Lett. **95**, (2005) 180602
3. J. Gemmer, M. Michel, Phys. Rev. E **29**, (2005) 136
4. M. Michel, J. Gemmer, G. Mahler, Phys. Rev. E **73**, (2006) 016101
5. L. Van Hove, Physica **XXI**, (1955) 517
6. L. Erdös, T.Hau , Comm. in Pure and App. Math., **53**, (2000) 667

Original publication Phys. Rev. E **77**, 011119 (2008)
available at http://pre.aps.org

Occurrence of exponential relaxation in closed quantum systems

Christian Bartsch,[1,*] Robin Steinigeweg,[1,†] and Jochen Gemmer[1,‡]

[1]*Fachbereich Physik, Universität Osnabrück, Barbarastrasse 7, D-49069 Osnabrück, Germany*

(Dated: January 28, 2010)

We investigate the occurrence of exponential relaxation in a certain class of closed, finite systems on the basis of a time-convolutionless (TCL) projection operator expansion for a specific class of initial states with vanishing inhomogeneity. It turns out that exponential behavior is to be expected only if the leading order predicts the standard separation of timescales and if, furthermore, all higher orders remain negligible for the full relaxation time. The latter, however, is shown to depend not only on the perturbation (interaction) strength, but also crucially on the structure of the perturbation matrix. It is shown that perturbations yielding exponential relaxation have to fulfill certain criteria, one of which relates to the so-called "Van Hove structure". All our results are verified by the numerical integration of the full time-dependent Schrödinger equation.

PACS numbers: 05.30.-d, 03.65.Yz, 05.70.Ln

I. INTRODUCTION

A substantial part of linear non-equilibrium thermodynamics essentially relies on a description by means of rate equations, often in the form of master equations [1]. The crucial quantities, such as the probability to find the system in some state i, j or the amount of particles, energy, etc. at points i, j in some space, are routinely believed to follow equations like

$$\frac{\partial}{\partial t} P_i = \sum_j R(j \to i)\, P_j - \sum_j R(i \to j)\, P_i, \qquad (1)$$

with time-independent transition rates from i to j, $R(i \to j)$. Pertinent examples are the decay of excitations in atoms, nuclear decay, etc. But also diffusive transport phenomena belong to that class, since the diffusion equation can also be formulated to take the above form (random walk dynamics). Another implementation of that scheme is the (linear) Boltzmann equation [1, 2] where particle scattering is taken into account by means of transition rates, and many more could be named.
However, regardless of the incontestable success of such descriptions, the strict derivation of rate equations from underlaying principles often remains a problem. Typically, the descriptiveness by means of rate equations is taken for granted. Since those rate equations yield an exponential decay towards equilibrium, the basic question may be formulated as: How can an exponential decay of some observable be derived from the Schrödinger equation?

On the basis of quantum mechanics the most popular approach to this question is probably Fermi's Golden Rule [3]. Despite the undisputed descriptive success of this scheme, it is simply derived from first order perturbation theory, e.g., its validity generally breaks down on a timescale much shorter than the resulting relaxation time. Therefore it can hardly describe a complete decay into equilibrium. One of the few concrete, concise derivations of exponential decay is the Weisskopf-Wigner theory for the relaxation of excitations in an atom due to the coupling of the atom to a zero-temperature, broad-band electromagnetic field [4]. However, this theory is hardly generalizable, since it only applies if just one state is coupled to a multitude of others, rather than many states coupled to many others, as is typically the case.
A more abstract, rather fundamental approach has been suggested by Van Hove [5, 6]. It is based on (infinite) quantum systems having continuous state densities and interactions which are described by smooth functions rather than discrete matrices. However, a lot of the findings for discrete systems in the paper at hand are quite parallel to Van Hove's, as will be pointed out below.
Other approaches are based on projection operator techniques, in particular the well-known Nakajima-Zwanzig (NZ) method. This method is commonly used in the context of open quantum systems, i.e., systems that allow for a partition according to a considered system (or simply "system") and an environment [1, 7]. For a specific choice of the initial condition, as pointed out below, the projection onto the system's degrees of freedom eventually leads to an autonomous master equation describing the dynamics of the system, based on a systematic perturbation expansion. But in general, due to the complexity of higher orders, only the leading order is taken into account. In the paper at hand we will demonstrate that this truncation may produce wrong results even and especially for the case of fast decaying correlation func-

*Electronic address: cbartsch@uos.de
†Electronic address: rsteinig@uos.de
‡Electronic address: jgemmer@uos.de

tions and arbitrarily weak interactions.
A further approach to this topic is based on the description of quasi-particle dynamics in many-particle systems by the use of Green's functions [8]. These considerations indicate the validity of a Boltzmann equation.
In the present paper we will employ another projection operator technique, the so-called time-convolutionless (TCL) method [9–14]. In the following we will follow the TCL-method as detailed in [14]. In Sec. II we introduce our rather abstract Hamiltonian for a "closed quantum" system (consisting of an unperturbed part and a perturbation) and define an also rather abstract observable, the dynamics of which we are going to investigate. In Sec. IV we demonstrate how the TCL technique can be used to compute the above dynamics of the variable. (This is somewhat reminiscent of projection techniques using "correlated projectors" [15, 16].) We tune our models such that a leading order truncation predicts exponential decay. For a "random interaction" this prediction turns out to be correct, as is verified by the numerically exact solution of the full time-dependent Schrödinger equation. In the following Sec. V non-random ("structured") perturbation matrices are discussed in more detail. While a leading order truncation still predicts exponential relaxation, it is demonstrated that this prediction may fail even for arbitrarily large models and arbitrarily small interactions. This breakdown stems from the fact that higher order contributions are not negligible if the interaction matrix violates certain criteria. Before we will close with a summary and conclusion in Sec. VI, these criteria will be also related to those conditions which Van Hove postulated in order to explain the occurrence of exponential relaxation.

II. MODELS, OBSERVABLES AND INTERPRETATION OF DYNAMICS

In the present paper we will analyze quantum models which are much simpler than most of the examples mentioned in the introduction. They are defined on a very general, rather formal level and are not meant to describe any specific, realistic quantum system in great detail. The Hamiltonian is taken to consist of a local part H_0 and an interaction part V such that $H = H_0 + V$. In particular, V is assumed to take the special form of an "off-diagonal block structure" in the eigenbasis of H_0, that is, the matrix representation of H may be written as

$$H = \left(\begin{array}{cc|cc} \ddots & 0 & & \\ & \frac{i}{n-1}\,\delta\epsilon & & v \\ 0 & \ddots & & \\ \hline & & \ddots & 0 \\ & v^\dagger & & \frac{j}{n-1}\,\delta\epsilon \\ & & 0 & \ddots \end{array}\right) \tag{2}$$

or, equivalently to the above notation, $H = H_0 + V$ may also be written as

$$\begin{aligned} H_0 &= \sum_{i=0}^{n-1} \frac{i}{n-1}\,\delta\epsilon\;|i\rangle\langle i| + \sum_{j=0}^{n-1} \frac{j}{n-1}\,\delta\epsilon\;|j\rangle\langle j|\;, \\ V &= \left(\sum_{i,j=0}^{n-1} v_{ij}\;|i\rangle\langle j| + \text{H.c.}\right), \end{aligned} \tag{3}$$

where $|i\rangle, |j\rangle$ form the basis in which (2) is represented. Obviously, the complete Hilbert space is divided into two subspaces, where i runs through the states of the first and j through the states of the second subspace, respectively. Obviously, H_0 may correspondingly be separated into two parts which we only specify very roughly at this point by two parameters: There are two identical "bands" with width $\delta\epsilon$ and n equidistant energy levels each.
The average strength of the interaction V is measured by

$$\lambda^2 = \frac{1}{n^2} \sum_{i,j=0}^{n-1} |v_{ij}|^2\;. \tag{4}$$

In our first example in Sec. IV we take the matrix elements v_{ij} in the off-diagonal blocks to be Gaussian, complex, random numbers. For the other examples V will be specified below. In all cases the matrix elements of V in the diagonal blocks are all zero, just to keep the picture as simple as possible.
We will investigate the (relaxation) dynamics of an abstract observable a, represented by an operator A, which is chosen in such a way that

$$[A, H_0] = 0\,,\ \mathrm{Tr}\{A\} = 0\,,\ \mathrm{Tr}\{A^2\} = 1\,. \tag{5}$$

The first of these properties states that A is diagonal in the eigenbasis of H_0, while the remaining two properties do not mean crucial restrictions on A. While all of the following will be correct for any A featuring the above properties, we mainly concentrate in our examples on "binary" operators, i.e., operators featuring only two different eigenvalues, namely, $+1/\sqrt{2\,n}$ in one

subspace and $-1/\sqrt{2\,n}$ in the other. This means that $a \equiv \mathrm{Tr}\{A\rho\} = +1/\sqrt{2\,n}$ indicates that the system entirely occupies one subspace and $a = -1/\sqrt{2\,n}$ indicates that it entirely occupies the other subspace. (Here, ρ is the density matrix for the state of the system.) If and only if $a(t)$ is found to relax exponentially to zero, the system allows for a merely statistical interpretation entirely beyond quantum physics: it is then in accord with a system featuring two distinguishable states in between it can "hop" with a given transition rate, the latter being equal for both directions. a then represents the difference between the probabilities of finding it in one or the other state, respectively.

In an abstract way the above model may represent many physical situations. It may be viewed as a simplified model for the exchange of an excitation between, e.g., two weakly coupled atoms, molecules, quantum dots, etc. A then represents the probability to find atom 1 excited, subtracted by the probability to find atom 2 excited, V represents the coupling in this scenario. Or it may model the momentum dynamics of a particle bound to one dimension which possibly changes its direction (forward-backward) due to some scattering. In a many-particle system the current operator could be identified with A and V may stand for a particle-particle interaction. This way the dynamics of the current autocorrelation function could be investigated based on the framework below. More detailed information about such models can be found in [17–22].

III. TCL SCHEME AND CHOICE OF THE PROJECTION OPERATOR

In this section we give a short overview of the time-convolutionless (TCL) projection operator technique [13, 14]. Furthermore, we introduce the pertinent equations which are applied to models with various interactions in Sec. IV and Sec. V. A detailed derivation of these equations is beyond the scope of this paper and can be found in [14, 20].

The TCL method is a projection operator technique such as the well-known Nakajima-Zwanzig technique [23, 24]. Both are applied in order to describe the reduced dynamics of a quantum system with a Hamiltonian of the type $H = H_0 + V$. Generally, the full dynamics of the system are given by the Liouville-von Neumann equation,

$$\frac{\partial}{\partial t}\,\rho(t) = -\imath\,[\,V(t), \rho(t)\,] = \mathcal{L}(t)\,\rho(t)\,. \tag{6}$$

(Now and in the following all equations are denoted in the interaction picture.) In order to describe the reduced dynamics of the system, one has to construct a suitable projection operator $\mathcal{P}$ which projects onto the relevant part of the density matrix $\rho(t)$. $\mathcal{P}$ has to satisfy the property $\mathcal{P}^2\,\rho(t) = \mathcal{P}\,\rho(t)$. Recall that in our case the relevant variable is chosen as the expectation value $a(t)$ of the binary operator A. For initial states $\rho(0)$ with

$$\mathcal{P}\,\rho(0) = \rho(0) \tag{7}$$

the TCL method yields a closed time-local equation for the dynamics of $\mathcal{P}\,\rho(t)$,

$$\frac{\partial}{\partial t}\,\mathcal{P}\,\rho(t) = \mathcal{K}(t)\,\mathcal{P}\,\rho(t) \tag{8}$$

with

$$\mathcal{K}(t) = \sum_{i=1}^{\infty} \mathcal{K}_i(t)\,. \tag{9}$$

The TCL technique avoids the usually troublesome time convolution which appears, e.g., in the context of the Nakajima-Zwanzig technique. Eq. (8) and (9) represent a formally exact perturbative expansion.

A brief comment on initial conditions should be made here. If (7) is not fulfilled, of course an additional inhomogeneity appears on the r.h.s. of (8). This may change the solutions of (8) drastically, c.f. [25] and references therein. However, for the model to be addressed below, there is substantial numerical evidence that, for a large set of initial states that do not fulfill (7), the dynamics are nevertheless reasonably well described by (8) (without inhomogeneity) [17, 20, 26–29]. Having mentioned this issue we consider in the following exclusively initial states in accord with (7).

For many models the odd cumulants of the expansion (9) vanish: $\mathcal{K}_{2i+1}(t) = 0$. This will turn out to apply to our model as well. The lowest non-vanishing order scales quadratically with λ and reads

$$\mathcal{K}_2(t) = \int_0^t dt_1\,\mathcal{P}\,\mathcal{L}(t)\,\mathcal{L}(t_1)\,\mathcal{P}\,. \tag{10}$$

For the fourth order term one finds

$$\begin{aligned}\mathcal{K}_4(t) \;=\; & \int_0^t dt_1 \int_0^{t_1} dt_2 \int_0^{t_2} dt_3 \\ & \mathcal{P}\,\mathcal{L}(t)\,\mathcal{L}(t_1)\,\mathcal{L}(t_2)\,\mathcal{L}(t_3)\,\mathcal{P} \\ & -\;\mathcal{P}\,\mathcal{L}(t)\,\mathcal{L}(t_1)\,\mathcal{P}\,\mathcal{L}(t_2)\,\mathcal{L}(t_3)\,\mathcal{P} \\ & -\;\mathcal{P}\,\mathcal{L}(t)\,\mathcal{L}(t_2)\,\mathcal{P}\,\mathcal{L}(t_1)\,\mathcal{L}(t_3)\,\mathcal{P} \\ & -\;\mathcal{P}\,\mathcal{L}(t)\,\mathcal{L}(t_3)\,\mathcal{P}\,\mathcal{L}(t_1)\,\mathcal{L}(t_2)\,\mathcal{P}\,.\end{aligned} \tag{11}$$

Note that the TCL approach is commonly used in the context of open quantum systems [1, 14, 23, 24]. The TCL method is, however, also applicable to our closed quantum system.

To those ends, we define the projection operator $\mathcal{P}$ by

$$\mathcal{P}\,\rho(t) \equiv \frac{1}{2n}\,\hat{1} + A\,\mathrm{Tr}\{A\,\rho(t)\} = \frac{1}{2n}\,\hat{1} + A\,a(t)\,. \tag{12}$$

As already mentioned above, $\mathcal{P}$ is constructed to project onto the time-dependent expectation value $a(t)$ of the binary operator A, in the Schrödinger picture. But since

A commutes with H_0, this expectation value is identical in the interaction and the Schrödinger picture. The full dynamics [Hilbert space: dimension $2n$, Liouville space of density matrices: dimension $(2n)^2$] is broken down to the time evolution of the single variable $a(t)$, all other information is neglected. As a suitable initial condition we can then choose $\rho(0) = (1/2n)\,\hat{1} + (1/\sqrt{2n})\,A$ which implies $a(0) = 1/\sqrt{2n}$. Inserting Eq. (12) into Eq. (8) yields the closed equation

$$\dot{a}(t) = \sum_{i=1}^{\infty} K_i(t)\, a(t) \tag{13}$$

with $K_i(t) = \mathrm{Tr}\{A\,\mathcal{K}_i(t)\,A\}$. Due to Eq. (12), the second order term reads

$$K_2(t) = -\int_0^t dt'\, C(t')\;, \tag{14}$$

where the two-point correlation function $C(t')$ is given by

$$C(t') = \mathrm{Tr}\Big\{\imath[\,V(t),A\,]\;\imath[\,V(t_1),A\,]\Big\}\;,\quad t' \equiv t - t_1\;. \tag{15}$$

A rather lengthy but straightforward calculation yields for the fourth order

$$\begin{aligned}
K_4(t) \;&=\; \int_0^t dt_1 \int_0^{t_1} dt_2 \int_0^{t_2} dt_3\; I_1 + I_2 + I_3 + I_4,\\
I_1 \;&=\; \mathrm{Tr}\Big\{[\,V(t_1),[V(t),A]\,]\,[\,V(t_2),[V(t_3),A]\,]\Big\},\\
I_2 \;&=\; -\;C(t-t_1)\,C(t_2-t_3)\;,\\
I_3 \;&=\; -\;C(t-t_2)\,C(t_1-t_3)\;,\\
I_4 \;&=\; -\;C(t-t_3)\,C(t_1-t_2)\;.
\end{aligned} \tag{16}$$

IV. SECOND ORDER TCL AND COMPLETELY RANDOM INTERACTION

In this section we apply the equations in second order TCL to a model with the completely random interaction introduced in Sec. II. The function $C(t')$ in Eq. (15) is identical to the autocorrelation function of the interaction, since it can also be written as

$$C(t') = \frac{4}{n} \sum_{i,j=0}^{n-1} |v_{ij}|^2\, \cos[\,\omega_{ij}\,(t-t_1)\,] \tag{17}$$

with frequencies $\omega_{ij} = (i-j)/(n-1)\,\delta\epsilon$ corresponding to H_0. Here, just like in many other examples, $C(t')$ decays within the correlation time τ_C which is of the order of $\tau_C \approx 4\pi/\delta\epsilon$ for our model. Afterwards the integral $K_2(t)$ becomes approximately time-independent and assumes a constant value R until the "Heisenberg time" $T = 2\pi\,n/\delta\epsilon$ is reached. This behavior can be inferred from integrating (17) and exploiting the properties of the sinc-function. From this analysis also R may be found with an accuracy determined by the law of large numbers. Thus the second order approximation of Eq. (13) eventually results in

$$\dot{a}(t) = -R\,a(t)\,,\quad R \approx \frac{4\pi\,n\,\lambda^2}{\delta\epsilon}\;. \tag{18}$$

We hence obtain a rate equation featuring the form of Eq. (1) and thus exponential dynamics for $a(t)$. The solutions for $a(t)$ decay exponentially with a relaxation time $\tau_R = 1/R$. However, this result is only valid within the boundaries $\tau_C \ll \tau_R < T$, because $K_2(t)$ can only be considered as time-independent up to the Heisenberg time. Recall to this end that our model features equidistant energies such that $C(t')$ is strictly periodic with T. These two boundaries also result in two necessary criteria for the system parameters which have to be fulfilled in order to produce the occurrence of exponential dynamics,

$$\frac{16\pi^2\,n\,\lambda^2}{\delta\epsilon^2} \ll 1\,,\quad \frac{8\pi^2\,n^2\,\lambda^2}{\delta\epsilon^2} > 1\,. \tag{19}$$

Remarkably, the whole derivation of the rate equation using second order TCL does not depend on the details of the interaction, i.e., the individual absolute values of the single matrix elements as well as their relative phases are not relevant. We should already mention here that the "structure", which we are going to introduce into the interaction in the following section, only concerns those details, hence the second order contribution K_2 will be the same in all our following examples.
In Fig. 1 the numerical solution of the Schrödinger equation is shown for the above repeatedly mentioned random interaction and compared with the TCL prediction. All parameters (the width of the Gaussian distribution according to which the matrix elements of V are generated, the bandwith, etc.) are adjusted such that the criteria (19) are well satisfied. This solution is obtained by exact diagonalization. And in fact, we find a very good agreement with the theoretical prediction of second order TCL.

V. FOURTH ORDER TCL AND NON-RANDOM INTERACTIONS

In this section we will be concerned with the structure of the interaction matrix and, especially, its influence on the time evolution of the expectation value $a(t)$. It will be demonstrated that the theoretical prediction (18) of second order TCL fails to describe the numerically exact solution of the Schrödinger equation correctly for certain "interaction types", even and especially if the conditions (19) are fulfilled, i.e., the "strength" is "adequate". We will outline that this failure stems from the fact that the fourth order contribution of the TCL expansion is not negligible on the relaxation timescale which is obtained from second order TCL. However, the exact evaluation of $K_4(t)$ turns out to be almost impossible, analytically

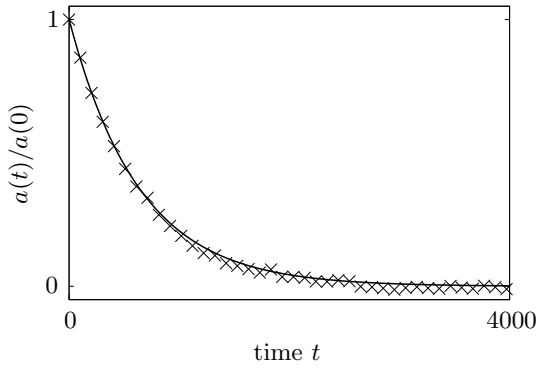

FIG. 1: Time evolution of the expectation value $a(t)$ for an interaction with completely random v_{ij}. The numerical result (crosses) indicates exponential behavior and is in very good agreement with the theoretical prediction (18) of second order TCL (continuous curve). The system parameters $n = 1000$, $\delta\epsilon = 0.5$, $\lambda = 2.5 \cdot 10^{-4}$ fulfill the conditions (19).

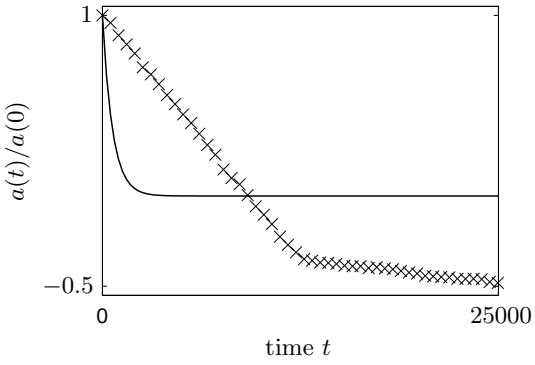

FIG. 2: Time evolution of the expectation value $a(t)$ for an interaction with $v_{ij} = \lambda$. The theoretical prediction (18) of second order TCL (continuous curve) fails to describe the numerical solution (crosses) correctly, although the system parameters $n = 1000$, $\delta\epsilon = 0.5$, $\lambda = 2.5 \cdot 10^{-4}$ still fulfill the conditions (19). V violates the Van Hove structure.

and numerically. Instead we will present feasible estimations of $K_4(t)/K_2(t)$ based on suitable approximations of $K_4(t)$ called $S(t)$ (see (23, 38)). Whenever

$$q(t) \equiv \frac{S(t)}{K_2(t)} < 1 \tag{20}$$

is violated the influence of higher order terms is not negligible. If this is the case for times t of the order of or shorter than τ_R, no exponential relaxation will result.

A. Uniform Interactions and Van Hove structure

Let us start with an example. Fig. 2 shows the time evolution of the expectation value $a(t)$ for an interaction with $v_{ij} = \lambda$. This type of interaction is, of course, highly non-random, since all matrix elements have the same absolute value and phase. The second order approximation obviously yields a wrong description for this interaction structure, that is, the dynamics are not exponential, although both of the conditions (19) are well fulfilled. It should be remarked again that the observed non-exponential behavior definitely is a structural issue. For instance, it can not be "repaired" by simply decreasing the overall interaction strength, because this decrease would eventually lead to the violation of the criteria (19).

To analyze this model we now develop our first estimate $S(t)$ for $K_4(t)$ which concerns the timescale $t >\approx \tau_C$. We start from from Eq. (16), where we abbreviate the triple time integration by a single "$\int$". One may hence write $K_4(t) = \int I_1 + I_2 + I_3 + I_4$. Fig. 3 shows a sketch for the integration volume of $K_4(t)$ in the 3-dimensional space which is spanned by t_1, t_2, t_3. The integration does not run over the whole cube with the edge length t, but only over the region where $t_3 \leq t_2 \leq t_1$ holds.
$C(t-t_1)$ is the autocorrelation function of the interaction which has already been mentioned in (15). Recall that

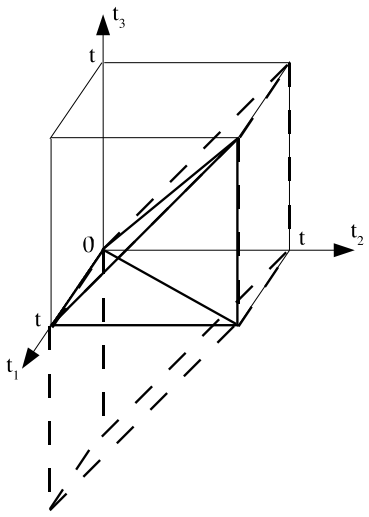

FIG. 3: Sketch for the integration volume of $K_4(t)$ for fixed t. The cube with the edge length t is drawn with thin lines, the actual integration volume is marked with thick lines. The dashed lines represent the changed integration volume which is used in the approximations.

$C(t')$ is only different from zero around $t' = 0$ in a small interval of the width τ_C. Thus, the integrands I_2, I_3, I_4 are only different from zero in a small volume around the region where both of the arguments are equal for each of the two multiplied correlation functions.
First of all let us focus on I_3 as well as I_4. The integrand I_3 contributes to $K_4(t)$ for $t = t_2$ and $t_1 = t_3$, while the integrand I_4 contributes to $K_4(t)$ for $t = t_3$ and $t_1 = t_2$, respectively. The sketch in Fig. 3 displays that both of these regions overlap only in the vicinity of one single point with the integration volume of $K_4(t)$, namely, at the point where all arguments are equal to t. Especially, this overlap does not increase with t. Therefore the triple time integration is estimated by $\int I_3 \approx \int I_4 \approx C(0)^2\, \tau_C^3$.

Using the estimate $R \approx C(0)\,\tau_C$, we eventually obtain for the ratio between the contributions from I_3, I_4 to the fourth order and the second order $K_2(t > \tau_C)$ for times $t > \tau_C$

$$\frac{\int I_3}{R} \approx \frac{\int I_4}{R} \approx C(0)\,\tau_C^2 \approx \frac{\tau_C}{\tau_R} \equiv \alpha\ . \tag{21}$$

Recall that the derivation of exponential behavior within second order TCL has required $\tau_C \ll \tau_R$ or, equivalently, $\alpha \ll 1$ such that the contributions to $K_4(t)$ which arise from I_3 and I_4 are negligible, at least in comparison with R.

Analogous conclusions cannot be made for the term I_2, because its overlap with the integration volume is larger and grows with t. We have to find another estimation for the contributions of I_2 as well as I_1, of course. Our estimation is based on the fact that neither I_2 nor I_1 can decay on a shorter timescale than τ_C in any possible direction of the (t_1, t_2, t_3)-space. This fact is obviously correct for I_2. But what about I_1? Since the term I_1 consists of summands which have the typical form

$$v_{ab}\,v_{bc}\,v_{cd}\,v_{da}\,\mathrm{e}^{-\imath\,\omega_{ab}\,t}\,\mathrm{e}^{-\imath\,\omega_{bc}\,t_1}\,\mathrm{e}^{-\imath\,\omega_{cd}\,t_2}\,\mathrm{e}^{-\imath\,\omega_{da}\,t_3}\ , \tag{22}$$

only those frequencies and, especially, those largest frequencies in I_1 which have already appeared in $C(t')$ contribute significantly to I_1. Consequently, I_1 can never decay faster than $C(t')$ in any possible direction of the (t_1, t_2, t_3)-space. In the (possibly unrealistic) "best case" $I_1 + I_2$ decays within τ_C around the point $I_{1/2}(t,t,t,t) = I_{1/2}(0,0,0,0) \equiv I_{1/2}(0)$. We can therefore estimate the value of $q(\tau_C)$ by

$$\frac{\int I_1 + I_2}{R} \approx \frac{[\,I_1(0) - C(0)^2\,]\,\tau_C^3}{C(0)\,\tau_C} = \left[\frac{I_1(0)}{C(0)^2} - 1\right]\alpha \equiv \beta\ . \tag{23}$$

β is a lower bound for the ratio between the fourth and the second order of TCL for times $t > \tau_C$. If $\beta \approx 1$ or even larger, then $K_4(t > \tau_C)$ dominates $K_2(t > \tau_C)$, that is, exponential behavior in terms of the second order prediction cannot occur. But $\beta \ll 1$, however, does not allow for a strict conclusion, since a slower decay of I_1 or I_2, as the case may be, raises their contribution to $K_4(t)$. Nevertheless, the condition $\beta \ll 1$ is an additional criterion for the occurrence of exponential decay which involves the structure of V.

In the following we will discuss why and to what extend β and, especially, the ratio $I_1(0)/C(0)^2$ is related to the conditions which have been postulated by Van Hove for the interaction V in order to explain the onset of exponential relaxation, see [5, 6]. To this end, let us define a hermitian operator G by

$$G \equiv [\,V, [V, A]\,]\ . \tag{24}$$

A straightforward calculation yields

$$I_1(0) = \mathrm{Tr}\{G^2\} = \sum_{i,j} |G_{ij}|^2\ , \quad C(0) = \mathrm{Tr}\{A\,G\}\ , \tag{25}$$

where G_{ij} represents the matrix elements of G in the eigenbasis of H_0. Furthermore, let us also introduce the superoperator $\mathcal{D}$ which is given by

$$\mathcal{D}\,M \equiv \sum_i |i\rangle\,M_{ii}\,\langle i| \tag{26}$$

and projects any operator M onto its diagonal elements in the eigenbasis of H_0. Then the expression

$$(A, G) \equiv \mathrm{Tr}\{A\,\mathcal{D}\,G\} \tag{27}$$

defines an inner product between the operators A and G, because $(A, G) = (G, A)^*[= (G, A)]$ holds and $(A, A) = 1$, as well as $(G, G) = \sum_i G_{ii}^2$, are both positive, real numbers. The Schwartz inequality $(A, G)^2 \leq (A, A)^2\,(G, G)^2$ can consequently be formulated. By the use of $(A, G) = C(0)$ we eventually obtain

$$C(0)^2 \leq \sum_i G_{ii}^2 \leq \sum_{i,j} |G_{ij}|^2 = I_1(0)\ , \tag{28}$$

i.e., $I_1(0)/C(0)^2 \geq 1$. $C(0)^2$ is at most as large as the sum of the squared diagonal elements of G, according to the above equation. Therefore $I_1(0)/C(0)^2 \approx 1$ and hence sufficiently small β can only be realized if the diagonal elements of G and thus the diagonal elements of V^2 are as large as possible in comparison with the remaining non-diagonal elements of V^2 (G). In principle, this is essentially what Van Hove proclaimed [5, 6].

In this sense, we define the "Van Hove structure" in the context of finite quantum systems: The interaction V is said to feature Van Hove structure if

$$\beta' \equiv \frac{I_1(0)}{C(0)^2}\,\alpha \ll 1\ , \tag{29}$$

while all conditions of second order TCL are simultaneously kept, of course. The latter refers to the validity of Eq. (19). The comparison with (23) shows that the Van Hove structure implies $\beta \ll 1$ and hence the relaxation may possibly be exponential, as described by the second order. Since the evaluation of β' is much more efficient than the complete computation of fourth order TCL (there is no time dependence left, e.g., $I_1(0)$ only depends on $t = t_1 = t_2 = t_3 = 0$), the Van Hove structure eventually is an assessable criterion for the possible occurrence of exponential decay. It is a criterion in the sense that only if (29) is satisfied, a use of the second order approximation is justified for any time longer than the correlation time, i.e., $t > \tau_C$.

Let us now apply these results to the already introduced models with random and non-random ($v_{ij} = \lambda$) interactions, respectively. The only term which varies for the different models is $I_1(0)$, since the terms $C(0)^2 \approx n^2\lambda^4$ and $\alpha \approx 16\pi^2 n\lambda^2/\delta\epsilon^2$ (again with an accuracy set by the law of large numbers for the random interaction) are the same for random and non-random interactions. For the random interaction a straightforward calculation leads to

$$I_1(0) = 32\,n^2\,\lambda^4\ , \quad \beta' = 2\,\alpha \ll 1 \tag{30}$$

such that the random interaction indeed features Van Hove structure. This agrees with the numerical results in Fig. 1 which yielded exponential relaxation. In the case $v_{ij} = \lambda$, however, we finally obtain

$$I_1(0) = 16\, n^3\, \lambda^4 \;, \quad \beta' = \frac{16\pi^2\, n^2\, \lambda^2}{\delta\epsilon^2} \;, \tag{31}$$

where $\beta' > 1$, according to Eq. (19). The absence of the Van Hove structure already suffices to explain the breakdown of exponential behavior in Fig. 2.
One may nevertheless be inclined to argue that the Van Hove structure is not the crucial difference between those two cases but simply the randomness of the matrix elements (which possibly induces quantum chaos). We therefore present a counter-example which immediately disproves such an argument. The example is slightly different from the others, since the complete system is not partitioned into equally large subspaces. n_1 and n_2 define the number of levels of the respective subspaces. One subspace consists of only one state ($n_1 = 1$). Thus, in the matrix V there is only a single column with non-zero elements and a single row, respectively. Although these non-zero elements are chosen to be all equal (non-random), it can be shown that this V features Van Hove structure. Note that such a Hamiltonian occurs, e.g., in the context of spin-boson models at zero temperature or the scenario addressed by the Weisskopf-Wigner theory, see [14].

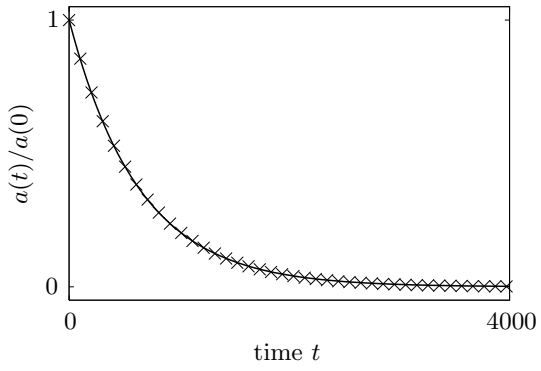

FIG. 4: Time evolution of the expectation value $a(t)$ for the interaction of spin-boson type. The numerical result (crosses) indicates exponential behavior and perfectly agrees with the theoretical prediction (18) of second order TCL (continuous curve). System parameters: $n_1 = 1$ (single level), $n_2 = 2000$ (many levels), $\delta\epsilon = 0.5$, $\lambda = 2.5 \cdot 10^{-4}$.

Fig. 4 shows an almost perfect correspondence between the numerical solution of the Schrödinger equation and the theoretical prediction (18) which is obtained by the use of second order TCL. Here, exponential relaxation is found, although V is not randomly chosen.

B. Sparse Interaction and Localization

So far, we numerically found exponential decay in accord with the second order for all considered models that showed the Van Hove structure. There is, however, non-exponential behavior for some types of interactions which feature the Van Hove property in the sense of (29) and are in accord with (19). Recall that those are only necessary but not sufficient conditions for the occurrence of exponential decay.
An example for such a situation is a model with a random but, say, "sparsely populated" interaction. This model is almost identical to the model with the completely random interaction. The only difference is that only 1/10 of the matrix elements are Gaussian distributed numbers, all others are zero. The non-zero numbers are randomly placed. Apparently, this type of interaction fulfills the Van Hove structure, since the completely random interaction already does.

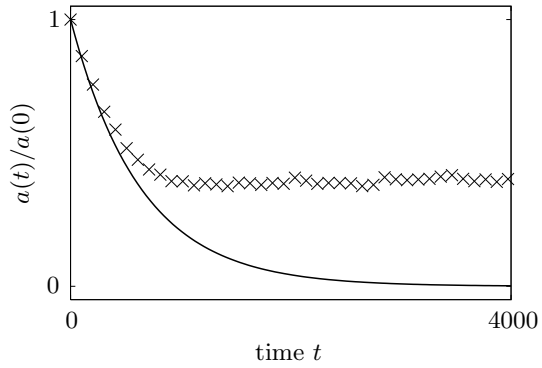

FIG. 5: Time evolution of the expectation value $a(t)$ for an interaction with random but "sparsely populated" v_{ij}. The theoretical prediction (18) of second order TCL (continuous curve) deviates from the numerical solution (crosses), even though the Van Hove structure as well as the conditions (19) are fulfilled. System parameters: $n = 1000$, $\delta\epsilon = 0.5$, $\lambda = 2.5 \cdot 10^{-4}$.

Fig. 5 displays the numerical solution of the Schrödinger equation and the theoretical prediction (18) of second order TCL. At the beginning there is a good agreement but then the numerical solution starts to deviate from a purely exponential decay and finally sticks at a clearly positive value. The latter non-zero value may be a hint towards localization effects which also appear, e.g., in the context of the Anderson model [30–33]. And in fact, the sparsely populated interaction takes a form which is very similar to the Hamiltonian of the, e.g., 3-dimensional Anderson model in the chaotic regime.
Apparently, we have to extend the analysis of the fourth order: There is no exponential behavior by the means of a complete exponential decay, although V fulfills the Van Hove property. Recall that the Van Hove criterion has been derived from the consideration of times $t <\approx \tau_C$ and thus $t = t_1 = t_2 = t_3 <\approx \tau_C$. Hence, we have to reconsider the full time dependence of the fourth order

to produce a feasible estimate for the timescale $t \approx \tau_R$. To this end, the integrand I_1 is expressed by

$$I_1 = \mathrm{Tr}\{\, G(t_1,t)\, G(t_2,t_3)\,\}\;, \tag{32}$$

where the hermitian operator $G(t_1,t)$ is again given by

$$G(t,t_1) \equiv [\,V(t),[V(t_1),A]\,]\;. \tag{33}$$

If $I_1(0) \approx C(0)^2$, the diagonal terms dominate at $t = t_1 = t_2 = t_3$. Based on this fact, we carefully assume that I_1 is dominated by these terms for other times as well. Of course, this assumption neglects the larger part of all terms but leads, as will be demonstrated below, to a criterion which may be evaluated with limited computational power. (For our simple example its validity can also be counterchecked by direct numerics.) However, following this assumption, I_1 can be approximated by

$$I_1 \approx \sum_i G_{ii}(t-t_1)\, G_{ii}(t_2-t_3)\;, \tag{34}$$

where $G_{ii}(t-t_1)$ are the diagonal matrix elements of $G(t,t_1)$ in the eigenbasis of H_0, namely,

$$G_{ii}(t-t_1) = 2\sum_j (A_{ii}-A_{jj})\,|V_{ij}|^2\,\cos[\,\omega_{ij}(t-t_1)\,]\;. \tag{35}$$

Furthermore, the correlation function $C(t-t_1)$ can, by the use of this notation, also be written as

$$C(t-t_1) = \sum_i A_{ii}\, G_{ii}(t-t_1) \tag{36}$$

such that I_2, the remaining fourth order integrand, can be expressed as well by

$$I_2 = -\sum_{i,j} A_{ii}\, G_{ii}(t-t_1)\, A_{jj}\, G_{jj}(t_2-t_3)\;. \tag{37}$$

In order to estimate with reasonable computational effort how $K_4(t)$ compares with $K_2(t)$ another approximation is necessary. Obviously, the expressions for I_1, I_2 are invariant along lines described by $t_1 = \text{const.}, t_2 = t_3$. Thus, as an approximation, we shift the integration volume from the original region, indicated with solid lines in Fig. 3, to a new region, indicated with dashed lines in Fig. 3. Obviously, this is a rather rough estimate but it will turn out to be good enough for our purposes. Now the coordinate transformation $x = t-t_1$, $y = t_2-t_3$, $z = t-t_2$ decouples the integrations within the new integration volume such that we eventually find for $S(t) \approx K_4(t)$ (if V features Van Hove structure)

$$S(t) = t\,\Big[\sum_i \Gamma_i(t)^2 - K_2(t)^2\Big]\;, \tag{38}$$

with the time integral $\Gamma_i(t) \equiv \int_0^t dt'\, G_{ii}(t')$. Now (20) may eventually be checked with very low computational power, based on $S(t)$ from (38). This adds to (19) and (29) as a further manageable criterion for exponential relaxation. Fig. 6 shows $q(t)$ [based on (38)] for the following interaction types: the completely random interaction, the interaction of spin-boson type, and the random but sparsely populated interaction. Fig. 6 apparently demonstrates that this approximation is able to explain the breakdown of exponential behavior in the case of a random, sparsely populated interaction: The fourth order becomes roughly as large as the second order at a time which agrees with the deviation between the second order theory and the numerical results in Fig. 5. In both other cases $q(t)$ remains sufficiently small, at least until the relaxation time is reached.

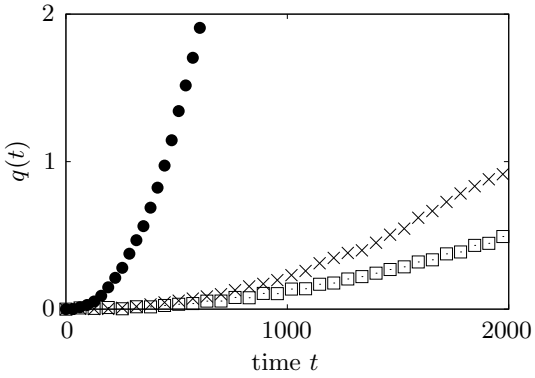

FIG. 6: Time evolution of the value $q(t)$ based on (38). $q(t)$ is numerically calculated for a completely random interaction (crosses), the interaction of spin-boson type (squares), and the random but sparsely populated interaction (circles). Note that $K_2(t)$ is a constant which is also identical for all three interactions. The system parameters are chosen according to Fig. 1, Fig. 4, and Fig. 5, respectively.

Obviously, regardless of the interaction type, $K_4(t)$ will eventually dominate $K_2(t)$ for large enough times (c.f. [34]). This, however, does not necessarily spoil the exponential decay: If $a(t)$ has already decayed almost completely into equilibrium, even a significant change of the rate $K(t)$ will not change the overall picture of an exponential decay (, as long as $K(t)$ remains negative). The influence of a large $K_4(t)$ will only be visible if it occurs, while $a(t)$ is still far from equilibrium, i.e., at times of the order of τ_R. If one now computes the ratio $q(t)$ for the time $t = \tau_R$, one finds

$$q(\tau_R) \approx \frac{\sum_i \Gamma_i(\tau_R)^2}{R^2} - 1\;, \tag{39}$$

where one has to take (38) and $K_2(\tau_R) = R = 1/\tau_R$ into account. This form has the advantage of being completely independent of the overall interaction strength λ. One can hence compute $q(\tau_R)$, taking τ_R as a free variable. The region in which $q(\tau_R) <\!\approx 1$ then represents the range of different τ_R for which exponential decay is possible and to be expected. The different "possible" τ_R can then be implemented by tuning λ appropriately. Often $q(\tau_R)$ is found to increase monotonously, essentially like in Fig. 6. Thus a good number to characterize

a class of models with different relaxation times (interaction strengths) would be τ_{max} as the largest time for which $q(\tau_{max}) <\approx 1$ holds true. This then indicates the largest timescale on which exponential relaxation can still be expected. We should note here that we intend to use this measure, τ_{max}, to investigate transport behavior in models of the Anderson-type in a forthcoming paper.

VI. SUMMARY AND OUTLOOK

We investigated the dynamics of some expectation values for a certain class of closed, finite quantum systems by means of the TCL projection operator method. This technique yields a perturbation expansion for those dynamics. Taking only the second (leading) order into account, we find that the evolution of these expectation values may be described by a rate equation, i.e., they relax exponentially if certain criteria are fulfilled. Those criteria, however, only depend on "rough" parameters like overall interaction strength, bandwidth and density of states but not on, e.g., the phases of the interaction matrix elements. An adequately computed numerical solution of the Schrödinger equation is in accord with this leading order result for random interaction matrices. However, numerics also show that this accordance breaks down if one considers non-random interactions, even if the above rough criteria are met. This, of course, indicates that higher orders are not negligible, depending on the structure, not only on the strength of the interaction. Subsequently, we established a numerically simple estimate for the absolute value of the fourth, i.e., the next higher order, in comparison to the second, for short times. From this approach it can be inferred that the fourth order remains negligible at small times if the interaction features a certain structure which we define as Van Hove structure according to [5]. However, numerics indicate that for certain interaction structures the fourth order may become non-negligible at larger times, thus spoiling the exponential relaxation, even if the interaction features Van Hove structure. Hence we suggest one more criterion (based on (20, 38)) that allows for the detection of such a behavior without diagonalizing the full system.

Diffusive transport in spatially extended quantum systems may be viewed as a form of exponential relaxation. Thus we intend to exploit the various criteria which are suggested in this paper to investigate the occurrence of diffusion in the Anderson model and/or other solid state models that do not allow for a full numerical diagonalization.

Acknowledgments

We sincerely thank H.-P. Breuer, M. Michel and M. Kadirōglu for their contributions to fruitful discussions. Financial support by the "Deutsche Forschungsgemeinschaft" is gratefully acknowledged.

[1] R. Kubo, M. Toda, and N. Hashitsume, *Statistical Physics II. Nonequilibrium Statistical Mechanics* (Springer, Berlin, 1991).
[2] C. Cercignani, *The Boltzmann Equation and its Applications* (Springer, New York, 1988).
[3] C. Cohen-Tannoudji, B. Diu, and F. Laloë, *Quantum Mechanics* (Wiley, New York, 1993).
[4] M. O. Scully and S. Zubairy, *Quantum Optics* (Cambridge University Press, Cambridge, 1997).
[5] L. Van Hove, Physica **21**, 517 (1955).
[6] L. Van Hove, Physica **23**, 441 (1957).
[7] U. Weiss, *Dissipative Quantum Systems* (World Scientific, Singapore, 1999).
[8] L. P. Kadanoff and G. Baym, *Quantum Statistical Mechanics* (Benjamin, New York, 1962).
[9] A. Fulinski, Phys. Lett. A **25**, 13 (1967).
[10] A. Fulinski and W. J. Kramarczyk, Physica A **39**, 575 (1968).
[11] P. Hänggi and H. Thomas, Z. Physik B **26**, 85 (1977).
[12] H. Grabert, P. Talkner, and P. Hänggi, Z. Physik B **26**, 389 (1977).
[13] S. Chaturvedi and F. Shibata, Z. Phys. B **35**, 297 (1979).
[14] H. P. Breuer and F. Petruccione, *Theory of Open Quantum Systems* (Oxford University Press, Oxford, 2007).
[15] C. D. Blanga and M. A. Despósito, Physica A **227**, 248 (1996).
[16] A. A. Budini, Phys. Rev. A **74**, 053815 (2006).
[17] M. Michel, G. Mahler, and J. Gemmer, Phys. Rev. Lett. **95**, 180602 (2005).
[18] J. Gemmer, R. Steinigeweg, and M. Michel, Phys. Rev. B **73**, 104302 (2006).
[19] R. Steinigeweg, J. Gemmer, and M. Michel, Europhys. Lett. **75**, 406 (2006).
[20] H. P. Breuer, J. Gemmer, and M. Michel, Phys. Rev. E **73**, 016139 (2006).
[21] R. Steinigeweg, H. P. Breuer, and J. Gemmer, Phys. Rev. Lett. **99**, 150601 (2007).
[22] M. Kadirōglu and J. Gemmer, Phys. Rev. B **76**, 024306 (2007).
[23] S. Nakajima, Progr. Theor. Phys. **20**, 948 (1958).
[24] R. Zwanzig, J. Chem. Phys. **33**, 1338 (1960).
[25] K. M. Fonseca Romero, P. Talkner, and P. Hänggi, Phys. Rev. A **69**, 052109 (2004).
[26] M. Esposito and P. Gaspard, Phys. Rev. E **68**, 066113 (2003).
[27] J. Gemmer and M. Michel, Eur. Phys. J. B **53**, 517 (2006).
[28] J. Gemmer and M. Michel, Eurohys. Lett. **73**, 1 (2006).
[29] J. Gemmer, M. Michel, and G. Mahler, *Quantum Thermodynamics* (Springer, New York, 2004).
[30] P. W. Anderson, Phys. Rev. **109**, 1492 (1958).
[31] R. Abou-Chacra, D. J. Thouless, and P. W. Anderson, J. Phys. C **6**, 1734 (1973).
[32] P. A. Lee and T. V. Ramakrishnan, Rev. Mod. Phys. **57**,

287 (1985).
[33] B. Kramer and A. MacKinnon, Rep. Progr. Phys. **56**, 1469 (1993).
[34] L. A. Khalfin, Sov. Phys. JETP **6**, 1053 (1958).

Original publication Phys. Rev. Lett. **102**, 110403(2009)
available at http://prl.aps.org

Dynamical typicality of quantum expectation values

Christian Bartsch[1,*] and Jochen Gemmer[1,†]

[1]*Fachbereich Physik, Universität Osnabrück, Barbarastrasse 7, D-49069 Osnabrück, Germany*

(Dated: January 28, 2010)

We show that the vast majority of all pure states featuring a common expectation value of some generic observable at a given time will yield very similar expectation values of the same observable at any later time. This is meant to apply to Schrödinger type dynamics in high dimensional Hilbert spaces. As a consequence individual dynamics of expectation values are then typically well described by the ensemble average. Our approach is based on the Hilbert space average method. We support the analytical investigations with numerics obtained by exact diagonalization of the full time-dependent Schrödinger equation for some pertinent, abstract Hamiltonian model. Furthermore, we discuss the implications on the applicability of projection operator methods with respect to initial states, as well as on irreversibility in general.

PACS numbers: 05.30.-d, 03.65.Yz, 05.70.Ln

In its broadest sense the term typicality may be explained as follows [1, 2]: If a set of states specified by some common feature (e.g., drawn according to the same distribution, sharing the same energy, etc.) yields a very narrow distribution of some other feature (e.g. some observable, etc.), then there is typicality. The concept of typicality as key to the occurrence of standard statistical equilibrium behavior (as opposed to ergodicity, mixing, etc.) especially in quantum mechanics has recently been established in various works [3–6].

One important implementation has been presented in [3, 4]. There it is shown that a majority of pure states of a compound system from some narrow energy shell yield almost the same reduced density matrix for a small subsystem. This happens to be the canonical equilibrium state in case of weak interactions and generic environment spectra [3].

In another typicality-based investigation [5] it is demonstrated that states drawn according to a certain type of probability distribution in Hilbert space feature very similar quantum expectation values (QEV's) of generic observables. Even more detailed results exist for the special case of a uniform distribution of normalized, pure states, i.e., a distribution which is invariant under all unitary transformations in Hilbert space [7]. Using the Hilbert space average method (HAM) [8, 9] one finds that the "Hilbert space average" (HA), i.e., the average of the QEV's of an observable D w.r.t. the above distribution, is given by

$$\mathrm{HA}[\langle\psi|D|\psi\rangle] = \frac{\mathrm{Tr}\{D\}}{n} = c_1 \tag{1}$$

and the corresponding "Hilbert space variance" (HV) by

$$\mathrm{HV}[\langle\psi|D|\psi\rangle] := \mathrm{HA}[(\langle\psi|D|\psi\rangle - \mathrm{HA}[\langle\psi|D|\psi\rangle])^2]$$
$$= \frac{1}{n+1}\left(\frac{\mathrm{Tr}\{D^2\}}{n} - \left(\frac{\mathrm{Tr}\{D\}}{n}\right)^2\right) = \frac{1}{n+1}\left(c_2 - c_1^2\right), \tag{2}$$

cf. [9]. Here n denotes the dimension of the corresponding Hilbert space and $c_i := \mathrm{Tr}\{D^i\}/n$ describes the i-th moment of the spectrum of D. Thus $c_2 - c_1^2$ is the spectral variance of D. Throughout this paper we focus on observables the low spectral moments of which do not change (significantly) under physically reasonable "upscaling". Pertinent examples are, e.g., a component of a specific spin in a system which is upscaled by adding more and more (interacting) spins, the occupation number of some momentum mode in an interacting many-particle system which is upscaled to comprise more and more momentum modes, or in general any local variable embedded in a growing system. For any such observable one may conclude from (2) that the Hilbert space variance, i.e., the width of the above distribution of QEV's vanishes with growing dimension n. In this sense bound observables in large systems yield typical QEV's.

In this paper we turn towards the typicality of dynamics of QEV's. In short, we demonstrate in the paper at hand that pure states from a set $\{|\phi\rangle\}$ featuring a common QEV of some observable A at some time t, i.e. $\langle\phi|A(t)|\phi\rangle = a$, most likely yield very similar QEV's at any later time, i.e. $\langle\phi|A(t+\tau)|\phi\rangle \approx \langle\phi'|A(t+\tau)|\phi'\rangle$ (with $|\phi\rangle, |\phi\rangle'$ both being states from the above set). We present some analytical derivations based on the HAM, in particular on Eqs. (1 and 2) and we additionally support the results with numerical calculations. Finally, we discuss what consequences arise for the validity of projection operator methods (Nakajima-Zwanzig (NZ), etc. [10–12]) w.r.t. initial states and the corresponding

inhomogeneities. Furthermore, we comment on the irreversibility of QEV's corresponding to individual pure states.

We specify our considered observable A only by the above mentioned moments, c_i, and specialize without substantial loss of generality to observables which are trace-free, $c_1 = 0$, and normalized to $c_2 = 1$. Furthermore we require the c_i with $i = 2, ..., 8$ to be of the order 1. Next, we introduce an ensemble of pure states $|\phi\rangle$ which is characterized as follows: All its states must feature the same QEV of the observable A, $\langle\phi|A|\phi\rangle = a$, must be normalized ($\langle\phi|\phi\rangle = 1$), and uniformly distributed otherwise. That means the ensemble has to stay invariant under all unitary transformations in Hilbert space that leave the expectation value of A unchanged, i.e. those transformations that commute with A, or, concretely, transformations of the form e^{iB}, with $[B, A] = 0$. This specifies the most general ensemble consistent with the restriction that all its states should yield a given a.

For the following calculations we further introduce some kind of "substitute" ensemble $\{|\omega\rangle\}$, which is much easier to handle. As will be shown below, this ensemble approximates the exact ensemble $\{|\phi\rangle\}$ described above very well for large Hilbert spaces.

The ensemble $\{|\omega\rangle\}$ is generated by

$$|\omega\rangle = (1/\sqrt{1+d^2})(1 + dA)|\psi\rangle \ , \tag{3}$$

where $|\psi\rangle$ are pure states drawn from a uniform distribution of normalized states without further restriction as described above (1). d is some small parameter which describes the deviation from the "equilibrium" ensemble $\{|\psi\rangle\}$. Since it is essentially the operator A itself that generates $\{|\omega\rangle\}$ from the entirely uniform distribution, $\{|\omega\rangle\}$ is invariant under the above uniform transformations that leave a invariant.

The construction (3) allows for an evaluation of moments of the distribution of $\langle\omega|C|\omega\rangle$ based on results on moments of the distribution of $\langle\psi|D|\psi\rangle$, or concretely

$$\begin{aligned} &\mathrm{HA}[\langle\omega|C|\omega\rangle^i] = \mathrm{HA}[\langle\psi|D|\psi\rangle^i] \\ &\text{with} \quad D = \frac{1}{1+d^2}(1 + dA)C(1 + dA) \ . \end{aligned} \tag{4}$$

(Of course the average on the l.h.s. corresponds to the substitute ensemble $\{|\omega\rangle\}$ while the average on the r.h.s is based on the completely uniform ensemble $\{|\psi\rangle\}$). Exploiting this, average and variance of $\langle\omega|C|\omega\rangle$ may be evaluated with the help of (1,2).

To assure that the ensemble $\{|\omega\rangle\}$ indeed approximates the ensemble $\{|\phi\rangle\}$, in the limit of large n, we evaluate the following four quantities

$$\begin{aligned} &\mathrm{HA}[\langle\omega|\omega\rangle], \qquad &&\mathrm{HA}[\langle\omega|A|\omega\rangle] \ , \\ &\mathrm{HV}[\langle\omega|\omega\rangle], \qquad &&\mathrm{HV}[\langle\omega|A(t)|\omega\rangle] \ , \end{aligned} \tag{5}$$

where $A(t)$ denotes the time dependence according to the Heisenberg picture. (For clarity: the results are given in Eqs. (6), (7), (8) and (10).)

The states $|\omega\rangle$ are not exactly normalized which would render them unphysical, of course. However, one finds from (1) and (4) (by implementing $C = 1$) that

$$\mathrm{HA}[\langle\omega|\omega\rangle] = 1 \ . \tag{6}$$

By exploiting (2) and (4) one finds analogously for the variance

$$\mathrm{HV}[\langle\omega|\omega\rangle] = \frac{1}{n+1} \cdot \frac{4d^2 + 4d^3c_3 + d^4(c_4 - 1)}{(1+d^2)^2} \ . \tag{7}$$

As defined above, the c_i are of the order 1, i.e. the HV of the norms scales with $1/n$ and becomes small for large Hilbert spaces. Therefore, the vast majority of the states $|\omega\rangle$ are approximately normalized for large n.

The average of the QEV's of A w.r.t. the ensemble $\{|\omega\rangle\}$ (which is meant to correspond to the above a) is calculated by exploiting (1) and (4) (by implementing $C = A$)

$$\mathrm{HA}[\langle\omega|A|\omega\rangle] = \frac{2d + d^2c_3}{1+d^2} \ . \tag{8}$$

That is, the mean QEV can be adjusted through the choice of the parameter d. However, the replacement ensemble is restricted on expectation values not too far away from zero (i.e. the average expectation value of the "equilibrium" ensemble $\{|\psi\rangle\}$) because by sweeping through all possible d not all possible expectation values up to the maximum eigenvalue of A are reachable.

The evaluation of $\mathrm{HV}[\langle\omega|A(t)|\omega\rangle]$ turns out to be somewhat more complicated, since we, in general, cannot fully diagonalize the Hamiltonian and thus do not know $A(t)$ in detail. However, we are able to perform an estimation for an upper bound. For this purpose we make use of the Hilbert Schmidt scalar product for complex matrices defined as $(X, Y) := \mathrm{Tr}\{X^\dagger Y\}$. Thus, one can formulate a Cauchy-Schwarz inequality of the form

$$\mathrm{Tr}\{X^\dagger Y\} \leq \sqrt{\mathrm{Tr}\{X^\dagger X\}\mathrm{Tr}\{Y^\dagger Y\}} \ . \tag{9}$$

Particularly, one obtains $\mathrm{Tr}\{A(t)A\} \leq \mathrm{Tr}\{A^2\}$. Evaluating $\mathrm{HV}[\langle\omega|A(t)|\omega\rangle]$ based on (2) and (4) (by implementing $C = A(t)$), realizing that $\mathrm{Tr}\{D\}^2$ is always positive and repeatedly applying (9) yields the inequality

$$\begin{aligned} \mathrm{HV}[\langle\omega|A(t)|\omega\rangle] \leq \frac{1}{n+1} \cdot \\ \frac{1 + 4d\sqrt{c_4} + 6d^2c_4 + 4d^3\sqrt{c_4}\sqrt[4]{c_4c_8} + d^4\sqrt{c_4c_8}}{(1+d^2)^2} \ . \end{aligned} \tag{10}$$

Again, since the c_i are of the order 1, the upper bound deceases with $1/n$. Thus, the variance (10) becomes small for large Hilbert spaces, just like the variance of the norms (7). This result yields two major direct implications.

First, if one evaluates (10) at $t = 0$, one finds that the majority of the states $|\omega\rangle$ feature approximately the same QEV of the observable A for large n. From this property together with the result that the states $|\omega\rangle$ are nearly normalized one concludes that the replacement ensemble $\{|\omega\rangle\}$ indeed approximates the exact ensemble $\{|\phi\rangle\}$ very well for large Hilbert spaces (with $a = \mathrm{HA}[\langle\omega|A|\omega\rangle]$ as given in (8)).

Second, the upper bound from (10) is valid for any time t. Thus, for large enough systems, the dynamical curves for $a_\omega(t) := \langle\omega|A(t)|\omega\rangle$ of the vast majority of pure states from the initial ensemble $\{|\omega\rangle\}$ are very close to each other and thus to the evolving ensemble average at any time t. Due to the similarity of $\{|\omega\rangle\}$ and $\{|\phi\rangle\}$ this should also hold true for the "exact" ensemble $\{|\phi\rangle\}$. Thus, there is a typical evolution for the expectation values $\langle\phi|A(t)|\phi\rangle$ or, to rephrase, there is "dynamical typicality". This statement represents the main result of this paper. Particularly, this typicality is independent of the concrete form of the dynamics, which may be a standard exponential decay into equilibrium or something completely different.

In the following we visualize these predictions for a model quantum system described by a Hamiltonian of the form $H = H_0 + V$, where H_0 is some unperturbed Hamiltonian with equidistant energy eigenvalues (number of states: $n = 6000$, level spacing: $\Delta E = 8.33{\cdot}10^{-5}$, $\hbar$ set to 1), and V some possibly but not necessarily small interaction. A is chosen as diagonal in the eigenbasis of H_0 with equally many, randomly placed elements 1 and -1. This is in accordance with the already mentioned conditions on the moments c_i ($c_1 = 0$, $c_2 = 1$). However, this specific form of the Hamiltonian and the observable A is not crucial for the main results of this paper concerning the typicality of expectation values. It is just an example for the numerical illustrations. We further calculate the dynamical curves of $a_{\omega(t)}$ as generated by three concrete interactions V that are chosen to represent different generic types of dynamical behavior. Thus, the matrix elements of V in the eigenbasis of H_0 (and A) are taken as (i.) random complex Gaussian numbers with $\overline{V_{ij}} = 0, \overline{|V_{ij}|^2} = 2.25 \cdot 10^{-8}$ (small perturbation), (ii.) random complex Gaussian numbers with $\overline{V_{ij}} = 0, \overline{|V_{ij}|^2} = 6.25 \cdot 10^{-6}$ (strong perturbation), (iii.) all identical constants, i.e., $V_{ij}^2 = 2.25 \cdot 10^{-8}$. We obtain the dynamics of the $a_\omega(t)$ by numerically solving the full time-dependent Schrödinger equation). These interactions give rise to three archetypical evolutions (i.) an exponential decay into equilibrium (Fig. 1(a)), (ii.) non-exponential decay into equilibrium (Fig. 1(b)), (iii.) no decay to equilibrium at all, even in the limit of many states and weak perturbations (Fig. 1(c)). The precise reasons for the emergence of these dynamics are beyond the scope of this text (for more details see [13]). For a clarification of the term "relaxation" in this context refer to [14].

In each of the figures the dynamics of $a_\omega(t)$ for three different pure states of the ensemble $\{|\omega\rangle\}$ as initial states are displayed. Furthermore, the evolution of the ensemble average is shown (averaged over 100 states). To numerically generate $\{|\omega\rangle\}$, the real and imaginary parts of the amplitudes of the states $|\psi\rangle$ (cf. (3)) w.r.t. the eigenbasis of H_0 are drawn as independent Gaussian numbers, similar to the Gaussian Adjusted Projected ensemble (GAP) (see [15, 16]). d is chosen as 0.1. Essentially, one finds that, for all three interactions, the dynamical curves of the pure states are close to the average curve for all displayed times t. Furthermore, the insets in Figs. 1(a),1(b),1(c) show the numerical variance $\sigma^2(t)$ of the $a_\omega(t)$ (calculated for 100 states), which turns out to be always smaller than the upper bound given in (10). Thus, all these numerics illustrate and back up our previously derived analytical results.

We now address further implications. The mean QEV, i.e., essentially a, can alternatively be reformulated using the notion of a density matrix as usually done in the framework of projection operator formalisms

$$a = \mathrm{HA}[\langle\omega|A|\omega\rangle] = \mathrm{HA}[\mathrm{Tr}\{A|\omega\rangle\langle\omega|\}] = \mathrm{Tr}\{A\,\mathrm{HA}[|\omega\rangle\langle\omega|]\}\,. \tag{11}$$

The $\mathrm{HA}[|\omega\rangle\langle\omega|]$ takes the role of the density matrix. Further evaluation gives (using the "substitute" ensemble $\{|\omega\rangle\}$) (see [3, 9])

$$\mathrm{HA}[|\omega\rangle\langle\omega|] = \frac{1 + 2dA + d^2A^2}{n(1+d^2)}\,. \tag{12}$$

For ensembles close to equilibrium, i.e., small d, which is fulfilled in the examples presented here, one can neglect the terms which grow quadratically in d. In this case, the density matrix takes approximately the same form as the initial state which is often used in projection operator calculations which aim at determining the dynamics of expectation values like $a(t)$ ([13]). There, for reasons given below, the (mixed) initial state is simply taken to be $\rho(0) = 1/n + cA$ such that $c = a(0)$. That means, correct dynamical results from the projection operator methods based on the above initial state describe the dynamics of the ensemble average of $\{|\omega\rangle\}$.

From this point of view some consequences on the applicability of projection operator theories (NZ, time-convolutionless, Mori formalism etc.), which are standard tools for the description of reduced dynamics, arise. These methods have in common the occurrence of an inhomogeneity in the central equations of motion that typically has to be neglected in order to solve them. Generally, the inhomogeneity depends on the true initial state, it, however, vanishes if the true initial state indeed is of some specific form determined by the pertinent projector [11, 12, 17]. For the above mentioned case the above $\rho(0)$ is exactly of that form, which means the dynamics of the ensemble are equal to the dynamics generated by the pertinent projected equation of motion without the

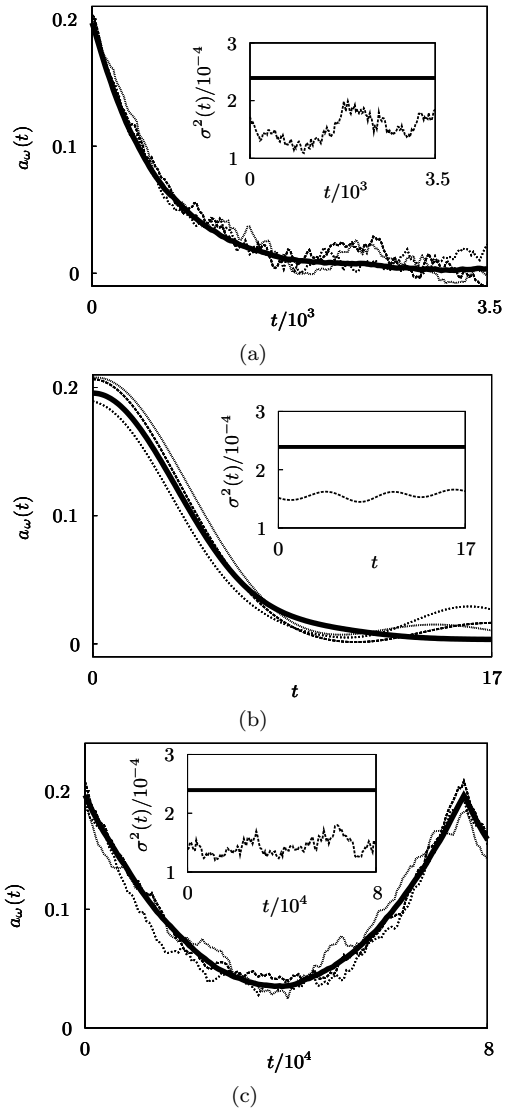

FIG. 1: Dynamics of some expectation values corresponding to a set of initial states $\{|\omega\rangle\}$, i.e., $\langle\omega|A(t)|\omega\rangle = a_\omega(t)$. The set is characterized by an "common" initial expectation value, i.e., all $|\omega\rangle$ yield $\langle\omega|A(0)|\omega\rangle \approx 0.2$. The figures illustrate that the individual evolutions typically stay close to the average over the set (solid line). The insets show evolutions of the variances $\sigma^2(t)$ which stay accordingly small and remain below some analytically predicted upper bound (solid line), cf. (10). The subfigures correspond to different Hamiltonians, generating different archetypical types of dynamics: a.) exponential relaxation, b.) non-exponential relaxation, c.) non-relaxing.

inhomogeneity. However, the evolution of the ensemble is typical, this implies that the inhomogeneity, as generated by most of the true initial states, should be negligible.

On the other hand, there are investigations in the field of open quantum systems, e.g., [18] and [19], suggesting that the true initial states may have an utterly crucial influence on the dynamics, such that, e.g., some correlated initial states may yield projected dynamics which are entirely different from the ones obtained by corresponding product states.

Nevertheless, to rephrase, the results of this paper indicate that in the limit of large (high dimensional) systems the inhomogeneity should become more and more irrelevant in the sense that the statistical weight of initial states, which yield an inhomogeneity that substantially changes the solution of the projected equation of motion, should decrease to zero. Note that this does not contradict the concrete results of [18] and [19].

The above results also shed some light on the relation of the apparently irreversible dynamics of QEV's to the, in some sense, reversible dynamics of the underlying Schrödinger equation. If a mean QEV as generated by some initial non-equilibrium ensemble (pertinent density matrix) relaxes to equilibrium [14] (which can often be reliably shown [11]) , then for the majority of the individual states that form the ensemble, the corresponding individual QEV's will relax to equilibrium in the same way. Thus, for the relaxation of the QEV's, the question whether or not the initial ensemble truly exists is largely irrelevant. Of course, there may be individual initial states giving rise to QEV evolutions that do not (directly) relax to equilibrium, but, to repeat, for high dimensional systems, their statistical weight is low.

Support by the Deutsche Forschungsgemeinschaft through the Graduiertenkolleg 695 is gratefully acknowledged.

* Electronic address: cbartsch@uos.de
† Electronic address: jgemmer@uos.de

[1] J. L. Lebowitz, Physics Today **46**, 32 (1993).
[2] J. L. Lebowitz, cond-mat/0709.0724.
[3] S. Goldstein, J. L. Lebowitz, R. Tumulka, and N. Zanghi, Phys. Rev. Lett. **96**, 050403 (2006).
[4] S. Popescu, A. J. Short, and A. Winter, Nature Phys. **2**, 754 (2006).
[5] P. Reimann, Phys. Rev. Lett. **99**, 160404 (2007).
[6] P. Reimann, Phys. Rev. Lett. **101**, 190403 (2008).
[7] One may consider all below investigations as applying to a part of the Hilbert space that corresponds to a certain energy region of the system rather than to the full Hilbert space. That amounts to microcanonical scenarios of a given finite temperatur rather than infinite temperature.
[8] J. Gemmer and G. Mahler, Eur. Phys. J. B **31**, 249 (2003).
[9] J. Gemmer, M. Michel, and G. Mahler, *Quantum Thermodynamics* (Springer, Berlin, 2004).
[10] H. P. Breuer, J. Gemmer, and M. Michel, Phys. Rev. E **73**, 016139 (2006).
[11] H. P. Breuer and F. Petruccione, *Theory of Open Quantum Systems* (Oxford University Press, Oxford, 2007).
[12] E. Fick and G. Sauermann, *The Quantum Statistics of Dynamic Processes* (Springer, Berlin, 1990).
[13] C. Bartsch, R. Steinigeweg, and J. Gemmer, Phys. Rev. E **77**, 011119 (2008).

[14] In a mathematical sense there is no relaxation since both the individual QEV's and their average are quasiperiodic for finite dimensional systems, cf. J.V. Neumann, Z. Phys. 57, 30 (1929). However, in pertinent scenarios recurrences usually occur on timescales which are long compared to any practically relevant timescale.
[15] S. Goldstein, J. L. Lebowitz, R. Tumulka, and N. Zanghi, J. Stat. Phys. **125**, 1197 (2006).
[16] P. Reimann, J. Stat. Phys. **132**, 921 (2008).
[17] U. Weiss, *Dissipative Quantum Systems* (World Scientific, Singapore, 1999).
[18] P. Pechukas, Phys. Rev. Lett. **73**, 1060 (1994).
[19] K. M. Fonseca Romero, P. Talkner, and P. Hänggi, Phys. Rev. A **69**, 052109 (2004).

Projection operator approach to master equations for coarse grained occupation numbers in non-ideal quantum gases

Christian Bartsch,[1,*] Robin Steinigeweg,[2,†] and Jochen Gemmer[1,‡]

[1] *Fachbereich Physik, Universität Osnabrück, Barbarastrasse 7, D-49069 Osnabrück, Germany*
[2] *Institut für Theoretische Physik, Technische Universität Braunschweig, Mendelsohnstrasse 3, D-38106 Braunschweig, Germany*

(Dated: January 28, 2010)

We aim at finding a set of quantitative, numerically manageable equations of motion for the occupation number dynamics in some non-ideal quantum gases featuring, e.g., electron-impurity scattering, electron-phonon scattering, electron-electron scattering, etc.. To this end we suggest the construction of a linear(ized) collision term which refers to a coarse grained set of occupation numbers by means of a projection operator technique. This collision term results as a concrete, non-singular, finite dimensional rate matrix. The coarse graining may be chosen to render the rate matrix as simple as possible, thus facilitating calculations of transport coefficients etc., as we demonstrate by a simple example.

PACS numbers: 05.30.-d, 05.70.Ln, 72.10.-d, 05.60.Gg

I. INTRODUCTION

There are many suggestions in the literature which address the mapping of the dynamics of non-ideal quantum gases onto Boltzmann equations. However, they often yield rather formal expressions for the collision terms, involving singular scattering rates, infinitely many dynamical occupation numbers, etc.. This makes them a challenging starting point for concrete numerical analysis. We first very briefly (and incompletely) review these suggestions, classified as three main groups of approaches: i) "Fermi's Golden Rule approaches", ii) "Green's-functions approaches" and iii) "factorization approaches". Of course there are many interconnections between them but for clarity we keep to this scheme here. (Readers who are familiar with the subject may simply skip this section.)

i): The square of the interaction matrix element that "connects" two occupation number eigenstates is here boldly taken as the weight of a singular, classical transition rate between those two states, which already implies a kind of random phase approximation [1]. Furthermore, it is assumed that the probabilities of the occupation number eigenstates are and remain such that mean occupation numbers factorize. This leads, e.g., to a scattering term like (1) where the n's are mean occupation numbers (see also [1–3]).

ii): The issue is approached by setting up the hierarchy of equations of motion for the Green's functions. The higher order Green's functions are then re-expressed by two-point-Green's functions using diagrammatic techniques and corresponding approximations. This results in a scattering term like (1) where the n's are related to one-mode-two-point-Green's functions, i.e., to some extent interpretable as mean occupation numbers. For details see, e.g., [4–6].

iii): The starting point are the Heisenberg equations of motion for the occupation numbers. Iterating those w.r.t. time and assuming full factorizability and diagonality of the occupation number operators at all times yields an autonomous set of equations for the mean occupation numbers. This yields a scattering term of the form denoted by (1). For details see, e.g., [7–9].

(Of course there are much more investigations of Boltzmann equations for quantum systems, some explore yet different approaches to non-ideal quantum gases such as, e.g.,[10–12], some treat other systems, e.g., [13–15], etc..)

Within the frame of quantum mechanics Boltzmann equations are routinely given as $\dot{n}_k + T_k^{\mathrm{drift}} = T_k^{\mathrm{col}}$ where $T^{\mathrm{drift}}, T^{\mathrm{col}}$ are the drift and the collision term, respectively, and k denotes the (quasi-)momentum. All the above approaches yield, e.g., for electron-impurity scattering, a collision term of the form

$$T_k^{\mathrm{col}} = 2\pi \sum_{il} |V_{k-i}|^2 \delta(E_l - E_i)(1-n_l)n_i(\delta_{lk} - \delta_{ik}) \ , \quad (1)$$

where E_k, E_i are the energies of the unperturbed single-particle modes k, i and V_{k-i} represents the respective Fourier-component of the perturbative potential due to the impurities. The δ-function results from considering a long-time limit. Since the n's are essentially mean occupation numbers of (quasi-)momentum eigenmodes the above equations of motion in this discrete form involve a number of dynamical variables that scales with the size of the crystal. This is, of course, numerically impossible to handle. Furthermore, the "rates" for the individual collision processes become singular in the long time limit as mentioned above. These difficulties eventually have to be cured by some sort of "coarse graining", i.e., by a change of perspective from considering individual occupation numbers to considering sums of occupation numbers corresponding to certain sets of modes, represented

*Electronic address: cbartsch@uos.de
†Electronic address: r.steinigeweg@tu-bs.de
‡Electronic address: jgemmer@uos.de

by the grains in momentum space. It is in general not obvious in full detail how this coarse graining has to be performed for a given, possibly rather complex model and what additional assumptions are required. And, on top of that, for many purposes in the context of linear non-equilibrium physics (, e.g., the calculation of transport coefficients, etc.), the collision term has to be linearized.

In this paper we thus suggest yet another construction of a pertinent collision term. Our construction is based on a time-convolutionless projection operator method. In a sense it "compactifies" all the above subtle steps: We start by specifying an adequate coarse graining in momentum space, thereby specifying the number of dynamical variables (which equals the number of grains). On the basis of this graining we define a pertinent corresponding projection (super-)operator. With this projector we simply perform the time-convolutionless (TCL) projection operator formalism, which is routinely used to find an autonomous set of equations of motion for the variables of interest. (Here these are, up to their equilibrium values, the joined occupation numbers of the grains.) This yields a linear(ized) collision term, i.e., a finite non-singular rate matrix for the joined occupation numbers of the grains. In this mathematical procedure no ill-controlled, additional assumptions for the dynamics have to be made. However, in the paper at hand we concentrate on a leading order truncation of the TCL-expansion (cf. (2)). Whether or not this is good enough is a somewhat subtle question but can in principle be checked by explicit evaluation of higher order terms [16]. The initial graining should be chosen with care, for it may have an influence on the validity of the truncation and it determines the concrete form of the rate-matrix. A more refined graining will facilitate the validity of the truncation (as may be inferred, e.g., from [16]) and produce a more detailed picture of the dynamics. On the other hand it will give rise to a higher dimensional rate-matrix. Thus, to put it in rough words, the graining should be chosen as coarse as possible but as fine as necessary.

Our paper is organized as follows: First (Sec.II) we give a very brief introduction to the results of the TCL projection operator formalism, again, the reader who is familiar with the subject may simply skip that. In (Sec.III) we introduce our models for the non-ideal quantum gases and specify our projection operator which is especially constructed to investigate the dynamics of the above mentioned, occupation number related variables. Then (Sec.IV) we perform leading order calculations on these models, namely for impurity scattering , electron-phonon interaction and electron-electron interaction. Those result in general but concrete expressions for the transition rates. Eventually we demonstrate (Sec.V) for the case of impurity scattering how the graining may be chosen to yield a collision term for which the relaxation-time approximation is actually exact. This facilitates the simple calculation of a diffusion coefficient.

II. TIME-CONVOLUTIONLESS PROJECTIVE APPROACH TO RELEVANT DYNAMICS

In this paragraph we give a short introduction to the TCL projection operator method [17–19]. In general, the latter is a perturbative projection operator technique which describes (the) reduced dynamics of a quantum system with a Hamiltonian of the type $H = H_0 + \lambda V$, where λV has to be small in some sense. It produces autonomous equations of motion for the variables of interest ("relevant information"). In order to apply this method one first has to construct a suitable projection (super) operator $\mathcal{P}$ which projects any density matrix $\rho(t)$ onto its relevant part. "Relevant part" here implies that $\mathcal{P}\rho(t)$, in spite of being significantly less complex than $\rho(t)$, should still contain all variables of interest. Furthermore, $\mathcal{P}$ has to satisfy the characteristic trait of a projection operator $\mathcal{P}^2\,\rho(t) = \mathcal{P}\,\rho(t)$. For initial states with $\mathcal{P}\rho(0) = \rho(0)$ the TCL scheme yields a closed time-local differential equation for the dynamics of $\mathcal{P}\rho$,

$$\frac{\partial}{\partial t}\mathcal{P}\rho(t) = \mathcal{K}(t)\mathcal{P}\rho(t), \qquad \mathcal{K}(t) = \sum_{i=1}^{\infty}\lambda^i\mathcal{K}_i(t), \qquad (2)$$

where the perturbative expansion used in the last equations is in principle (formally) exact. In this paper we exclusively focus on initial states which satisfy the above relation. For a discussion of the legitimacy of this approach see [19–22].

As already mentioned in the introduction, we furthermore focus on a description to leading order of (2). which is typically and certainly in our case the second order, i.e., we have to determine $\mathcal{K}_2(t)$. A widely accepted indicator for the validity of the truncation is a clear timescale separation between the resulting relaxation dynamics and the decay of the correlation function, the latter being introduced below.

In the literature [19] one finds

$$\mathcal{K}_2(t) = \int_0^t \mathrm{d}t_1\,\mathcal{P}\,\mathcal{L}(t)\,\mathcal{L}(t_1)\,\mathcal{P}\,. \qquad (3)$$

where $\mathcal{L}(t)\rho = -\frac{i}{\hbar}[V(t),\rho]$ corresponds to the Liouville-(super-) operator. Here and in the following all equations are denoted in the interaction picture. For a concrete application we have to specify the underlying quantum model and further a suitable projection operator.

III. STRUCTURE OF THE MODELS AND A PERTINENT PROJECTION OPERATOR

The systems we discuss here may in general be all sorts of quantum gases, but for clarity and brevity we focus on the "spinless fermions"- type here. (This refers to

the particles for which the collision term is to be constructed.)

$$H = \underbrace{\sum_{\mathbf{k}} \varepsilon_{\mathbf{k}} a^\dagger_{\mathbf{k}} a_{\mathbf{k}}}_{H_0} + V \tag{4}$$

$a^\dagger_{\mathbf{k}}, a_{\mathbf{k}}$ are electronic creation/annihilation operators in some momentum eigenmodes and $\varepsilon_{\mathbf{k}}$ denotes the corresponding dispersion relation.

The latter depends on the underlying model which is assumed to describe the non-interacting electrons, e.g., a free electron gas, a tight binding model, etc.. Or an adequate dispersion relation may be determined from an advanced solid state method such as density functional theory, etc..

Here, V refers to different pertinent interaction types, which we specify and investigate below in paragraph IV. In detail, these are electron-impurity-scattering, electron-phonon-interaction and electron-electron-interaction. All of them are treated as small perturbations (in the sense of the TCL method).

Now, in order to introduce a pertinent projection operator, we firstly need to define some basic operators. For the non-interacting many-particle system we may directly write down the wavenumber (momentum) dependent "single particle equilibrium density operator" on the mode $\mathbf{j}$ as:

$$\rho^{\mathrm{eq}}_{\mathbf{j}} := f_{\mathbf{j}}(\mu, T) a^\dagger_{\mathbf{j}} a_{\mathbf{j}} + (1 - f_{\mathbf{j}}(\mu, T)) a_{\mathbf{j}} a^\dagger_{\mathbf{j}}, \tag{5}$$

with $f_{\mathbf{j}}(\mu, T) = (\exp((\varepsilon(\mathbf{j}) - \mu)/k_B T) + 1)^{-1}$ being the Fermi distribution. Since we are interested in low temperature regimes we may substitute (approximate) the chemical potential μ by the Fermi energy ε_F. Further we abbreviate $f_{\mathbf{j}}(\varepsilon_F, T)$ as $f_{\mathbf{j}}$.

The equilibrium density operator, again for the non-interacting case, of the total system (, i.e., H_0), ρ^{eq}, may be written as the tensor product of the single particle density operators, i.e.,

$$\rho^{\mathrm{eq}} := \bigotimes_{\mathbf{i}} \rho^{\mathrm{eq}}_{\mathbf{i}}. \tag{6}$$

We should mention here for later reference that, while ρ^{eq} is strictly speaking just the equilibrium state of the non-interacting system, it is routinely considered to describe the equilibrium single particle properties of the weakly interacting system more or less correctly. Thus, if single particle observables relax towards equilibrium due to the interactions (scattering), we expect them to relax towards values corresponding to ρ^{eq}.

Furthermore, we define an operator $\Delta_{\mathbf{j}}$ as

$$\Delta_{\mathbf{j}} := (1 - f_{\mathbf{j}}) a^\dagger_{\mathbf{j}} a_{\mathbf{j}} - f_{\mathbf{j}} a_{\mathbf{j}} a^\dagger_{\mathbf{j}} = a^\dagger_{\mathbf{j}} a_{\mathbf{j}} - f_{\mathbf{j}}, \tag{7}$$

which describes the deviation of the mode occupation number $n_{\mathbf{j}} = a^\dagger_{\mathbf{j}} a_{\mathbf{j}}$ from its thermal equilibrium.

In order to concretize the projector further we must now introduce the afore mentioned coarse graining in momentum space. Eventually this means that we have to define domains in momentum space; we label those regions by Greek indices (κ, η). Different occupation numbers corresponding to the same region will no longer be investigated separately from each other, the remaining variables will simply be the sums over occupation numbers belonging to the various domains. The concrete choice of the domains substantially influences the result of the following considerations, as will become clear in the remainder of this paper. However, at this point we simply mathematically define operators Δ^κ describing the summed deviations (from equilibrium) of all occupation numbers belonging to a common domain

$$\Delta^\kappa = \sum_{\mathbf{j} \in \kappa} \Delta_{\mathbf{j}} \ . \tag{8}$$

Furthermore, we define operators

$$D_{\mathbf{j}} := \bigotimes_{\mathbf{i} \neq \mathbf{j}} \rho^{\mathrm{eq}}_{\mathbf{i}} \otimes (a^\dagger_{\mathbf{j}} a_{\mathbf{j}} - a_{\mathbf{j}} a^\dagger_{\mathbf{j}}) \tag{9}$$

$D_{\mathbf{j}}$ corresponds to a diagonal product operator that equals the equilibrium density operator on all modes except $\mathbf{j}$.

Moreover, we abbreviate the time dependent expectation value of Δ^κ, which we are mainly interested in by $d^\kappa(t)$:=$\mathrm{Tr}\{\Delta^\kappa \rho(t)\}$, where $\rho(t)$ is the density operator which describes the actual state of the system.

With these preliminary definitions we construct a suitable projector as follows:

$$\mathcal{P}\rho(t) = \rho^{\mathrm{eq}} + \sum_\kappa \frac{1}{N_\kappa} (\sum_{\mathbf{j} \in \kappa} D_{\mathbf{j}}) d^\kappa(t) \tag{10}$$

(Note that a similar projector has recently been used in the context of investigations on electronic lifetimes in aluminum [23].)

It is straightforward to prove that this projector indeed features the crucial property of a projection operator, i.e., $\mathcal{P}^2 = \mathcal{P}$. It furthermore obviously captures the dynamical variables of interest, namely the d^κ.

Before we eventually concretely apply (2) we make the following approximation for an expression that appears in the computation of (2):

$$\frac{\imath}{\hbar}[V(t), \rho^{\mathrm{eq}}] \approx 0 \tag{11}$$

The neglected commutator term essentially describes the dynamics of the equilibrium state of the non-interacting system. Eventually we are interested in a single particle observable. As already mentioned above, the equilibrium state of the non-interacting system is believed to reasonably describe single particle observables in equilibrium even for weakly interacting systems. Since an equilibrium state is constant, the above commutator should

not significantly contribute to the relevant dynamics, thus we drop it. Keeping the term and performing all following steps eventually yields an expression which can be explicitly shown to be indeed negligible in the weak coupling limit. For clarity and briefness we omit this calculation here.

Now, we explicitly evaluate (2) to leading, i.e., second order using the above projector. In order to extract from this equation of motion for operators an equation of motion for the scalar observables of interest (which are the $d^\eta(t)$) we multiply by Δ^η and take a trace:

$$\frac{\partial}{\partial t}\mathrm{Tr}\{\Delta^\eta \mathcal{P}\rho(t)\} = \mathrm{Tr}\{\Delta^\eta \mathcal{K}_2(t)\mathcal{P}\rho(t)\} \tag{12}$$

Realizing that $\mathrm{Tr}\{D_\mathbf{j}\Delta_\mathbf{l}\} = \delta_{\mathbf{j},\mathbf{l}}$ and $[V(t),\Delta_\mathbf{k}] = [V(t),n_\mathbf{k}]$, furthermore employing (11) and some invariance properties of the trace, we find after a lengthy but straightforward calculation:

$$\dot{d}^\eta(t) = \sum_\kappa \int_0^t \mathrm{d}t_1 \underbrace{\frac{1}{\hbar^2 N_\kappa}\sum_{\substack{\mathbf{i}\in\kappa,\\ \mathbf{k}\in\eta}} -\mathrm{Tr}\{D_\mathbf{i}[V(t_1),[V(t),n_\mathbf{k}]]\}}_{C_{\eta\kappa}(t,t_1)} d^\kappa(t) \tag{13}$$

This is our first main result. Obviously (13) may be interpreted as a rate equation for the dynamics of the coarse grained occupation numbers. It thus corresponds to a linear(ized) collision term. The rates, which are typically finite and directly computable, are given by $R_{\eta\kappa}(t) := \int_0^t \mathrm{d}t_1 C_{\eta\kappa}(t,t_1)$. They may in general be time-dependent which does not fit in to the standard picture. But, as they are given by integrals over correlation functions, they can be expected to converge to constant values after some correlation times under some rather mild conditions on the model and the graining. For a concrete example for the evaluation of the rates see Sec.V.

For most routinely considered interactions (and all interactions analyzed in this paper) the particle number within the specifically addressed system (e.g., electron system) ($N = \sum_\mathbf{k} n_\mathbf{k}$) is conserved. Thus

$$\sum_{\mathbf{k}\in\eta} n_\mathbf{k} = N - \sum_{\kappa\neq\eta}\sum_{\mathbf{l}\in\kappa} n_\mathbf{l} \tag{14}$$

holds. Exploiting this feature, we may determine the diagonal rate terms of the rate equation (13) from the non-diagonal terms by inserting (14) into (13)

$$R_{\eta\eta} = -\sum_{\kappa\neq\eta} R_{\kappa\eta}\ . \tag{15}$$

Thus, the rate equation (13) may here be classified as a master equation which is consistent with its interpretation as a collision term in a Boltzmann equation.

For the following calculations it turns out to be convenient to reformulate the trace term from (13):

$$\begin{aligned} &-\mathrm{Tr}\{D_\mathbf{i}[V(t_1),[V(t),n_\mathbf{k}]]\} = \\ &-(\mathrm{Tr}\{V(t)V(t_1)n_\mathbf{k}D_\mathbf{i}\} + h.c.) \\ &+(\mathrm{Tr}\{V(t)n_\mathbf{k}V(t_1)D_\mathbf{i}\} + h.c.)\ , \end{aligned} \tag{16}$$

where we have used that $D_\mathbf{i}$ commutes with $n_\mathbf{k}$. Note that the Hermitian conjugate is of identical form, respectively, except exchanged time arguments.

The physical implications of (13) may become more transparent if it is applied to concrete models and some pertinent interactions are inserted. This is done for some examples in the next Section.

IV. APPLICATION TO MODELS WITH DIFFERENT INTERACTIONS

A. Electron-Impurity-Scattering

Firstly, we apply the method introduced above to a quantum gas model with electronic impurity scattering, i.e., in addition to a periodic crystal lattice potential the electron is subject to a weak, random non-periodic potential. The latter of course induces the scattering. (One may think here for example of an Anderson model with very weak on-site disorder, way down below the critical disorder, cf. [24].) A corresponding Hamiltonian may be given by

$$H = \underbrace{\sum_\mathbf{n} \varepsilon_\mathbf{n} a^\dagger_\mathbf{n} a_\mathbf{n}}_{H_{0,\mathrm{el}}} + \underbrace{\sum_{\mathbf{k},\mathbf{q}} \frac{W(\mathbf{q})}{\sqrt{\Omega}} a^\dagger_{\mathbf{k}+\mathbf{q}} a_\mathbf{k}}_{V}\ . \tag{17}$$

Here $W(\mathbf{q})$ simply denotes the corresponding spatial Fourier component of the random impurity potential and Ω corresponds to the total number of discrete (quasi-)momenta, i.e., Ω scales with the volume of the crystal. The above "interaction term V" has to be inserted into Eq.(13) to determine the scattering rates $R_{\eta\kappa}(t)$. We evaluate the traces in (16) by identifying all contributing diagonal terms, i.e., terms that contain equally many creation and annihilation operators acting on a single $\mathbf{k}$-mode. In doing so it proves to be advantageous that both $D_\mathbf{i}$ and $n_\mathbf{k}$ factorize onto the single $\mathbf{k}$-modes and, furthermore, are diagonal on each $\mathbf{k}$-mode. After some straightforward calculation we arrive at

$$\begin{aligned} &-\mathrm{Tr}\{D_\mathbf{i}[V(t_1),[V(t),n_\mathbf{k}]]\} = \\ &\frac{|W(\mathbf{k}-\mathbf{i})|^2}{\Omega}(f_\mathbf{k} + (1-f_\mathbf{k}))\cdot 2\cos[\frac{1}{\hbar}(\varepsilon_\mathbf{i}-\varepsilon_\mathbf{k})(t-t_1)], \end{aligned} \tag{18}$$

where we have used $W(\mathbf{q}) = W^*(-\mathbf{q})$ (, since the interaction potential should be real in configuration space).

We finally obtain for the rates

$$R_{\eta\kappa}(t) = \int_0^t \mathrm{d}\tau \frac{2}{\hbar^2 N_\kappa} \sum_{\substack{\mathbf{i}\in\kappa,\\ \mathbf{k}\in\eta}} \frac{|W(\mathbf{k}-\mathbf{i})|^2}{\Omega} \cos[\frac{1}{\hbar}(\varepsilon_{\mathbf{i}} - \varepsilon_{\mathbf{k}})\tau] \ , \tag{19}$$

with $\tau := t - t_1$.

Note, that the resulting rates are completely independent of any equilibrium occupation numbers, i.e, the linear dynamics do not depend on the position in momentum space at which particles have been added or taken away. Or, to rephrase, deviations from equilibrium relax all in the same way regardless of whether they occur above, below, or at the Fermi-level.

B. Electron-Phonon-Interaction

One important mechanism that is commonly believed to mainly control electronic transport in metals is electron-phonon-scattering. To investigate this case, we routinely assume a Hamiltonian of the following form:

$$H = \underbrace{\sum_{\mathbf{n}} \varepsilon_{\mathbf{n}} a^\dagger_{\mathbf{n}} a_{\mathbf{n}}}_{H_{0,\mathrm{el}}} + \underbrace{\sum_{\mathbf{i}} \omega_{\mathbf{i}} b^\dagger_{\mathbf{i}} b_{\mathbf{i}}}_{H_{0,\mathrm{ph}}} + \underbrace{(\sum_{\mathbf{k},\mathbf{q}} \frac{W(\mathbf{q})}{\sqrt{\Omega}} a^\dagger_{\mathbf{k}+\mathbf{q}} a_{\mathbf{k}} b_{\mathbf{q}} + h.c.)}_{V}, \tag{20}$$

where $b^\dagger_{\mathbf{i}}, b_{\mathbf{i}}$ are (bosonic) creation/annihilation operators corresponding to some phonon eigenmodes (labelled by $\mathbf{i}$) and $\omega_{\mathbf{i}}$ denotes the corresponding phononic dispersion relation. This Hamiltonian is of the quantum gas type we have introduced above (4), but with an additional phononic Hamiltonian $H_{0,\mathrm{ph}}$. The interaction V may be viewed as representing processes in which an electron is scattered under the annihilation/creation of a phonon such that the complete momentum is conserved.

We choose here to project onto deviations from equilibrium in the electronic system only, i.e., phononic occupation numbers are not treated as dynamical variables but their equilibrium values rather enter as parameters. To this end we keep the projection operator essentially as given in (10) but multiply ρ^{eq} and $D_{\mathbf{j}}$ by $\rho^{\mathrm{eq,\ Ph}}$, the latter being the equilibrium state of the phononic system (which in itself is an ideal gas). A corresponding calculation (which is essentially very similar to the previous one for electron-defect-scattering) yields

$$\begin{aligned}
&-\mathrm{Tr}\{D_{\mathbf{i}}[V(t_1),[V(t),n_{\mathbf{k}}]]\} = \\
&\frac{|W(\mathbf{i}-\mathbf{k})|^2}{\Omega}(f_{\mathbf{k}} g_{\mathbf{i}-\mathbf{k}} + (1-f_{\mathbf{k}})(1+g_{\mathbf{i}-\mathbf{k}})) \\
&\cdot 2\cos[\frac{1}{\hbar}(\varepsilon_{\mathbf{i}} - \varepsilon_{\mathbf{k}} - \omega_{\mathbf{i}-\mathbf{k}})(t-t_1)] \\
&+\frac{|W(\mathbf{k}-\mathbf{i})|^2}{\Omega}(f_{\mathbf{k}}(1+g_{\mathbf{k}-\mathbf{i}}) + (1-f_{\mathbf{k}}) g_{\mathbf{k}-\mathbf{i}}) \\
&\cdot 2\cos[\frac{1}{\hbar}(\varepsilon_{\mathbf{i}} - \varepsilon_{\mathbf{k}} + \omega_{\mathbf{k}-\mathbf{i}})(t-t_1)] \ ,
\end{aligned} \tag{21}$$

where we have used $\mathrm{Tr}\{\rho^{\mathrm{eq,\ Ph}} b^\dagger_{\mathbf{q}} b_{\mathbf{q}}\} = g_{\mathbf{q}}$.

In many pertinent systems, the phonon energies are considered to be small compared to the electron energies. Thus, neglecting the phonon energies ($\omega_{\mathbf{k}-\mathbf{i}} \approx 0$) and again exploiting $W(\mathbf{q}) = W^*(-\mathbf{q})$, we may further simplify (21) and obtain for the transition rates of Eq.(13) ($\kappa \neq \eta$)

$$\begin{aligned}
&R_{\eta\kappa}(t) = \\
&\int_0^t \mathrm{d}\tau \frac{2}{\hbar^2 N_\kappa} \sum_{\substack{\mathbf{i}\in\kappa,\\ \mathbf{k}\in\eta}} \frac{|W(\mathbf{k}-\mathbf{i})|^2}{\Omega}(1+g_{\mathbf{k}-\mathbf{i}}+g_{\mathbf{i}-\mathbf{k}}) \cos[\frac{1}{\hbar}(\varepsilon_{\mathbf{i}}-\varepsilon_{\mathbf{k}})\tau].
\end{aligned} \tag{22}$$

Thus, according to this approximation, the rate matrix is essentially of the same form as in the case of impurity scattering, except for the equilibrium phonon occupation numbers. (For another time-convolutionless master equation approach to the dynamics of phonon-coupled systems see [25].)

C. Electron-Electron-Interaction

In this paragraph we apply the above method to a system featuring electron-electron-interaction. A corresponding Hamiltonian may read

$$H = \underbrace{\sum_{\mathbf{n}} \varepsilon_{\mathbf{n}} a^\dagger_{\mathbf{n}} a_{\mathbf{n}}}_{H_{0,\mathrm{el}}} + \underbrace{\frac{1}{2} \sum_{\mathbf{k},\mathbf{l},\mathbf{q}} \frac{W(\mathbf{q})}{\Omega} a^\dagger_{\mathbf{k}+\mathbf{q}} a^\dagger_{\mathbf{l}-\mathbf{q}} a_{\mathbf{k}} a_{\mathbf{l}}}_{V} \ . \tag{23}$$

The evaluation of the trace term (16) is basically similar to the previous examples. Nevertheless, identifying all contributing terms proves in this case to be somewhat subtle. However, simply following the scheme, we arrive after some lengthy calculation at

$$\begin{aligned}
&R_{\eta\kappa}(t) = \int_0^t \mathrm{d}\tau \frac{2}{\hbar^2 N_\kappa} \sum_{\substack{\mathbf{i}\in\kappa,\\ \mathbf{k}\in\eta}} \sum_{\mathbf{l}} \\
&(\mathrm{Re}(W(\mathbf{i}-\mathbf{k})) - \mathrm{Re}(W(\mathbf{k}-\mathbf{l})))^2 \cdot \frac{1}{\Omega^2} \\
&(f_{\mathbf{l}}(1-f_{\mathbf{i}-\mathbf{k}+\mathbf{l}})(1-f_{\mathbf{k}}) + f_{\mathbf{k}} f_{\mathbf{i}-\mathbf{k}+\mathbf{l}}(1-f_{\mathbf{l}})) \\
&\cos[\frac{1}{\hbar}(\varepsilon_{\mathbf{i}} + \varepsilon_{\mathbf{l}} - \varepsilon_{\mathbf{k}} - \varepsilon_{\mathbf{i}-\mathbf{k}+\mathbf{l}})\tau] \\
&-(\mathrm{Re}(W(\mathbf{l}-\mathbf{i})) - \mathrm{Re}(W(\mathbf{k}-\mathbf{l})))^2 \cdot \frac{1}{\Omega^2} \\
&(f_{\mathbf{k}}(1-f_{\mathbf{i}+\mathbf{k}-\mathbf{l}})(1-f_{\mathbf{l}}) + f_{\mathbf{l}} f_{\mathbf{i}+\mathbf{k}-\mathbf{l}}(1-f_{\mathbf{j}})) \\
&\cos[\frac{1}{\hbar}(\varepsilon_{\mathbf{k}} + \varepsilon_{\mathbf{i}} - \varepsilon_{\mathbf{i}+\mathbf{k}-\mathbf{l}} - \varepsilon_{\mathbf{l}})\tau] \ .
\end{aligned} \tag{24}$$

Here we have again used that $W(\mathbf{q}) = W^*(-\mathbf{q})$ and therefore $W(\mathbf{q}) + W(-\mathbf{q}) = 2\mathrm{Re}(W(\mathbf{q}))$.

Collecting all terms that can be converted into each other by permutation of creation/annihilation operators gives rise to the emergence of anti-symmetric interaction

matrix elements. For the electron-electron interaction the rates contain an additional sum over all states in momentum space that does not appear in the previous examples. This makes the computation perhaps more extensive, but does not cause any principle problems.

V. APPLICATION: DIFFUSION COEFFICIENT OF THE 3-DIM ANDERSON MODEL WITH WEAK DISORDER

In this section we aim at finding the diffusion coefficient for a 3-d Anderson model including very weak, uncorrelated disorder, i.e., such that almost all states are non-localized, cf. Sec. IV A. To this end we first determine a pertinent scattering rate matrix. Especially, we choose a specific coarse graining that yields a rate matrix which strictly obeys the relaxation time approximation (cf. [26]) and therefore allows for a simple computation of a diffusion coefficient. The underlying Hamiltonian has the form of Eq. (17) (electron-defect-scattering). The corresponding dispersion relation is given by

$$\varepsilon_{\mathbf{k}} = -2J(\cos k_x + \cos k_y + \cos k_z) \ , \tag{25}$$

where J is an energy determining the bandwidth (bandwidth=$12J$). We focus here on random uncorrelated on-site disorder, i.e., the $W(\mathbf{q})$'s are assumed to be given by independent random numbers, generated according to some distribution. As explained below, for this setting only the mean square of the $W(\mathbf{q})$'s eventually enters the rate matrix, thus for our purposes we do not even need to explicitly name the type of distribution here.

At this point, we specify the graining in detail. The momentum space is firstly divided into domains corresponding to energy shells of equal energy width ΔE (according to the dispersion relation). Then we further divide the energy shells (labelled by E) into g_E domains, such that each of these domains contains equally many states N which implies equal volumes in momentum space. Fig. 1 shows an example of this type of coarse graining for the 2-dimensional case. We assume that the grains are small enough that the dispersion relation may be linearized on each grain. Further, we define

$$\overline{W^2_{\eta\kappa}} = \sum_{\substack{\mathbf{i}\in\kappa,\\ \mathbf{k}\in\eta}} |W(\mathbf{k}-\mathbf{i})|^2 \cdot \frac{1}{N_\kappa N_\eta} \ . \tag{26}$$

Due to the disorder being uncorrelated we get $\overline{W^2_{\eta\kappa}} = W^2 = \text{const.}$, i.e., $\overline{W^2_{\eta\kappa}}$ is independent of the domains. Exploiting this (and routinely the properties of the *sinc*-function) we can approximately perform the integration in (19), thus finding for times larger than the correlation time the non-diagonal elements of the rate matrix ($\eta \neq \kappa$)

$$R_{\eta\kappa} = \frac{2\pi W^2}{\hbar}\frac{N}{\Delta E}\delta_{E(\eta),E(\kappa)} \ , \tag{27}$$

where $\delta_{E(\eta),E(\kappa)}$ is 1 if η and κ belong to the same energy shell and 0 otherwise. So, there are only transition rates between domains within the same energy shell. Furthermore, due to the specific coarse graining, these rates are equal for all transitions within one energy shell, i.e., there is no dependence on η and κ.

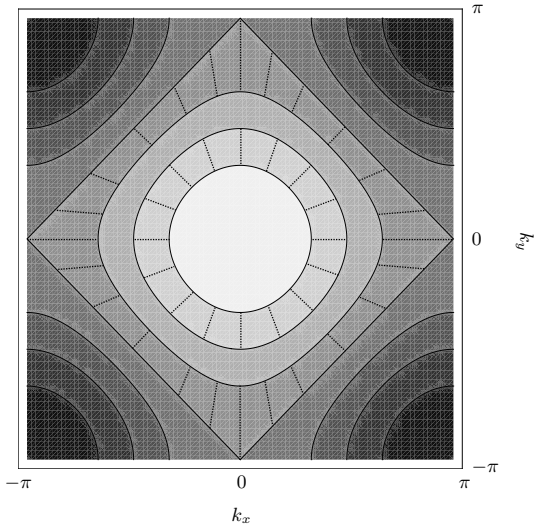

FIG. 1: Sketch of our specific coarse graining in momentum space for a 2-d Anderson model. Contour lines of equal energy define energy shells of equal energy width ΔE. Within two exemplary shells the full detailed graining is displayed: the shell is orthogonally partitioned into g_E domains of equal area. This amounts to an equal number of states per domain.

The total number of states within some energy shell E, which we label by N_E, is $Ng_E = N_E$. As already mentioned, the diagonal terms of the rate matrix may be obtained from the master equation property (Eq.(15)). By means of the abbreviation

$$R^E := \frac{2\pi W^2}{\hbar}\frac{N_E}{\Delta E} \ , \tag{28}$$

the rates may be eventually written as

$$R^E_{\eta\kappa} = \frac{R^E}{g_E} - \delta_{\eta,\kappa}R^E \ . \tag{29}$$

To repeat, the non-diagonal elements of this rate matrix are all equal and thus, this specific graining yields symmetric detailed balance. As well-known the equilibrium state, i.e., equilibrium set of "grain occupation probabilities" (mathematically: the eigenvector belonging to the eigenvalue 0) for this type of master equation is the uniform distribution. The corresponding vector of probabilities (all concentrated at the energy E) reads:

$$\vec{P}_0 : P_{0,\kappa} = \frac{1}{g_E} \tag{30}$$

Furthermore, all other states $\vec{X}$ which are orthogonal to the equilibrium state ($\vec{X}\vec{P}_0 = 0$) span the (highly degenerate) eigenspace of the rate matrix with eigenvalue

$-R^E$. Thus all deviations from equilibrium at energy E relax exponentially with a rate R^E. This is precisely what is called the relaxation time approximation [26].

Having found this rate matrix we are all set for the calculation of the corresponding diffusion coefficient. There are several approaches to the derivation of a diffusion coefficient from a linear(ized) Boltzmann equation. Here we follow [15] and references therein by using the formula

$$D = -v_\eta R^{-1}_{\eta\kappa} v_\kappa P^0_\kappa \ , \tag{31}$$

where D is the diffusion coefficient, v_η, v_κ are the velocities corresponding to the respective momenta, $R^{-1}_{\eta\kappa}$ is the (pseudo-)inverted rate matrix (neglecting the null-space) and P^0_κ denotes the equilibrium distribution. For the velocities v_κ we routinely plug in the slope of the dispersion relation in, say, x-direction at the respective grains κ (group velocity). These slopes are approximately constant within one grain, given one employs the above mentioned graining. Due to the symmetry of the dispersion relation the vector $v_\kappa P^0_\kappa$ does not have any overlap with the null-space of the rate matrix, i.e., $\sum_\kappa P^0_\kappa v_\kappa P^0_\kappa = 0$. Hence $R^{-1}_{\eta\kappa}$ from (31) may simply be replaced by $-1/R^E$, i.e., the inverse of the eigenvalue of the eigenspace that is complementary to the null-space. Hence, we can evaluate formula (31) and eventually find for the diffusion coefficient at energy E

$$D_E = \frac{1}{R^E} \sum_{\kappa \in E} v_\kappa^2 \frac{1}{g_E} = \frac{1}{R^E} \overline{v^2} \ . \tag{32}$$

Thus the (shell-specific) diffusion coefficient is completely determined by the total decay rates R^E and the averaged squared velocity in x-direction $\overline{v^2}$. This expression (32) may easily be evaluated using any standard computer. The result is displayed in Fig.2.

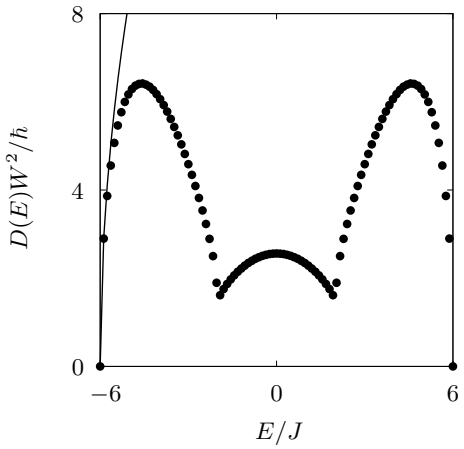

FIG. 2: Energy dependent diffusion coefficient for a 3-d Anderson model with weak disorder according to formula (32) (dotted curve). The structure is much richer than the one obtained from a free-electron approximation (solid line).

Obviously the spectrum of diffusion coefficients features a non-trivial structure. A "free-electron approximation", i.e., replacing the true dispersion relation by a pertinent parabolic one, makes the calculation much easier (can be done analytically), but only describes the true diffusion coefficients at the outer edges of the peaks more or less correctly.

VI. SUMMARY AND OUTLOOK

We computed linear(ized) master equations describing the dynamics of some coarse grained set of occupation numbers in non-ideal quantum gases, featuring i) impurity scattering, ii) electron-phonon scattering and iii) electron-electron scattering, by means of the TCL projection operator method. The resulting rate matrices are of finite dimension and contain only finite rates. Their concrete forms, including their dimensions, depend crucially on the way the coarse graining is performed (and on the concrete models of course). The rates are given as sums or integrals of pertinent functions over domains in (quasi-)momentum space. They may in general efficiently be numerically evaluated using moderate computing power. The choice of a specific graining may yield an especially convenient form of the rate matrix, e.g., all non-diagonal entries equal, etc.. Such simple forms may facilitate further considerations based on those rate matrices such as, e.g., computation of diffusion coefficients. As an instructive example we presented the calculation of the diffusion coefficient for a 3-d Anderson model with weak, uncorrelated disorder. The expressions for the rate matrices may also serve as a basis for computations of diffusion coefficients in other systems. One may think of electronic diffusion in bulk metals (primarily due to phonon coupling) but also of electronic diffusion in low dimensional systems such as nanowires embedded in bulk insulators. Furthermore, diffusion coefficients in low dimensional systems controlled by particle-particle interactions may be addressed (cf. [27]). The diffusion coefficients may be converted to conductivities using a generalized Einstein relation (cf. [28]). Thus the results presented here may be used for certain concrete transport-theoretical investigations. The feasibility of such an approach is supported by the fact that a similar approach has been demonstrated to yield reasonable results for electronic lifetimes in aluminum [23].

Acknowledgments

We sincerely thank M. Kadirogˇlu for his contributions to fruitful discussions. Financial support by the "Deutsche Forschungsgemeinschaft" is gratefully acknowledged.

[1] R. E. Peierls, *Quantum Theory of Solids* (Clarendon, Oxford, 2001).
[2] S. Lepri, R. Livi, and A. Politi, Phys. Rep. **377**, 1 (2003).
[3] J. Jäckle, *Einführung in die Transporttheorie* (Vieweg, Braunschweig, 1978).
[4] L. P. Kadanoff and G. Baym, *Quantum Statistical Mechanics* (Benjamin, New York, 1962).
[5] J. Rammer and H. Smith, Rev. Mod. Phys. **58**, 323 (1968).
[6] D. N. Zubarev, V. Morozov, and G. Ropke, *Statistical Mechanics of Nonequilibrium Processes: Basic Concepts, Kinetic Theory* (John Wiley and Sons, 1996).
[7] L. Erdös, M. Salmhofer, and H.-T. Yau, arXiv:math-ph/0302034 (2003).
[8] H. Haug, *Statistische Physik: Gleichgewichtstheorie und Kinetik* (Springer, Berlin Heidelberg, 2006).
[9] L. A. Banyai, *Lectures on Non-Equilibrium Theory of Condensed Matter* (World Scientific, 2006).
[10] K. Aoki, J. Lukkarinen, and H. Spohn, J. Stat. Phys. **124**, 1105 (2006).
[11] J. Koide, J. Phys. A: Math. Gen. **33**, 127 (2000).
[12] D. Benedetto, F. Castella, R. Esposito, and M. Pulvirenti, J. Stat. Phys. **114**, 381 (2004).
[13] K. Hornberger, Phys. Rev. Lett. **97**, 060601 (2006).
[14] B. Vacchini, Int. J. Theor. Phys. **4**, 1011 (2005).
[15] M. Kadirōglu and J. Gemmer, Phys. Rev. B **76**, 024306 (2007).
[16] C. Bartsch, R. Steinigeweg, and J. Gemmer, Phys. Rev. E **77**, 011119 (2008).
[17] S. Chaturvedi and F. Shibata, Z. Phys. B **35**, 297 (1979).
[18] H. P. Breuer, J. Gemmer, and M. Michel, Phys. Rev. E **73**, 016139 (2006).
[19] H. P. Breuer and F. Petruccione, *Theory of Open Quantum Systems* (Oxford University Press, Oxford, 2007).
[20] H. Grabert, P. Talkner, and P. Hänggi, Z. Physik B **26**, 389 (1977).
[21] K. M. Fonseca Romero, P. Talkner, and P. Hänggi, Phys. Rev. A **69**, 052109 (2004).
[22] C. Bartsch and J. Gemmer, Phys. Rev. Lett. **102**, 110403 (2009).
[23] M. Kadirōglu and J. Gemmer, Phys. Rev. B **79**, 134301 (2009).
[24] H. Grussbach and M. Schreiber, Phys. Rev. B **51**, 663 (1995).
[25] V. Pouthier, Phys. Rev. B **80**, 144304 (2009).
[26] C. Kittel, *Introduction to Solid State Physics* (John Wiley and Sons, 2004).
[27] J. Sirker, R. G. Pereira, and I. Affleck, Phys. Rev. Lett. **103**, 216602 (2009).
[28] R. Steinigeweg, H. Wichterich, and J. Gemmer, Europhys. Lett. **88**, 10004 (2009).

Width dependence of transport coefficients for models of atomic wires coupled to phonons

Christian Bartsch[1,*] and Jochen Gemmer[1,†]

[1] *Fachbereich Physik, Universität Osnabrück, Barbarastrasse 7, D-49069 Osnabrück, Germany*

(Dated: January 29, 2010)

We consider models of quasi-1-d, planar atomic wires consisting of several, laterally coupled rows of atoms, with mutually non-interacting electrons. This electronic wire system is coupled to phonons, corresponding, e.g., to some substrate. We aim at computing diffusion coefficients in dependence on the wire widths and the lateral coupling. To this end we firstly construct a numerically manageable linear collision term for the dynamics of the electronic occupation numbers by following a certain projection operator approach. By means of this collision term we set up a linear Boltzmann equation. A formula for extracting diffusion coefficients from such Boltzmann equations is given. We find in the regime of a few atomic rows and intermediate lateral coupling a significant and non-trivial dependence of the diffusion coefficient on both, the width and the lateral coupling.

PACS numbers: 05.30.-d, 05.70.Ln, 72.10.-d, 05.60.Gg

I. INTRODUCTION

The strong desire for an ongoing miniaturization of electronic circuits has led to the idea of molecular electronics. Very roughly molecular electronics include all implementations of basic electronic functional devices on the scale of atoms or molecules. The most basic device surely is a wire, meaning a system in which an electronic current may flow as a response to an electric field in a prescribed direction. Various implementations of such atomic wires have been suggested and experimentally explored. Some suggestions are based on the concept of running current through chemically synthesized, mechanically more or less chainlike molecules [1]. Others are essentially continuations of existing lithographic techniques, imprinting extremely small structures into semiconductors [2]. Yet another scheme relies on the formation of chains or rows of atoms or molecules, most likely on the surface of some substrate. The current is then supposed to flow from molecule to molecule (and not or only negligibly into the substrate). The formation of such linear molecular structures is thought to be achieved by self-assembly, possibly influenced or controlled by structures on the substrate surface [3]. Present experimental efforts mainly concentrate on the sufficiently controlled fabrication of the respective system that represents the wire. Mechanical and chemical stability are still to be considered. So far not much experimental data on the conductivities of such wires is available, except for the implementation of the single molecule contacted at both ends [4, 5].

Nevertheless we address the question of transport properties of some "ideal" atomic wire of the "self-assembled-atoms-type" in the paper at hand. Our investigations are based on an extremely simplified model. We consider a periodic, infinitely long, linear structure of atoms. The structure consists of several, parallel, monoatomic chains of atoms. The chains are coupled to each other with some coupling strength. Primarily for simplicity we consider the electrons on the wire as mutually non-interacting which makes the isolated wire itself a ballistic conductor. However, there are investigations indicating that one-dimensional structures tend towards ballistic behavior even if the particles are interacting, due to integrability [6–9]. In our model the ballistic electronic system is coupled to phonons, which may be viewed as being due to the lattice dynamics of the substrate. As expected this phonon-coupling is found to induce diffusive transport behavior. We calculate the diffusion coefficient in dependence on the number of parallel rows and the coupling between the rows finding a strong dependence on both.

This paper is organized as follows. In Sec. II we firstly introduce the above quantum model of the wire in detail. In Sec. III we formulate, based on the model, a linear(ized) master equation for the dynamics of some variables which correspond to (coarse grained) occupation numbers of electronic momentum modes. This is done on the basis of an approach from [10]. In Sec. IV we suggest an approach for calculating a diffusion coefficient from a pertinent, linear Boltzmann equation. By means of the previously formulated master equation we set up such a linear Boltzmann equation describing the electronic dynamics of our model. Finally, in Sec. V we numerically evaluate the obtained formula for the diffusion coefficient and analyze the dependence of the diffusion coefficient on the number of neighboring rows as well as on on the lateral coupling strength between neighboring rows. We close with summary and outlook.

*Electronic address: cbartsch@uos.de
†Electronic address: jgemmer@uos.de

II. INTRODUCTION OF THE MODEL

Routinely we open the considerations by specifying the underlying quantum model on the basis of which we below analyze the dynamical properties of the atomic wires. The Hamiltonian consists of three parts: an electronic part $H_{0,\mathrm{el}}$ describing the hypothetically unperturbed electrons on the wire, a phononic part $H_{0,\mathrm{ph}}$ representing a standard set of decoupled phononic modes and an interaction V which couples the electrons to the phonons:

$$H = \underbrace{\sum_{\mathbf{j}}\sum_{r=1}^{B}\varepsilon_{\mathbf{j},r}a^{\dagger}_{\mathbf{j},r}a_{\mathbf{j},r}}_{H_{0,\mathrm{el}}} + \underbrace{\sum_{\mathbf{i}}\omega_{\mathbf{i}}b^{\dagger}_{\mathbf{i}}b_{\mathbf{i}}}_{H_{0,\mathrm{ph}}} + \underbrace{(\sum_{\mathbf{k},\mathbf{q}}\sum_{r,s=1}^{B}\frac{W_{rs}(\mathbf{q})}{\sqrt{\Omega}}a^{\dagger}_{\mathbf{k}+\mathbf{q},r}a_{\mathbf{k},s}b_{\mathbf{q}}+h.c.)}_{V}, \quad (1)$$

with $\Omega = BL$.

A real space sketch of the electronic part is depicted in Fig. 1. We assume a quasi-1-d, planar, cubic lattice of atoms that forms the wire. Concretely we assume that the electrons may occupy localized (Wannier) states at those lattice sites, i.e., a standard tight-binding description. The wire now consists of a finite, possibly small integer number B of parallel rows of atoms. The motion of the electrons along the rows is controlled by nearest neighbor hopping matrix elements of strength $T_{\parallel}$. The hopping from one row to the adjacent row(s) is controlled by matrix elements of strengths $T_{\perp}$. The electrons on the wire are assumed to experience no mutual interactions, i.e, without any further coupling their dynamics would be simply ballistic. Since the wire is furthermore strictly periodic along the rows, its Hamiltonian may be denoted based on the dispersion relation $\varepsilon_{\mathbf{j},r}$ as done in (1). Here $\varepsilon_{\mathbf{j},r}$ denotes the one-particle-energy corresponding to the lattice-momentum $\mathbf{j}$ and the "branch" r. Due to the B parallel rows the dispersion relation features B branches or "bands". Fourier transforming the Hamiltonian described by Fig. 1 essentially yields

$$\varepsilon_{\mathbf{j},r} = \underbrace{-2T_{\parallel}\cos\mathbf{j}}_{\varepsilon_{\mathbf{j}}} + T_{\perp}\varepsilon_r \ , \quad (2)$$

where the concrete ε_r have to be determined from the subsequent diagonalization of a BxB-Matrix. (For an $B = 2$ example see Fig. 2.) Hence, the bandwidth of each band (which we label E_B) is determined by the longitudinal coupling $E_B = 4T_{\parallel}$, whereas the displacement $T_{\perp}\varepsilon_r$ scales linearly with the lateral coupling $T_{\perp}$.

The phononic dispersion relation $\omega_{\mathbf{i}}$ may take some standard form for acoustic or optical phonons. Below it will turn out that the details are irrelevant within the frame of our considerations as long as phononic energies are much smaller than electronic energies, i.e., $\omega_{\mathbf{i}} << \varepsilon_{\mathbf{j},r}$. The latter will be assumed.

The interaction V is also of standard lowest order form, it may be viewed as corresponding to an electron scattering under creation or annihilation of a phonon, with the phonon essentially compensating for the electronic momentum change.

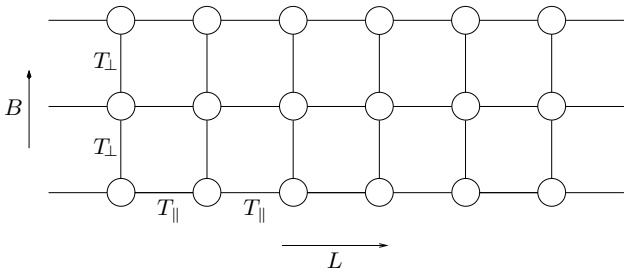

FIG. 1: Sketch of the quantum model we use to describe the properties of an atomic wire. Circles denote localized electronic states on a regular (quasi-)1-d lattice in configuration space. Lines indicate couplings with strength $T_{\parallel}$ parallel and strength $T_{\perp}$ perpendicular to the wire.

III. FORMULATION OF A MASTER EQUATION FOR COARSE GRAINED OCCUPATION NUMBERS

As a first step in our analysis we now aim at mapping the quantum dynamics of some set of "coarse grained occupation number deviations" in momentum space on a master equation. To this end we follow directly the scheme described in [10]. For an overview over mappings of quantum dynamics onto Boltzmann equations also see [10] and references therein. This scheme produces a linear master equation for a finite number of variables. These variables are sums of deviations of electronic occupation numbers from their equilibrium values. To make this well defined we have to specify which occupation number deviations should contribute to a certain sum. Only with this specification the scheme from [10] may be implemented. We call all modes, the occupation number deviations of which contribute to a certain sum, a "grain". Thus the number of variables as well as the concrete rates from the above master equation depend on this graining. Since this graining is to some extent arbitrary we must make sure that eventually our diffusion coefficient converges for a systematic refinement of the graining. This convergence then in turn sets the scale for a "correct" graining. In the following we first describe our choice for the graining and then give precise definitions for the above dynamical variables of the master equation.

Our graining is realized by primarily partitioning the momentum space into M "energy shells" of equal energy width ΔE. We then define the grains within one shell by means of the intersections of the electronic dispersion relation with the respective energy shell as depicted exemplarily in Fig. 2. We label the entity of all grains serially by Greek indices (, e.g., κ). (This may correspond to a consecutive numbering from left to right (see

Fig. 2) within one shell, which is then accordingly continued through the shells with increasing energy.) Note that these grain indices already contain the information to which band the respective grain belongs, that is, the band indices r are absorbed into the grain indices. As mentioned above the necessary refinement of the graining is eventually determined by the convergence of the diffusion coefficient. However, we generally focus on grains that are small enough to allow for a linearization of the dispersion relation on each grain.

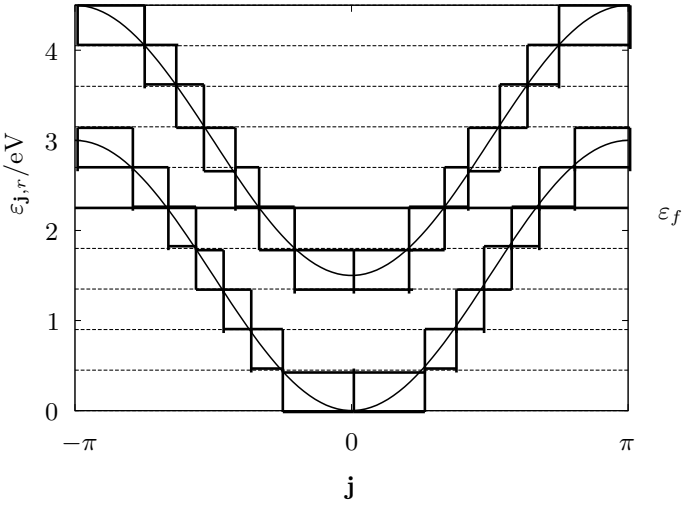

FIG. 2: Sketch of our specific coarse graining in momentum space for a model featuring $B = 2$ rows, i.e., the dispersion relation consists of 2 bands. Parallel dashed lines define energy shells of equal energy width ΔE. Rectangular boxes mark the individual grains. The Fermi edge is indicated by a thick line. Some shells contain grains from one band, some from both bands. Other model parameters: $E_B = 3\text{eV}$, $T_\perp = T_\parallel$, $M = 10$ energy shells and half filling ($\varepsilon_f = 2.25\text{eV}$).

Now we give a mathematical definition for the above deviations of electronic occupation numbers from their equilibrium values which are summed over a grain to form a dynamic variable of the above master equation. An operator representing such a deviation is given by

$$\Delta_{\mathbf{j},r} := a^\dagger_{\mathbf{j},r} a_{\mathbf{j},r} - f_{\mathbf{j},r}, \tag{3}$$

where $f_{\mathbf{j},r}$ is the equilibrium value of the electronic occupation number. Since we are interested in weak electron-phonon coupling we may take $f_{\mathbf{j},r}$ from the Fermi distribution for the occupation numbers of the isolated electronic system. Since we are furthermore interested in low temperature regimes we may routinely replace the chemical potential μ in the corresponding Fermi distributions $f_{\mathbf{j},r}(\mu, T) = (\exp((\varepsilon_{\mathbf{j},r} - \mu)/k_B T) + 1)^{-1}$ by the Fermi energy ε_F. With the help of such "individual mode deviation operators" $\Delta_{\mathbf{j},r}$ the deviation operators for the whole grains Δ^κ may simply be defined by the corresponding sums

$$\Delta^\kappa = \sum_{\mathbf{j},r\in\kappa} \Delta_{\mathbf{j},r} \ , \tag{4}$$

where the sum of course runs over all modes belonging to some grain. The dynamical variables of the above master equation are then defined as the expectation values of the grain deviation operators $d^\kappa(t)$ for the actual quantum state $\rho(t)$ of the full system evolving according to the coupled Hamiltonian H, i.e., $d^\kappa(t) := \mathrm{Tr}\{\rho(t)\Delta^\kappa\}$. Naturally, the dynamics of $\rho(t)$ are not directly accessible. But, as explained above, the considerations in [10] (which we, for brevity, do not intend to repeat or discuss here) provide a scheme by means of which the dynamics of the $d^\kappa(t)$ may be mapped onto a linear master equation. The scheme is believed to be valid as long as the electron-phonon coupling may be considered a small perturbation to the electronic system $H_{0,\mathrm{el}}$). Thus, simply applying this scheme casts the dynamics into the form:

$$\dot{d^\eta}(t) = \sum_{\kappa\neq\eta} R_{\eta\kappa}(t) d^\kappa(t) - \sum_{\kappa\neq\eta} R_{\kappa\eta}(t) d^\eta(t) \ . \tag{5}$$

The concrete expressions of the rates may also be read off from the results of [10]. As mentioned above we focus here on the case of negligible phonon energies which is explicitly treated in [10]. Exploiting this leaves us with

$$R_{\eta\kappa}(t) = \int_0^t \mathrm{d}\tau \frac{2}{\hbar^2 N_\kappa} \sum_{\substack{\mathbf{i},s\in\kappa,\\ \mathbf{k},r\in\eta}} \frac{|W_{rs}(\mathbf{k}-\mathbf{i})|^2}{\Omega} (1+g_{\mathbf{k}-\mathbf{i}}+g_{\mathbf{i}-\mathbf{k}}) \cdot \cos[\frac{1}{\hbar}(\varepsilon_{\mathbf{i},s}-\varepsilon_{\mathbf{k},r})\tau], \tag{6}$$

where N_κ denotes the number of states within the grain κ and $g_{\mathbf{q}}$ is the equilibrium occupation number of the phonon mode $\mathbf{q}$, as taken from the Bose distribution for the isolated phononic system $H_{0,\mathrm{ph}}$. Basically, the rates appear as integrals over some correlation functions, which usually decay within some correlation time τ_c, we generally assume the latter to be short compared to the time scale of the relaxation dynamics (weak coupling limit). Further, we define

$$\overline{\Gamma^2_{\eta\kappa}} = \sum_{\substack{\mathbf{i},s\in\kappa,\\ \mathbf{k},r\in\eta}} |W_{rs}(\mathbf{k}-\mathbf{i})|^2 (1+g_{\mathbf{k}-\mathbf{i}}+g_{\mathbf{i}-\mathbf{k}}) \cdot \frac{1}{N_\kappa N_\eta} \ . \tag{7}$$

Using this abbreviation and routinely exploiting the properties of the *sinc*-function as well as the linearizability of the dispersion relation on each grain, we can approximately perform the integration in (6), finding for times larger than the correlation time for the rates

$$R_{\eta\kappa} = \frac{2\pi\overline{\Gamma^2_{\eta\kappa}}}{N\hbar} \frac{N_\eta}{\Delta E} \delta_{E(\eta),E(\kappa)} \ . \tag{8}$$

The $\delta_{E(\eta),E(\kappa)}$ is meant to indicate that transitions only occur between grains from the same energy shell, i.e., all other rates vanish. Note that the resulting rates are completely independent of the electronic equilibrium occupation numbers, i.e, scattering above, below, or at the Fermi-level is in this approximation qualitatively the same.

IV. CALCULATION OF A DIFFUSION COEFFICIENT FROM A LINEAR BOLTZMANN EQUATION

Eventually we intend to calculate the diffusion coefficient from a type of linear Boltzmann equation. To this end we are simply going to interpret the rates from (8) as the entries of the corresponding collision term. But even if the Boltzmann equation is fully defined we have to tell how to calculate a diffusion coefficient from it. There are several approaches to the derivation of diffusion coefficients from linear(ized) Boltzmann equations [11–14]. However, since we are here confronted with a subtlety that may not occur in other cases, namely a non-symmetric rate matrix, we suggest an alternative approach to the diffusion coefficient. This approach is outlined in the following.

We start from a linear Boltzmann(-like) equation describing the dynamics of some probability distribution $\rho_\eta(\mathbf{x}, t)$ in a velocity discretized one-particle phase space:

$$\dot{\rho}_\eta(\mathbf{x}, t) = -v_\eta \nabla_{\mathbf{x}} \rho_\eta(\mathbf{x}, t) + \sum_\kappa R_{\eta\kappa} \rho_\kappa(\mathbf{x}, t) \ . \quad (9)$$

The two addends represent the drift and the collision term, respectively. The velocity v appears as depending on some index η. Eventually this index will be identified with the quantum mechanical momentum mode. After Fourier transforming with respect to $\mathbf{x}$ we find for the (Fourier transformed) probability distribution $\rho_\eta := \rho_\eta(\mathbf{q}, t)$

$$\dot{\rho}_\eta = \sum_\kappa (\underbrace{-\imath \mathbf{q} v_\eta \delta_{\eta\kappa}}_{R_1} + \underbrace{R_{\eta\kappa}}_{R}) \rho_\kappa \ , \quad (10)$$

where the drift term R_1 now enters as a diagonal matrix and the collision term R as a non-diagonal matrix with respect to the above representation.

Eq. (10) is formally identical to a non-specific, abstract time dependent Schrödinger equation where $R_1 + R$ corresponds to some Hamilton operator. However, since $R_1 + R$ is not Hermitian, eigenvalues may (and will) not be real. Furthermore, eigenstates represent spatial particle-density waves with wavevectors $\mathbf{q}$ which decay mono-exponentially. Such a behavior is in accord with diffusive transport. The corresponding decay constant is given by the imaginary part of the corresponding eigenvalue. For arbitrarily small $\mathbf{q}$ (long wavelengths) one may treat the drift term R_1 as a small perturbation to the collision term R. Therefore, in order to find the decay constant, we may calculate corrections to eigenvalues of R induced by R_1 via a procedure that is essentially analogous to standard time-independent perturbation theory as given in textbooks. In doing so, the eigenvectors of R represent the eigenstates of the unperturbed Hamiltonian. The eigenvector $\vec{P}_0$ of R featuring the eigenvalue zero corresponds to the total, isotropic equilibrium distribution in the above phase space. Thus, assuming that the evolving distribution that corresponds to a diffusion process exhibits locally (with respect to real space) more or less the equilibrium distribution with respect to velocities (momenta), we have to analyze the decay dynamics of $\vec{P}_0$ induced by R_1. In other words we have to calculate the correction to the eigenvalue of $\vec{P}_0$. Before going in any detail we note that the second order correction scales as $\propto \mathbf{q^2}$. Thus, in case the first order vanishes, the decay constants for the corresponding density waves will scale as $\propto \mathbf{q^2}$ as well. The latter dynamics represent a solution to a diffusion equation with a diffusion coefficient given by the prefactor of the $\mathbf{q^2}$-term of the decay constants. Thus, calculating the second order correction to $\vec{P}_0$ may and will turn out as being equivalent to calculating the diffusion coefficient.

Nevertheless, as already mentioned above, we encounter here the difficulty that the collision term R is in general non-symmetric and therefore the eigenvectors of R, denoted by $\{\vec{P}_i\}$, are not necessarily orthonormal. This problem may be dealt with by introducing a dual basis $\{\vec{P}^i\}$ such that

$$\vec{P}^j \vec{P}_i = \delta_{ji} \ . \quad (11)$$

Like, e.g., in the context of relativity, the dual basis is constructed by means of some metric tensor G_{ij} featuring

$$\vec{P}^i = G_{ij} \vec{P}_j \ . \quad (12)$$

A straightforward calculation yields for the inverse of the metric tensor

$$G^{-1}_{ij} = \vec{P}_i \cdot \vec{P}_j \ . \quad (13)$$

That is, its matrix elements are simply given by the scalar products of the eigenvectors of R. For the construction of the dual basis G^{-1} has still to be inverted of course.

Within this framework we are finally able to determine the corrections to the eigenvalue zero. As already outlined, we hereby follow precisely the scheme of standard time independent perturbation theory, except for replacing basis "bra"-vectors by vectors from the dual basis. For the eigenvalue correction (to the eigenvalue of $\vec{P}_0$, i.e., zero) to first order we thus obtain

$$E_1 = -i\mathbf{q} \vec{P}^0 \hat{v} \vec{P}_0 \ , \quad (14)$$

where $\hat{v}$ is a diagonal matrix in the matrix representation used in (10) with the corresponding velocities v_η as diagonal elements, i.e., it is given by $R_1 = -\imath \mathbf{q} \hat{v}$. If the system in question features full spatial mirror-symmetry (as our atomic wire system does) the eigenvectors $\vec{P}_j$ of R as well as their dual counterparts $\vec{P}^i$ separate into two symmetry classes, symmetric and antisymmetric. Those two classes do not mix or overlap (in the sense of a regular scalar product). Since $\vec{P}_0$ and $\vec{P}^0$ belong to the symmetric class but $\hat{v}\vec{P}_0$ belongs to the antisymmetric class, the first order correction E_1 vanishes. As outlined above this is exactly what is required for the corresponding solution

of the Boltzmann equation in order to describe diffusive dynamics at all. Thus we may indeed extract the diffusion coefficient from the second order. A straightforward calculation yields for the latter

$$D = \frac{E_2}{-\mathbf{q}^2} = -P^0_\eta v_\eta R^{-1}_{\eta\kappa} v_\kappa P_{0,\kappa} \ , \tag{15}$$

where R^{-1} corresponds to the inverse matrix to R neglecting the null-space.

Thus we eventually found a diffusion coefficient describing a diffusive class of solutions of a velocity-discretized, linear Boltzmann equation. Or to rephrase: given a specific linear Boltzmann equation we may calculate the corresponding diffusion coefficient based on (15). Thus, in our case we now have to specify a pertinent Boltzmann equation, i.e., the v_η and $R_{\eta\kappa}$. Of course we do that on the basis of the considerations in Sec. III. We formulate a Boltzmann equation which is discretized according to the previously described graining. Concretely we identify the v_η with the slope of the dispersion relations at the centers of the corresponding grains. This is the standard concept of identifying particle velocities with group velocities. The scattering rates $R_{\eta\kappa}$ are taken from (8). With those allocations the Boltzmann equation is fully specified. However, since the rates as given in (8) only give rise to transitions within an energy shell, the dynamics completely decouple with respect to energy shells. Due to this decoupling the equilibrium state $\vec{P}_0$ is not completely determined by the Boltzmann equation, the latter does not fix the equilibrium particle numbers for full shells, it only sets the distribution onto the grains within one shell. Thus we have to pick a $\vec{P}_0$ in accord with the Boltzmann equation but additionally with reasonable overall particle numbers assigned to the shells. Here we do that based on the standard idea of transport being due to particles above the Fermi edge and due to holes below. Thus we weigh the equilibrium distribution within the shells by the probabilities of finding holes or particles, respectively at the corresponding energies. Doing so we find:

$$\vec{P}_0 : P_{0,\kappa} \propto f(E,T) N_\kappa \tag{16}$$

for $E > \varepsilon_f$ and

$$\vec{P}_0 : P_{0,\kappa} \propto (1 - f(E,T)) N_\kappa \tag{17}$$

for $E < \varepsilon_f$. This construction ensures that the diffusion coefficient is dominated by processes occurring near the Fermi energy for common temperatures which appears physically reasonable. Since the diffusion coefficient as given in (15) involves the dual counterpart of the equilibrium distribution, an overall prefactor, i.e., the total number of particles does not alter its value (, hence such a prefactor is not specified above). This also appears physically reasonable. With this choice for the equilibrium distribution all quantities in (15) are eventually specified.

V. NUMERICAL COMPUTATION OF THE DIFFUSION COEFFICIENT

In this paragraph we concretely determine a diffusion coefficient for the model describing the atomic wire as introduced in Sec. II by explicitly and straightforwardly evaluating formula (15). The respective computations may be done on standard computers. The numerical effort of course depends on the finesse of the chosen/necessary graining, however most of the diffusion coefficients presented below have been found within minutes of computation time.

The calculations mainly aim at describing the typical, characteristic dependence of the diffusion coefficient on two crucial system properties, i.e., the width of the atomic wire and the lateral coupling; we do not intend here to determine diffusion coefficients with extreme (numerical) precision or to describe concrete experimental realizations in great detail.

Along those lines the bandwidth of the electronic dispersion relation is chosen as $E_B = 3\text{eV}$, i.e., $T_\parallel = 0.75\text{eV}$. Furthermore, we apply a temperature of 300K. In this case the equilibrium distribution $\vec{P}_0$ is mainly concentrated around the Fermi energy, i.e., mainly the grains belonging to the shells in the vicinity of the Fermi edge contribute to the diffusion coefficient. Furthermore, we exclusively focus here on half-filling situations. For simplicity we assume that the electron-phonon coupling elements $W_{rs}(\mathbf{q})$ from (1) show no strong $\mathbf{q}$-dependence and also that there is no decisive dependence on the band indices r, s, i.e., we consider all momentum modes as being equally strongly coupled, no matter which grain they belong to. Consequently, we set $W_{rs}(\mathbf{q})^2 = W^2$ with $W = 0.03\text{eV}$, thus weak coupling is implemented in the sense of electron-phonon coupling being much smaller than the electronic bandwidth. Additionally, also for simplicity, we set the phononic dispersion to a constant with $\omega_{\mathbf{i}} = 0.03\text{eV}$. This satisfies the above mentioned requirement of phonon energies being much smaller than electronic energies.

As outlined above, we expect the diffusion coefficient to converge towards some value for finer and finer grainings. We clearly observe this feature in the calculations. So, all plotted diffusion coefficients refer to in this sense converged values, i.e., are taken from sufficiently fine grainings which here means about 100 shells per bandwidth E_B. This amounts to a total number of grains $g \approx 200B$.

Fig. 3 shows the resulting diffusion coefficients for different widths of the molecular wire, i.e., different number of parallel rows B, for two lateral couplings $T_\perp = 2T_\parallel$ and $T_\perp = T_\parallel$.

One finds that the corresponding diffusion coefficients for $T_\perp = 2T_\parallel$ come out rather discontinuous and show large jumps for increasing width. In fact, the diffusion coefficient becomes very small (almost 0) for certain widths, e.g., $T_\perp = 2T_\parallel$, 2 rows). This especially occurs when the slopes of the dispersion relations near the Fermi edge are very small, i.e., almost 0, in one or more bands. In such

a case the velocities v_κ become small and the rates $R_{\eta\kappa}$ become large thus giving rise to a small diffusion coefficient.

For $T_\perp = T_\parallel$ one finds a relatively smooth, continuous curve without such distinctive jumps as for $T_\perp = 2T_\parallel$. However, in both cases we observe a dependency of the diffusion coefficient on the width of the atomic wire, which has to be classified as a finite size effect. Of course this effect should vanish in the limit of infinitely large widths $B \to \infty$, i.e., the diffusion coefficient is expected to become constant, since the model then passes into a regular 2-d lattice. The plots in Fig. 3 suggest such a convergence at a width of approximately 50 rows and are therefore in accord with the above educated guess. Although a numerical verification was possible we omit such a calculation here for it would be numerically rather costly.

From the plots in Fig. 3 one may infer that the "discontinuity" of the diffusion coefficient with regard to the width of the molecular wire seems to crucially change with varying lateral coupling $T_\perp$.

This feature is further analyzed in Fig. 4 which shows the dependence of the diffusion coefficient on the lateral coupling $T_\perp$ for several numbers of rows (2 to 6).

According to these graphs the diffusion coefficient drops for a all analyzed widths when $T_\perp$ is increased from 0, slightly faster for larger widths. As already observed in Fig. 3 the diffusion coefficients here decrease partly to very small values, but then jump up at certain lateral coupling strengths to values which vary significantly for different widths. Recall that $T_\perp$ determines the displacement of the different energy bands. The jumps occur whenever a band edge is driven through the Fermi edge, since the slope of the dispersion relation is 0 at the band edges. Especially note that these jumps cause a significant spreading of the curves above $T_\perp \approx 1.3T_\parallel$, i.e., when the lateral coupling becomes stronger than the longitudinal (which is in accord with the discontinuous curve for the in this sense large enough lateral coupling $T_\perp = 2T_\parallel$ displayed in Fig. 3).

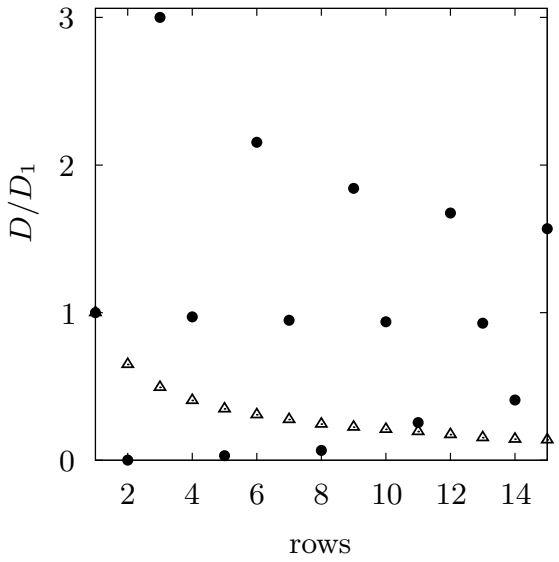

FIG. 3: Plot of the diffusion coefficient D against the number of rows, i.e., the width for $T_\perp = 2T_\parallel$ (black dots) and $T_\perp = T_\parallel$ (white triangles). The plot is normalized to the D obtained for 1 row, denoted by D_1. Other parameters: $E_B = 3$eV, $T_\parallel = 0.75$eV, $T = 300$K, half filling.

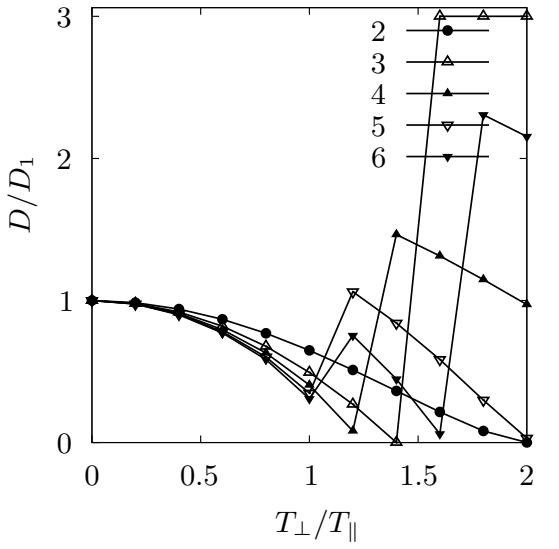

FIG. 4: Plot of the diffusion coefficient D against the lateral coupling $T_\perp$ for different widths, i.e., different numbers of rows, according to the legend. The plot is normalized to the D obtained for 1 row, denoted by D_1. Other parameters: $E_B = 3$eV, $T_\parallel = 0.75$eV, $T = 300$K, half filling.

VI. SUMMARY AND OUTLOOK

We investigated diffusive transport behavior of electrons in atomic wires, described on the basis of some pertinent quantum model. The rather simplified model is meant to schematically describe planar atomic wires with a width of a few atoms, formed, e.g., on a crystal surface (or embedded in some crystal bulk). The electrons within the wire are taken to be mutually non-interacting, diffusive behavior is solely induced by coupling to the crystal phonons. To this end we firstly computed a linear master equation describing the dynamics for some, with respect to momentum space, coarse grained occupation numbers, hereby closely following an approach from [10]. The resulting rate matrix is then interpreted as the collision term of a pertinent linear Boltzmann equation.

Furthermore, we analyzed solutions of linear Boltzmann equations which can be characterized as representing diffusive transport dynamics. An explicit expression connecting the diffusion coefficient to the parameters of the Boltzmann equation is given. Based on this formula we numerically computed diffusion coefficients for wires of different types. In particular, we investigated the dependency of the diffusion coefficient on the width of the

atomic wire as well as the dependency on the lateral coupling strength between neighboring rows. We found that the resulting diffusion coefficient varies significantly and non-regularly with the width. If the lateral exceeds the longitudinal atomic coupling within the wire, the diffusion coefficient exhibits large jumps with respect to varying widths. This feature may be clearly classified as a finite size effect. Concretely the diffusion coefficient may become very small and even nearly vanish for certain combinations of widths and lateral couplings. There is also a rather strong dependence on the lateral coupling for fixed widths showing jumps for strong lateral coupling. The corresponding curves differ significantly subject to the width. Thus, to summarize this results: the diffusion coefficient depends strongly and in a non-trivial way on both, the wire width and the lateral coupling.

By using a generalized Einstein relation [15] the diffusion coefficients may be converted into conductivities, which would probably be better accessible by experiments. Therefore, the approach introduced here may serve as a basis for concrete transport-theoretical analyzations to be performed in the near future.

To obtain more realistic quantitative results, the model parameters used in this approach may be better adjusted to some concrete (experimental) realizations, e.g., a more realistic electron-phonon coupling, possibly including electron-electron interactions, etc..

Acknowledgments

We sincerely thank M. Kadirogˉlu for his contributions to fruitful discussions. Financial support by the "Deutsche Forschungsgemeinschaft" is gratefully acknowledged.

[1] J. Lehmann, S. Kohler, P. Hänggi, and A. Nitzan, Phys. Rev. Lett. **88**, 228305 (2002).
[2] A. Fuhrer, A. Dorn, S. Lüscher, T. Heinzel, K. Ensslin, W. Wegschneider, and M. Bichler, Superlatt. and Microstr. **31 (1)**, 19 (2002).
[3] A. Kühnle, L. M. Molina, T. R. Linderoth, B. Hammer, and F. Besenbacher, Phys. Rev. Lett. **93**, 086101 (2004).
[4] W. Haiss et al., J. Phys. Chem. B **111 (24)**, 6703 (2007).
[5] G. J. Ashwell, B. Urasinska, C. Wang, M. R. Bryce, I. Grace, and C. J. Lambert, Chem. Commun. p. 4706 (2006).
[6] X. Sotos, Phys. Rev. Lett. **82**, 1764 (1999).
[7] B. N. Narozhny, A. J. Millis, and N. Andrei, Phys. Rev. B **58**, R2921 (1998).
[8] F. Heidrich-Meisner, A. Honecker, D. C. Cabra, and W. Brenig, Phys. Rev. B **68**, 134436 (2003).
[9] X. Sotos and P. Prelovšek, *Interacting Electrons in Low Dimensions* (Kluwer Academic Publishers, 2003), vol. 25 of *Physics and Chemistry of Materials with Low-Dimensional Structures*, chap. Transport inOne-Dimensional Quantum Systems.
[10] C. Bartsch, R. Steinigeweg, and J. Gemmer (2010), invited for resubmission to Phys. Rev. E.
[11] R. Balescu, *Equilibrium and Nonequilibrium Statistical Mechanics* (John Wiley and Sons, New York, London, Sydney, Toronto, 1975).
[12] W. Brenig, *Statistical Theory of Heat* (Springer Verlag, Berlin, Heidelberg, New York, 1989).
[13] J. Jäckle, *Einführung in die Transporttheorie* (Vieweg, Braunschweig, 1978).
[14] M. Kadirogˉlu and J. Gemmer, Phys. Rev. B **76**, 024306 (2007).
[15] R. Steinigeweg, H. Wichterich, and J. Gemmer, Europhys. Lett. **88**, 10004 (2009).

Eidesstattliche Erklärung

Hiermit erkläre ich, dass ich die vorliegende Dissertation selbstständig, ohne unerlaubte Hilfe Dritter und ohne Benutzung anderer als der von mir angegebenen Quellen und Hilfsmittel angefertigt habe. Die den verwendeten Quellen wörtlich oder inhaltlich entnommenen Stellen habe ich als solche kenntlich gemacht. Ich habe keine vorherigen Promotionsversuche unternommen.

Osnabrück, d. 29.01.2010

Christian Bartsch